# Proteomic Analysis of Merkel Cell Polyomavirus

## Thesis

# Proteomic Analysis of Merkel Cell Polyomavirus

Gianluca Triolo

A Thesis Submitted in Fulfillment of the Requirements

Of the Faculty of Life Science of the Open University (UK) For the

Degree of Master of Philosophy


International Centre for Genetic Engineering and Biotechnology

Trieste, Italy

Director of Studies: Dr. Michael P. Myers
External Supervisor: Dr. James Chong

November, 2019

# TABLE OF CONTENTS

LIST OF TABLES

LIST OF FIGURES

# DEDICATION

This Master's thesis is dedicated to the **friendship** and **memory** of Prof Arturo Falaschi (21 January 1933, Rome – 1 June 2010, Montopoli in Val d'Arno). I'm sure you would have appreciated. And to all those who are suffering from or have died of Merkel cell carcinoma.

ACKNOWLEDGEMENTS

The last five years have been an incredible journey. I have faced many tough challenges, learned numerous skills, madded accomplished many goals. Various fine individuals have helped me. I have been extremely fortunate to encounter such nice people and am grateful to all of them. First and foremost I would like to thank my mentor Dr Michael Paul Myers. I don't know where to begin to express my gratitude for your time, guidance, patience and encouragement. Thank you for sharing your strong belief that research should be fun, for your enthusiasm and genuine interest and for you're good sense of humor. Thank you for always taking time to make sure that everything is okay and also for creating a friendly atmosphere in the group. I will always be grateful to you for the opportunities and project that you gave me, for all your support and the freedom to listen some of my crazy ideas. Thank you for be such great person and one inspirational scientists.

Thanks to Dr Rabab Abdelaleem for her support, help and sincere friendship. Thanks to Dr Lawrence Banks and to his group (in particular Justyna Broniarczyk and David Pim) for fruitful discussions and good collaboration. Thanks to Paola Massimi and Valentina Martinelli, for being such a good friends, and for the interesting discussions.

Finally, and most importantly, I will be forever grateful to my wonderful family. Thanks to my wife Monica, for the enormous support and calm; to my son Cesare for always was showing an interest in science and your mere existence.

Sincerely,

Triolo Gianluca

ABBREVIATIONS

All the abbreviations can also be found in the text when introduced for the first time. The abbreviations used only once are not included in this list.

| | |
|---|---|
| aa | Amino acid |
| Ab | Antibody |
| ACN | Acetonitrile |
| AmAc | Ammonium Acetate |
| AmBic | Ammonium Bicarbonate |
| AP | Atmospheric Pressure |
| BKPyV | BK polyomavirus |
| BSA | Bovine Serum Albumin |
| CBB | Coomassie Brilliant Blue |
| CID | Collision Induced Dissociation |
| DTT | DL-Dithiothreitol |
| E. coli | Escherichia coli |
| ECD | Electron Capture Dissociation |
| EBV | Epstein-Barr virus |
| ESI | Electrospray Ionization |
| ER | Early Reagion |
| ETD | Electron Transfer Dissociation |
| FBS | Fetal bovine serum |
| GFP | Green fluorescent protein |
| HEPES | 4-(2-hydroxyethyl)-1-Piperazineethanesulfonic |
| HPLC | High Performance Liquid Chromatography |

| | |
|---|---|
| HPV | Human papillomavirus |
| IARC | International Agency for Research on Cancer |
| IP | Immune-precipitation |
| IT | Ion trap |
| JCPyV | JC polyomavirus |
| LC | Liquid Chromatography |
| LC-MS/MS | Liquid chromatography mass spectrometry |
| LR | Late Reagion |
| LTAg | Large tumor antigen |
| m/z | Mass-to-charge ratio |
| MALDI | Maxtrix-Assisted Laser Desorption/Ionization |
| MCPyV | Merkel Cell Polyomavirus |
| Mgf | Mascot generic file |
| MPyV | Murine polyomavirus |
| MS | Mass Spectrometry |
| MS/MS | Tandem Mass Spectrometry |
| MTAg | Middle tumor antigen |
| MW | Molecular weight |
| ORF | Open reading frame |
| PAGE | Polyacrylamide gel electrophoresis |
| PBS | Phosphate buffered saline |
| PCR | Polymerase chain reaction |
| PDB | Protein Database |
| PMF | Peptide mass fingerprinting |
| pRb | Retinoblastoma protein |
| PTM | Post-translational Modification |

| | |
|---|---|
| Rf | Radio-frequency |
| RP | Reverse phase |
| Rpm | Rotations per minute |
| SDS | Sodium dodecyl sulphate |
| SDS-PAGE | Sodium Dodecyl Sulfate Polyacrylamide Gel Electrophoresis |
| sTAg | Small tumor antigen |
| SV40 | Simian virus 40 |
| TCEP | Tris(2-carboxyethyl)phosphine |
| TEAB | Triethyl ammonium bicarbonate |
| TFA | Trifluoro Acetic Acid |
| TIC | Total ion current |
| VLP | Virus-like particle |
| VP | Viral protein |
| wt | Wild type |

**Abstract**

Over the past 8 years, the discovery of 11 new human polyomaviruses (HPyVs) has revived interest in this DNA tumor virus family. Although HPyV infection is widespread and largely asymptomatic, one of these HPyVs, Merkel cell polyomavirus (MCPyV), is a human tumor virus. JC virus (JCPyV), BK virus (BKPyV), HPyV7, and trichodysplasia-spinulosa virus (TSPyV) can cause non-neoplastic diseases in the setting of immunosuppression. Probably, one of the most common themes among the oncogenic viruses rests in the ability of one or more of the viral proteins to deregulate pathways involved in the control of cell proliferation.

The focus of this work is on MCPyV, which is a human pathogen. In addition to its importance in human health, there is growing interest in adapting MCPyV for drug delivery and other biotechnology applications, several viral coat proteins can spontaneously assemble into capsids in vitro with morphologies identical to the native virions and virion assembly is a powerful model system for studying protein complex formation. The protein capsid of the virion is a non-covalent association of protein subunits that is responsible for an array of functions, including cell attachment, cell entry, and DNA release. Even for the best studied family members, the mechanism of assembly is still poorly understood.

Studies on the proteins of MCPyV provide information about the composition of the virus, as well as individual virus-virus protein and virus-host protein interactions. Mass spectrometry offers a unique perspective on the properties of viruses. Its broad application to viral structure provides unique insights into many biological processes, including viral–antibody binding, protein–protein interactions and protein dynamics. Electrospray ionization (ESI) mass spectrometry is a powerful approach for analyzing biomolecules and biomolecular complexes. Previous studies have provided evidence that

non-covalent biomolecular complexes can be observed by ESI mass spectrometry. Mass spectrometry of viral proteins is now routine and since viruses are typically well characterized, in that the capsid protein and genome sequences are known, identifying a virus based on the mass of the protein or based on enzymatic digestion is relatively straightforward.

This thesis describes the use of mass spectrometry for the identification of proteins associated with the MCPy virion and for the analysis of the post-translational modifications of the capsid proteins, such as ubiquitinylation, phosphorylation and acetylation.

# 1. INTRODUCTION

## 1.1 Viruses

The first viruses were discovered at the end of the nineteenth century by the Russian botanist Iwanowski who demonstrated that the extracts of a diseased plant could transmit the disease to healthy plants, even after passing through fine filters. At that point a virus (from the Latin for poison) was called "soluble living germ" (*Cann 2001*).

Viruses are organisms that cause diseases that depend largely on their host for survival and reproduction because they can only multiply within cells. Viruses are the smallest known organisms and it was not until the 1930s that it was possible to separate viruses from their host cell material. Studies of bacterial viruses, e.g. bacteriophages, in the 1940s, confirmed that viruses consist of genetic material (RNA or DNA) and a protein shell, the capsid, which surrounds it (*Hershey, Chase 1952*). The capsid helps to transport the virus and it also protects the virus from degradation when it is outside of cells. Many viruses also have a lipid envelope surrounding the capsid. Each virus type can only infect a limited range of hosts and some viruses can only infect one species. Viruses are also normally tissue specific, for example some common cold viruses only infect cells of the upper respiratory tract.

The isolated viral particles are incapable of reproducing without assistance, because they lack enzymes and all the other equipment necessary to produce their own proteins. However, when they enter a host cell, they take control of the cellular machinery to promote their reproduction. This multiplication of the virus is often lethal to the infected cell, which in turn lyses, and releases numerous new viral particles that infect new cells. Many of the symptoms of a viral infection are due to this tissue damage, but also due to

the activation of the immune system, e.g. the inflammatory responses (*Rous, Landmark 1983*).

The immune system typically manages to control the virus within a few weeks. However, some viruses do not kill the cell; and are able to integrate their genes into the host genome and can remain more or less dormant in the host inducing a persistent, latent, or recurrent viral infection. Some of these viruses may contain genes that regulate cell growth and can transform normal cells into cancer cells and these are the tumor viruses (*Gross 1953*).

## 1.2 Viruses and Cancer

About 20 % of all cancer cases worldwide are believed to be caused by viruses (*Parkin 2001; Parkin 2006*). The strongest link is between Human Papilloma Virus (HPV) and cervical cancer, where the virus has been estimated to be responsible for 93% of the cervical cancers (*Bosch et al. 1995*). Moreover, liver cancer is linked to Hepatitis B and C viral infection (*Bradley 1999*). Epstein-Barr virus (Burkitt's lymphoma), human herpes virus (Kaposi's sarcoma) and human T-lymphotropic retrovirus (leukemia) also represent identified human tumor viruses (*Zur Hausen 1999*). The first tumor virus was discovered by Francis Peyton Rous more than 100 years ago and considerable research has been devoted to understanding this group of viruses (*Rous 1910*). Vaccination programs for the prevention of two common tumor virus infections, hepatitis B virus (HBV) and HPV have begun to make a difference in the burden of cancer and the general health of the world population (*Goldie et al. 2004; Lavanchy 2004*).

Francis Peyton Rous showed that viruses could induce cancer. He transplanted sarcoma from a 15-month old hen into other chickens using cell-free tumor extracts (*Rous 1910; Rous 1983*). The isolated etiologic agent, Rous sarcoma virus (RSV), was the first tumor virus identified. It took 50 years, with Ludwik Gross's discovery of an acute transforming

murine retrovirus and a polyomavirus that caused murine tumors (*Gross 1953*), for the interest in tumor viruses to re-emerge. The impact of these achievements was enormous. Just after Rous received the Nobel Prize for his discoveries other studies of the Rous Sarcoma Virus resulted in the discoveries of reverse transcription and the cellular origin of viral oncogenes (*Stehelin 1976; Baltimore 1970*).

The first tumor viruses were discovered in fowls by Rous in 1911 (*Rous 1910 and Rous 1911*). In the 1930s, Rous et al., infected rabbits with cottontail rabbit papillomavirus and found that the rabbits developed tumors (*Rous 1936*). In 1951 Gross found the first murine tumor virus, the murine leukemia virus (MLV) (*Gross 1951*). Regarding human tumor viruses, it was not until 1976, that Zur Hausen could demonstrate that human papillomavirus (HPV) causes cervical cancer (*Zur Hausen 1976*). Numerous tumor viruses have been identified that include members of the retrovirus, polyomavirus, adenovirus and herpesvirus groups (*McLaughlin-Drubin and Munger 2008*).

### 1.3 Human tumor viruses

The first human tumor virus was discovered in 1964 by Anthony Epstein, Bert Achong and Yvonne Barr. They identified herpesvirus-like particles in cell lines from African patients with an unusual, geographically confined childhood cancer called Burkitt's lymphoma (*Epstein, Barr 1964*). The virus was subsequently named the Epstein-Barr virus (*Golden 1968*). Although studies that showed EBV infection is ubiquitous in adults worldwide, EBV-associated tumors were rare. The dissociation between infection and the onset of cancer confounded scientists on how viruses cause tumors (*Proceedings of the IARC Working Group on the Evaluation of Carcinogenic Risks to Humans 1997; Griffin 2000*). In addition, sporadic Burkitt lymphomas, often lacking EBV, have been observed in developed countries, but these cases often maintain a characteristic mutation of Burkitt's lymphoma (*Kelly and Rickinson 2007*). Understanding how cancer developes and the

recognition that chronic viral infections work together with various non-viral host factors to contribute to cancer, ultimately led to the acceptance of EBV as a human cancer virus. The International Agency for Research on Cancer (IARC) declared EBV as a Group I human carcinogen in 1997 (*No. 70 IARC Working Group on the Evaluation of Carcinogenic Risk to Humans. Lyon (FR): International Agency for Research on Cancer; 1997*). Scientists have made numerous attempts to search for human tumor viruses using a similar electron microscopy approach, however these were mostly negative. It was later understood that oncogenic viruses generally do not replicate as virions in tumors, but exist as latent episomes or physically integrated into the host genome (*Berger, Concha 1995; Imperiale 2000*). Many other classes of human tumor viruses have been identified since EBV (Table 1.1). Interestingly, almost all of these human tumor viruses have closely related family members that do not cause human cancer.

**Table 1.1** Human tumor viruses (from *Moore, Chang, 2010*)

| Virus | Year identified | Method of identification | Genome | Cancer associations | Reference |
|---|---|---|---|---|---|
| Epstein–Barr virus (EBV) | 1964 | Electron microscopy | Double-stranded DNA herpesvirus | Most Burkitt's lymphoma and nasopharyngeal carcinoma, most lymphoproliferative disorders, some Hodgkin's disease, some non-Hodgkin's lymphoma and some gastrointestinal lymphoma | Epstein *et al*., Lancet, 1964 |
| Hepatitis B virus (HBV) | 1965 | Serologic screening | Single-stranded and double-stranded DNA hepadenovirus | Some hepatocellular carcinoma | Blumberg *et al*., JAMA, 1965 |
| Human T-lymphotropic virus-I (HTLV-I) | 1980 | Tissue culture | Positive-strand, single- stranded RNA retrovirus | Adult T cell leukaemia | Poiesz *et al*., PNAS, 1980 |
| High-risk human papillomaviruses (HPV) | 1983–1984 | DNA cloning | Double-stranded DNA papillomavirus | Most cervical cancer and penile cancers and some other anogenital and head and neck cancers | Durst *et al*., PNAS, 1983 Boshart *et al*., EMBO J, 1983 |
| Hepatitis C virus (HCV) | 1989 | cDNA cloning | Positive-strand, single- stranded RNA flavivirus | Some hepatocellular carcinoma and some lymphomas | Choo *et al*., Science, 1989 |
| Kaposi's sarcoma herpesvirus (KSHV) | 1994 | Representational difference analysis | Double-stranded DNA herpesvirus | Kaposi's sarcoma, primary effusion lymphoma and some multicentric Castleman's disease | Chang *et al*., Science, 1994 |
| Merkel cell polyomavirus (MCV) | 2008 | Digital transcriptome subtraction | Double-stranded DNA polyomavirus | Most Merkel cell carcinoma | Feng *et al*., Science, 2008 |

In adults, primary HBV infection causes either acute hepatitis or may be asymptomatic. However, in about 5% of infected infants and adults where the primary infection fails to resolve, a chronic infection is observed. Persistent chronic infection, along with other risk factors, increases the risk of developing hepatocellular carcinoma (*Shah 2004; Carbone et al. 1997*).

HBV-induced liver cancer is responsible for more than 300,000 deaths a year worldwide. An important milestone in the prevention of these tumors was provided by Merck's HBV vaccine. It is a recombinant vaccine produced in yeast cells and protects against not only acute and chronic hepatitis, but also the development of HCC (*Javier, Butel 2008*).

HTLV-1, the first retrovirus that causes human cancer was discovered in the 1980's (*Poiesz et al. 1980*). HTLV-1 infects healthy individuals, but is kept in check by the immune

system and remains latent/dormant for long periods. HTLV-1 infection causes a life-long infection for infected subjects. HTLV-1 is endemic in various parts of the world and it has been estimated that over 10 million individuals are infected with HTLV-1 (*Edlich et al. 2003*), but most infected persons are asymptomatic.

Cervical cancer is the third most common cancer in women worldwide (*Smith et al. 2004*). Based on the emerging evidence at the time, linking human papillomaviruses (HPV) to gential warts, Harald zur Hausen reasoned that HPV was the etiologic agent for cervical cancer, despite the general belief that herpes simplex virus 2 (a sexually transmitted virus) was the likely cause. In his landmark studies in 1983 and 1984, his group discovered two novel HPV genotypes (HPV16 and HPV18) (*Tsai et al. 2003; Gilbert et al. 2004*). These genotypes are now confirmed as the causative agents for 70% of cervical cancers worldwide. HPVs are associated with more human cancers than any other virus (*Mannova et al. 2003; Friedet al. 1981; Sinibaldi et al. 1990; Liu et al. 1998*). The success of the HBV vaccine prompted HPV biologists to develop a safe HPV vaccine. This was achieved by using quadrivalent virus like particles (VLP)-based on recombinant capsid protein L1 from HPV types 6, 11, 16 and 18) and clinical trials in 2006 demonstrated that immunized women had type-specific protection against HPV infection, as well as protection against associated cervical, vulvar and vaginal disease (*Block et al. 2006*). VLPs are non-infectious virions resulting from the self-assembly of viral capsid proteins, and are used in making conformational viral epitope-based vaccines (*Michel et al. 1967*). The vaccines, marketed as the quadrivalent Gardisil®9 and the bivalent CervarixTM, are widely used and recommended for young individuals (both girls and boys, ages 9 through 26). Based on current estimates, these vaccines can lead to the prevention of greater than 400,000 cervical cancer cases per year.

Investigations of viruses as agents of human neoplasms led to the discovery of two new human tumor viruses, KSHV and MCPyV. Kaposi's sarcoma-associated herpesvirus (KSHV) is the virus that causes Kaposi's sarcoma (KS), the most common neoplasm that

occurs in individuals with untreated HIV / AIDS. Kaposi sarcoma oncogenesis has been shown to be associated with loss of T-cell-mediated control of KSHV-infected cells.

KSHV can establish an asymptomatic infection for life in immunocompetent subjects and when the number of T cells decreases (AIDS or treatment with immunosuppressive drugs) both the prevalence of KSHV infection and the incidence of KS in KSHV carriers increases significantly (*Chang et al. 1994; Robey et al. 2010*).

Merkel cell carcinoma is a rare and aggressive primary skin tumor that often has a poor prognosis (*Gheysen et al. 1989; Delchambre et al. 1989*). The risk of developing MCC is 13 times higher in patients with AIDS and 10 times higher after solid organ transplantation (*French et al. 1990*). MCC is also more common in patients undergoing immunosuppressive therapy, in elderly subjects and in patients with other tumors such as chronic lymphatic leukemia, basal cell carcinoma and squamous cell carcinoma. Importantly, none of these tumors has being casually associated with MCPyV infection (*Reety et al. 2012*). Based on the strong association between immunosuppression and its epidemiology, Merkel Cell Carcinoma (MCC) was subjected to a direct sequencing method called Digital Transcriptome Subtraction (DTS) designed to discover viral sequences (*Murata et al. 2003; Paliard et al. 2000*). cDNA libraries were created from the mRNA of four MCC tumor tissues and sequenced to generate a transcriptome database of MCC tumors. An in silico subtraction of known human sequences using databases of human genomic sequences (made available through the Human Genome Project) identified non-human sequence candidates for further testing. From these candidate sequences, a transcript with homology to other poliomaviruses was identified, which paved the way for the discovery of a new polyoma virus associated with MCC (GenBank access numbers EU375803 and EU375804) (*Murata et al. 2003*).

## 1.4 Polyomaviruses

### 1.4.1 Classification

The name Polyomaviridae derives from the study of the first discovered member of this family, the murine polyomavirus (MPyV) that was discovered by Gross in 1953. He noted that MPyV induced multiple (poly: Greek meaning many) tumors (oma: Greek meaning tumors) when injected into mice. Polyomaviruses have been found in mammals and birds. The genome sequences of 30 polyomaviruses have been deposited in GenBank, including more than 10 disinct viruses infecting humans (Figure 1.1) (*Van Ghelue et al. 2012*).

The first Human polyomaviruses, BK and JC, named using the affected patients' initials, were isolated in 1971 from the urine of a kidney transplant recipient and from the brain of a Hodgkin lymphoma patient, respectively (*Gardner et al. 1971; Padgett et al. 1971*). Others new viruses were found using DNA sequencing techniques. In 2007, the Karolinska Institute (KI) and Washington University (WU) polyomaviruses (KIPyV and WUPyV) were found in nasopharyngeal aspirates. In 2008, the Merkel cell polyomavirus (MCPyV) was discovered in Merkel cell carcinoma transcriptomes (*Feng et al. 2008*). HPyV-6 and HPyV-7 were found in skin swabs of healthy individuals in 2010 (*Schowalter et al. 2010*). In the same year, Trichodysplasia spinulosa (TS) associated polyomavirus (TSPyV) was found in a patient with the rare skin disease TS (*Van der Meijden et al. 2010*). To date, the latest HPyVs described are HPyV-9, and HPyV-10 which were found in the serum of a kidney transplant patient (*Scuda et al. 2011*) and in skin specimens of a patient with a rare genetic disorder known as myelokathexis syndrome (*Buck et al. 2012*). One more possible Human polyomavirus was identified in a child from Malawi and named Malawi polyomavirus (MWPyV) (*Siebrasse et al. 2012*). HpyV-10 and MWPyV are likely to be the same virus as sequence similarity of these is greater than 95% (*Buck et al. 2012*).

This close relationship is also seen in a phylogenetic tree of the polyomaviruses and is also indicates that MCPyV is the most distant family member (Figure 1.1).

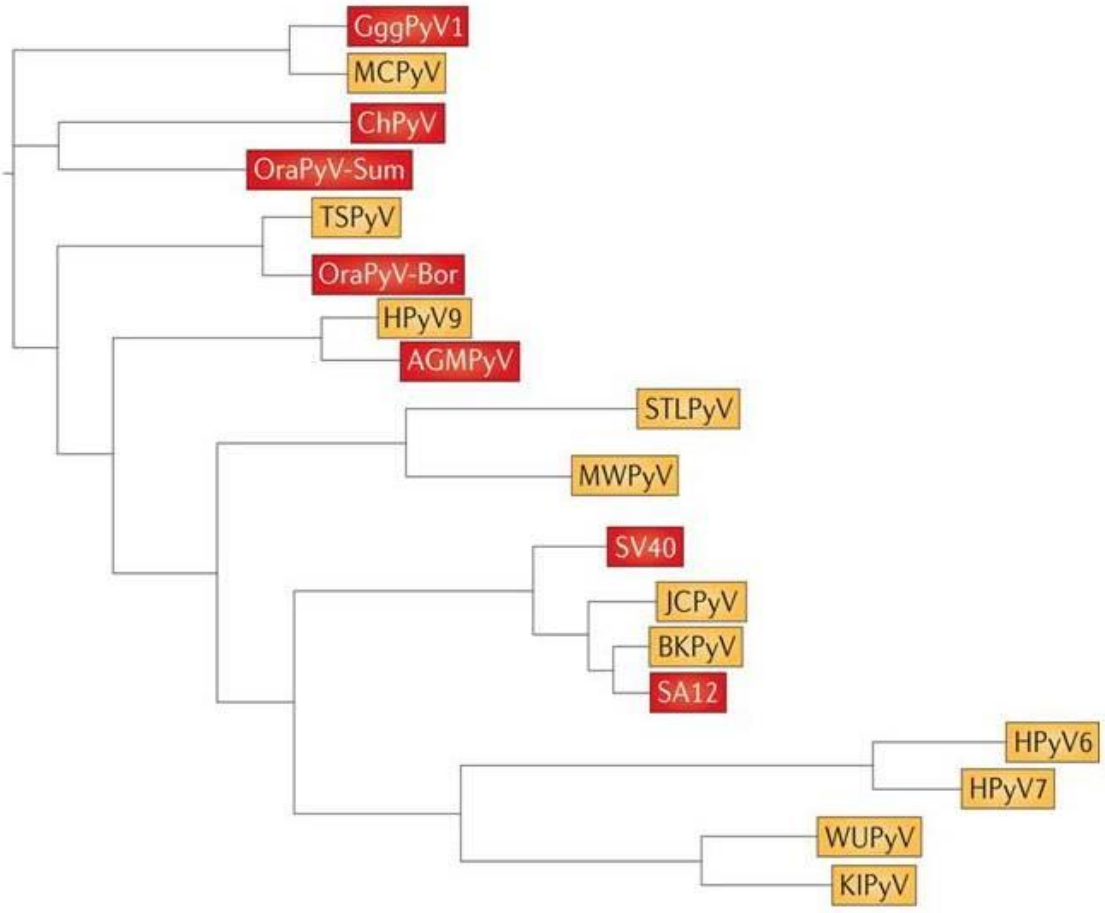


**Figure 1.1 Polyomaviridae phylogrnetic tree including 11 HpyVs.** In yellow are shown viruses identified from human isolates, and viruses identified from primate isolates are shown in red. This simplified tree was build using the relationships between the amino acid sequences of human and primate polyomavirus large T antigen and capsid protein VP1 of each species. Sequences were then aligned using multiple alignment programs. (DeCaprio & Garcea 2013)

**Figure 1.2** Structure of the polyomavirus capsid. Adopted from *Cann 2001*.

### 1.4.2 Morphology, genomic arrangement and viral proteins

The polyomaviruses are non-enveloped small viruses with a circular double-stranded DNA (dsDNA) genome of ~5000 base pairs. The genome is packaged in an icosahedral (T=7 symmetry) capsid of approximately 40-45 nanometers in diameter (Figure 1.2). Capsids are composed of 72 pentameric capsomeres of the VP1 protein, which is capable of self-assembly into a closed icosahedron; (*Salunke et al. 1986*) with each VP1 pentamer associated with one of the other two capsid proteins, VP2 or VP3 (*DeCaprio et al. 2013*). The MCPyV capsid consists of the structural proteins VP1 and VP2 in a ratio of 5:2, the VP3 protein, is not incorporated into MCPyV capsids but it is found in other polyomaviruses. Polyomavirus genomes are divided into two transcriptional regions called the early (ER) and the late region (LR) encoded on opposite strands (Figure 1.3). The early region usually codes for two proteins, the Large T antigen (LTAg) and the Small T antigen (sTAg). LTAg is a multifunctional nuclear phospho-protein with distinct roles in promoting viral DNA replication by forming a complex with cellular replication proteins, unwinding the viral genome and stimulating cell-cycle advancement into S- phase. In order to stimulate S-phase entry, LTAg inactivates both the p53 and the retinoblastoma (pRB) tumor suppressor pathways (*Hermannstadter et al. 2009; Kazem et al. 2014*). LTAg-

induced cell-cycle progression is the principal contributor to oncogenic transformation, because the expression of LTAg alone is sufficient to cause tumor formation in many systems (*Cheng et al. 2009*). The sTAg stimulates viral DNA replication and the sTAg C-terminus binds to and deregulates the PP2A phosphatase (*Sullivan et al. 2005*). Without sTAg, polyomaviruses are viable, but grow more slowly and less productively.

The late region (LR) contains the three capsid proteins VP1, VP2, and VP3 (*Decaprio et al. 2013*). Avian polyomaviruses contain a VP4 capsid protein (*Johne et al. 2007*), and some mammalian polyomaviruses produce an agnoprotein that is involved in transcription, virus maturation and release. SV40 encodes a 17 kT protein that is produced by alternative splicing of the LTAg transcript (*Zerrahn et al. 1993*) (Figure 1.4). Each region is transcribed by the host cell's RNA polymerase II, as a single pre-messenger RNA containing multiple genes. These two regions are separated by a non-coding regulatory region (NCCR) containing the origin of replication (ori) and binding sites for transcription factors (Figure 1.3).

### 1.4.3 Simian Virus 40

The Simian 40 virus (SV40), also called the vacuolating virus of the monkey, is a polyomavirus found in monkeys (Macaques Rhesus), and as a zoonotic infection in humans (*Shah 2004*). SV40 infection has been shown to transform tissue culture cells and cause tumors in laboratory animals. The virus was first described in 1960, in a culture of monkey kidney cells used to produce the polio vaccine (*Sweet et al. 1960*). This vaccine was administered to over 100 million people from 1955 to 1963 and the possibility that SV40 causes human diseases, especially cancer, has been the subject of debate ever since. For example, it has been described that SV40 is present in mesotheliomas in humans (*Carbone et al. 1997*), but fortunately, an important role of this virus in human tumors has not been established.

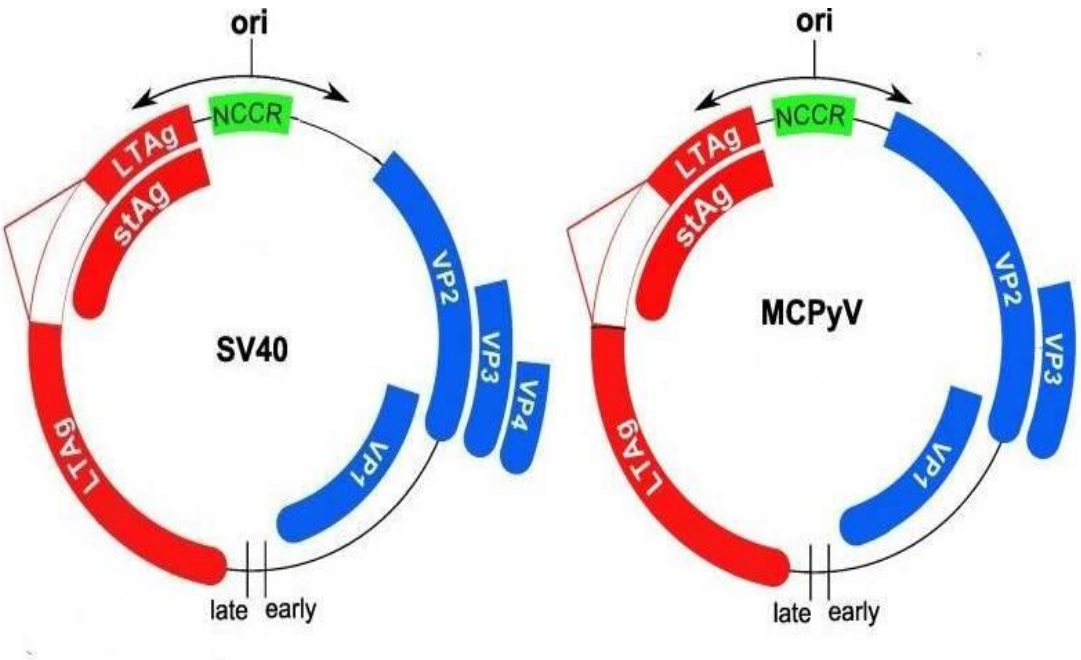


**Figure 1.3 SV40 and MPyV genome.**
The genomes of SV40 (5,243 bp) NC_001669 and MPyV (5,297 bp) NC_001515 are outlined. They are divided into an early region that encodes the T (TAgs) antigens (shown in red) and in the late region that encodes the capsid VP1- 4 proteins (shown in blue). The non-coding regulatory region (NCRR) separates the two regions (early and late). Several open reading frames are generated by alternating splicing. The complete genome sequences were obtained from the NCBI database (NC_001669-SV40 and NC_001515-MPyV) (modified from Lagatie O et al. 2013).

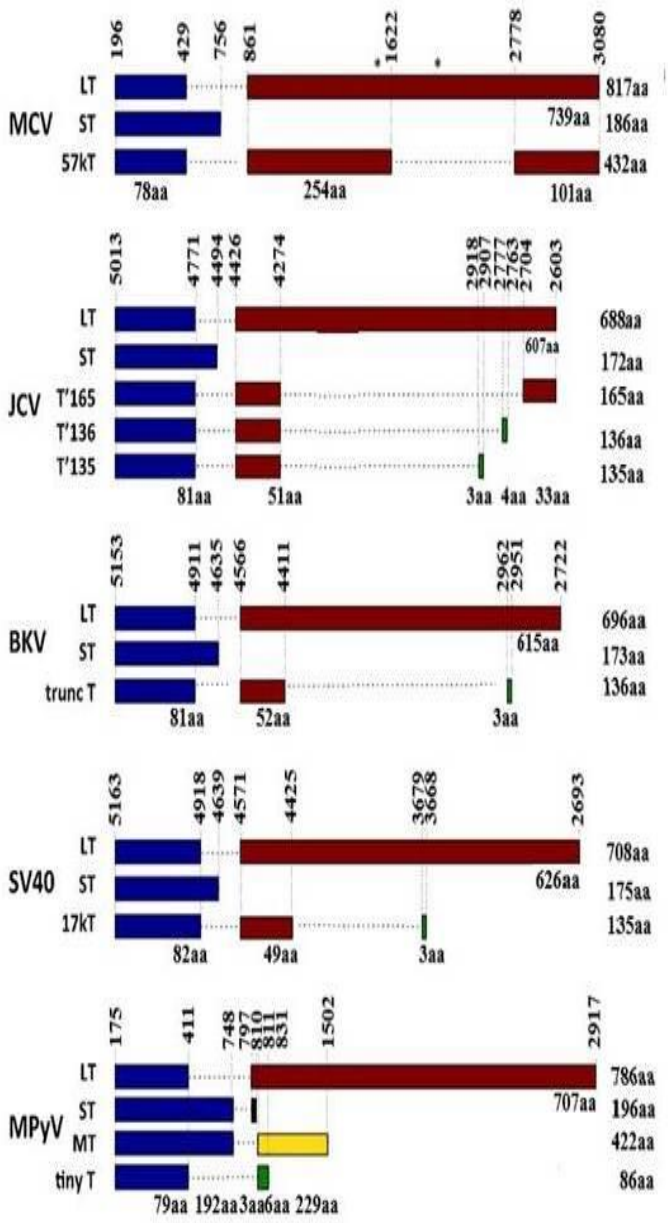


**Figure 1.4 Splicing patterns of various polyomavirus T antigens**

The MCPyV splicing patterns are compared to JCV, BKV, SV40 and MPyV. With different colors are represent different reading frames and the dotted lines represent introns. The nucleotide positions and amino acid (aa) residue lengths of the different proteins are also shown. The N-terminus of each T antigen is shared (exon 1, range = 78-82 aa), but the C-terminus is most often unique (except 57kT and T'165). The asterisks on MCPyV LTAg reveal the premature stop codons found in truncated LTAg's (350 and 339 prototypes in that order respectively). (Modified from Reety Arora, Thesis Submitted for the PhD degree, University of Pittsburgh, USA 2012).

### 1.4.4 Viral life cycle

The polyomavirus life cycle begins with the interaction of the VP1 capsid proteins with sialic acid or other ganglioside receptors. Ganglioside GM1 is the best characterized

receptor for SV40, GD1a and GT1b for MPyV, GD1b and GT1b for BKV, GT1b and the serotonin receptor 5HT2AR for JCV and GT1b and heparin sulphate, a glycosaminoglycan, for MCPyV (*Tsai et al. 2003; Low et al. 2006; Elphick et al. 2004; Erickson et al. 2009*). Gangliosides are components of the plasma membrane that comprise glycosphingolipids with one or more sialic acids. Whenever the virus binds to the receptor, the initial phase of the life cycle proceeds with internalization of the virus through caveole, or clathrin-dependent endocytosis (*Eash et al. 2006*). Cellular factors in the lipid bilayer of the internalized vessicle allow for the release of the viral genome into the cytoplasm. Viral DNA passes into the nucleus where transcription factors are recruited to induce transcription of the early region. This results in the expression of LTAg and sTAg which promotes entry of the infected cells into S phase, where LTAg recruits cellular DNA replication factors and initiates DNA replication of the viral genome from the origin in the NCRR (*Simmons, 2000*). The start of viral replication leads to transition into the late phase of the viral life cycle. Viral DNA replication progresses bidirectionally on the circular genome, involving leading and lagging strands. When the two-replication forks meet, replication terminates (*Fanning et al. 2009*). LTAg activates transcription from the late gene promoter and represses the early promoter. This results in the expression of the capsid proteins, which then assemble into capsids and encapsulate the viral genome. Virus is released by cell lysis and the process can begin again. An SV40 infection cycle takes 3-4 days in permissive cells (such as African green monkey cells) in vitro, eventually resulting in cell death and the production of ~300 infectious progeny virions per infected cell (*Pipas 2009*) (Figure 1.5).

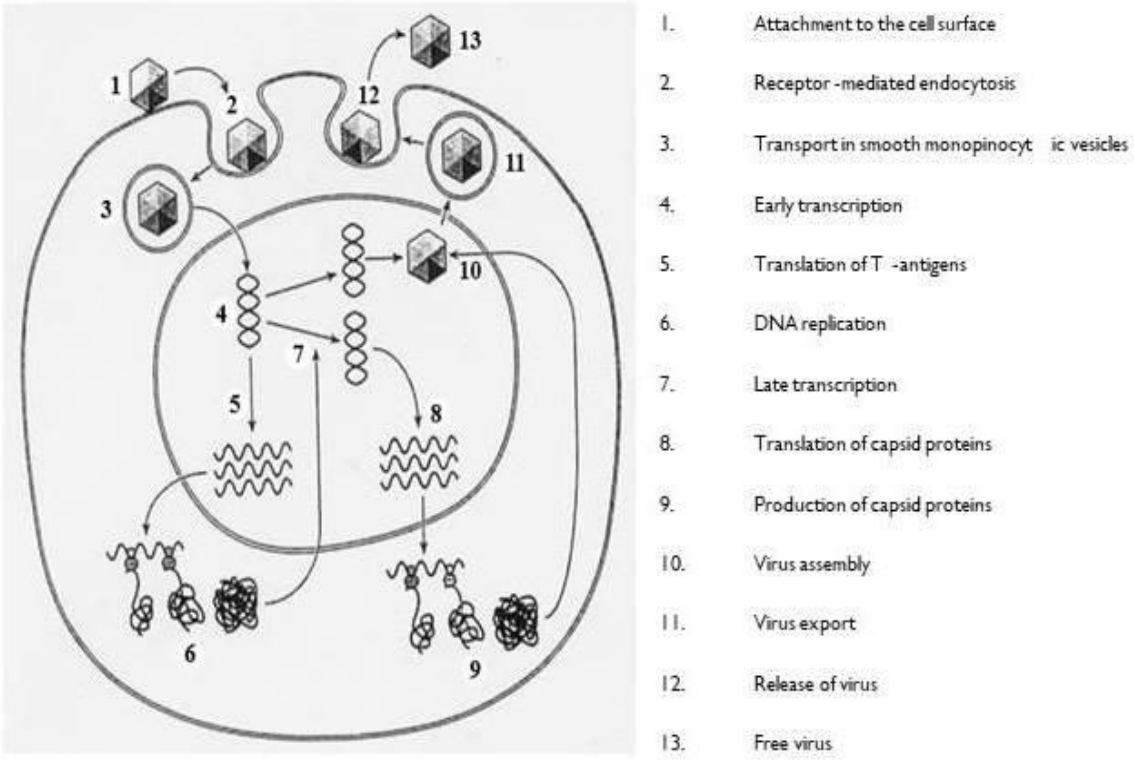


**Figure 1.5** Viral cell entry and reproduction (from Cole et al. 2001).

In human systems, only the life cycles of JCPyV and BKPyV have been well studied. During the lytic phase, the virus attaches onto the cell surface via receptors such as gangliosids and the serotonin receptor (*Elphick et al. 2004; Erickson et al. 2009; Low et al. 2006*). The virus is trafficked through the caveolae and the endoplasmatic reticulum (RE) to the nucleus, where it is uncoated and the early region is transcribed. Caveolae are dedicated lipid rafts that form 50-70 nm flask-shaped invaginations of the plasma membrane. The virion is presumably internalized in the caveolae on binding to host receptors. In the case of JCPyV this process is clathrin-dependent and the clathrin coated vesicles mature into late endosomes. The maturation is accompanied by a pH acidification down to pH 6.0, which promotes uncoating of the viral genome (*Eash et al. 2006*).

After transcription and translation, LTAg begins to promote DNA replication of the viral genome. The shift to late viral protein expression is not fully clear, but likely involves

transcriptional activation of the late promoter and repression of the early promoter by LTAg (*Gjoerup et al. 2010*). Capsid proteins assemble around the replicated genomes to form new mature virions, which are released by mechanisms that include cell lysis (*Atkin et al. 2009*).

The cell-transforming properties have been studied using the model polyomaviruses SV40 and the murine polyomavirus (MPyV), both of which induce tumours in mice. Transformation is largely the result of a failed lytic infection, either because the host cell is not permissive for replication or because the virus is defective in replicative functions. This non-replicative viral DNA can integrate into the host genome randomly and typically infective virus cannot be isolated from tumour material (*Atkin et al. 2009*).

### 1.4.5 Human polyomaviruses.

So far nine human polyomaviruses have been identified (Table 2). The JC virus (JCPyV) and the BK virus (BKPyV), which take their names from the initials of their respective patients, were the first human polymaviruses to be discovered. They were isolated from cultures of diseased tissues of immunosupressed patients, JCPyV from brain tissue of a progressive multifocal leukoencephalopathy pateint and BKPyV from the urine of a patient with nephropathy and poor renal function (*Gardner et al. 1971; Padgett et al. 1971*). JCPyV has a limited tissue tropism and infects only kidney, bone marrow, oligodendrocytes and astrocytes (*Maginnis et al. 2009*). The researchers found that in animal models, JCPyV causes tumors in rodents and primates (*Houff et al. 1983; WT et al. 1978; Ohsumi et al. 1986; Ohsumi et al. 1985; Walker et al. 1973; Horie et al. 1989*). As with JCPyV, the expression of BKPyV early region (ER) also transforms mouse and hamster cells and immortalizes human cells (*Grossi et al. 1982; Portolani et al. 1978*). BKPyV inoculation of newborn mice, rats and hamsters causes various tumors including ependymoma, neuroblastoma, fibrosarcoma and osteosarcoma (*Tognon et al. 2003; Corallini et al. 1982*).

Based on these results, many studies investigated the link between JCPyV and BKPyV and various cancers (brain, colorectal and gastric), but an association between these viruses and any type of human cancer has not been made (*Maginnis et al. 2009; Tognon et al. 2003; Imperiale 2000; Jiang et al. 2009; Caldarelli-Stefano et al. 2000; Jung et al. 2008; Ricciardiello et al. 2000; Laghi et al. 1999; Ricciardiello et al. 2001; Murai et al. 2007; Rencic et al., 1996; Shin et al. 2006*). Both viruses are still common in the general population and maintain lifelong disease-free infection in immunocompetent individuals (*Kean et al. 2009*). Seroprevalence studies show an overall seroprevalence rate of 81-82% for BKPyV and 35-58% for JCPyV among healthy blood donors from the UK, Switzerland and the United States (*Kean et al. 2009; Knowles et al. 2003; Egli et al. 2009*). Seroconversion occurs early in childhood and dampens in elderly individuals for BKPyV but increases steadily up to ~50% in 60-69 aged individuals for JCPyV (*Knowles et al. 2003*).

In 2007 two more closely related human polyomaviruses were found by the Karolinska Institute (KIPyV) and the Washington University (WIPyV) polyomavirus. Both were isolated from children with acute respiratory tract infections by constructing cDNA libraries, deep sequencing, and BLASTing against NCBI databases for non-human sequences (*Allander et al. 2007; Gaynor et al. 2007*). Present experimental proof does not support causation of any respiratory disease and no other link between illnes and symptomatic infection has been found (*Wattier et al. 2008; Zhuang et al. 2010; Ren et al. 2008; Jartti et al. 2012*). Both viruses show a wide geographic distribution and estimates of seroprevalence range widely from 1-65% among the general healthy population (*Kean et al. 2009; Venter et al. 2009; Bialasiewicz et al. 2010; Bialasiewicz et al. 2007; Dang et al. 2011; Furuse et al. 2010; Zhao et al. 2010*). Three more polyomaviruses were discovered recently by using a method called rolling circle amplification (RCA). RCA is a random primer extension technique that uses a DNA-dependent polymerase that preferentially amplifies circular DNA and can displace an annealed DNA strand (*Johne et al. 2009*). During a search for MCPyV on skin surfaces using RCA, Schowalter et al. serendepitiously

discovered Human polyomavirus 6 and 7 (HPyV6 and HPyV7) from the skin of healthy humans (*Schowalter et al. 2010*). Subsequent studies failed to reveal any link between HPyV6 or HPyV7 and basal cell carcinomas, melanomas, and cutaneous B and T cell lymphomas (*Schrama et al. 2012*). The HPyV6 and HPyV7 are most similar to WUPyV and KIPyV and are classified into the WuKipolyomaviruses group in the new ICTV taxonomical classification (*Johne et al. 2011*).

**Table 1.2**: **Human Polyomaviruses** (*From Chang & Moore, Annual Reviews Pathology 2011*)

| Virus | Year identified | Method of identification | Prevalence in human population | Disease associations | Genome size | GenBank | Reference |
|---|---|---|---|---|---|---|---|
| BK virus (BKV) | 1971 | Culture isolation from urine of renal transplant recipient | >90% of adults | Cystitis, polyomavirus-associated nephropathies, ureteral stenosis | 5153bp | NC_001538 | Gardner *et al*., Lancet, 1971 |
| JC virus (JCV) | 1971 | Culture isolation from brain tissue with progressive multifocal leukoencephalopathy | >70% of adults | Progressive multifocal leukoencephalopathy | 5130bp | NC_001699 | Padgett *et al*., Lancet, 1971 |
| Karolinska Institute polyomaviurs (KIV) | 2007 | Deep sequencing of DNAase-treated respiratory fluids | 55–70% of adults | Not defined | 5040bp | NC_009238 | Allander *et al*., JVI, 2007 |
| Washington University polyomavirus (WUV) | 2007 | Deep sequencing of DNAase- treated respiratory fluids from children with upper respiratory infections | 69–80% of adults | Not defined | 5229bp | NC_009539 | Gaynor *et al*., PLoS Pathogens, 2007 |
| Merkel cell polyomavirus (MCV) | 2008 | Digital transcriptome subtraction of Merkel cell carcinoma tissue | 42–70% of adults | Merkel cell carcinoma | 5387bp | NC_010277 | Feng *et al*., Science, 2008 |
| Human Polyomavirus 6 (HPyV6) | 2010 | Rolling-circle amplification of skin and hair samples | Not defined | Not defined | 4926bp | NC_014406 | Schowalter *et al*., Cell host&microbe, 2010 |
| Human Polyomavirus 7 (HPyV7) | 2010 | Rolling-circle amplification of skin and hair samples | Not defined | Not defined | 4952bp | NC_014407 | Schowalter *et al*., Cell host&microbe, 2010 |
| Trichodysplasia spinulosum polyomavirus (TSV) | 2010 | Rolling-circle amplification of trichodysplasia spinulosum lesion in transplant recipient | Not defined | Transplant-associated trichodysplasia spinulosum | 5232bp | NC_014361 | Van der Meijden *et al*., PLoS Pathogens, 2010 |
| Human Polyomavirus 9 (HPyV9) | 2011 | Consensus PCR and deep sequencing | Not defined | Not defined | 5026bp | NC_015150 | Scuda *et al*., JVI, 2011 |

An eighth human polyomavirus was isolated in 2010 from virus-associated trichodysplasia spinulosum (VATS), a rare type of dysplasia seen only in transplant and immunosuppressed patients. Based on previous ultrastructural detection of polyomavirus like particles in VATS (*Wyatt et al. 2005*) and its close association with immunosuppression, van der Meijden and collaborators applied RCA to VATS tissue and found trichodysplasia spinulosum polyomavirus (TSaPyV) (*Van der Meijden et al. 2010*). TSaPyV exhibits abundant expression of viral proteins only in the affected hair follicles, suggesting a causative role in trichodysplasia spinulosa disease (*Tan et al. 2011; Kazem, et al. 2012*). In 2011, HPyV9 was identified from the serum of an immunosuppressed kidney transplant patient by using consensus PCR (*Scuda et al. 2011*). Most of these recently discovered human polyomaviruses appear to be previously unrecognized infections with a high seroprevalence in the general population. With improvement of detection techniques and assays the subfamily of human polyomaviruses is likely to expand with new polyomaviruses being linked to disease as well as being part of the normal human microbial flora.

### 1.4.6 SV40 Tag - classic models for studying cancer

The Polyomaviruses, and in particularly SV40, have been used as model systems for understanding the basic cellular biology relating to cellular immortalization and oncogenic transformation. Since they were discovered, studies on Polyomaviruses and their target pathways have lead to critical insights into key biological processes. These viruses rely on the multifunctional T antigen proteins and the cellular machinery to carry out various functions in their life cycle (*Pipas 2009; Pipas 1992*).The TAgs start by reprogramming the host cell cycle to induce progression into the S-phase, creating an optimal environment for viral replication. This is especially important for SV40 infection in its natural host

rhesus macaque, because SV40 typically infects non-cycling, growth-arrested, epithelial cells of the kidney (*Ahuja et al. 2005*).

Changes in cell morphology, anchorage independent growth, loss of density-dependent growth inhibition, a decrease in the dependence on serum growth factors, and the ability to form tumors in animal hosts are indicators that distinguish a tumor cell from a normal cell (*Raptis et al. 2001; Hanahan et al. 2011*). Multiple assays have been developed to study the transformation phenotype induced by SV40 and other polyomaviruses. In each of these assays, cells are cultured under conditions of selective growth pressure so that only the transformed cells are able to survive and proliferate, whereas the normal cells die or enter senescence. These form the basis by which SV40 and other polyomaviruses ability to transform cells have been assessed (*Raptis et al. 2001*).

### 1.4.7 Large tumor antigen (LTAg)

SV40 TAgs target and modify different cellular pathways that are important for preparing the cellular environment for DNA replication and these pathways have also proven to be important for the ability of TAgs to transform cells.

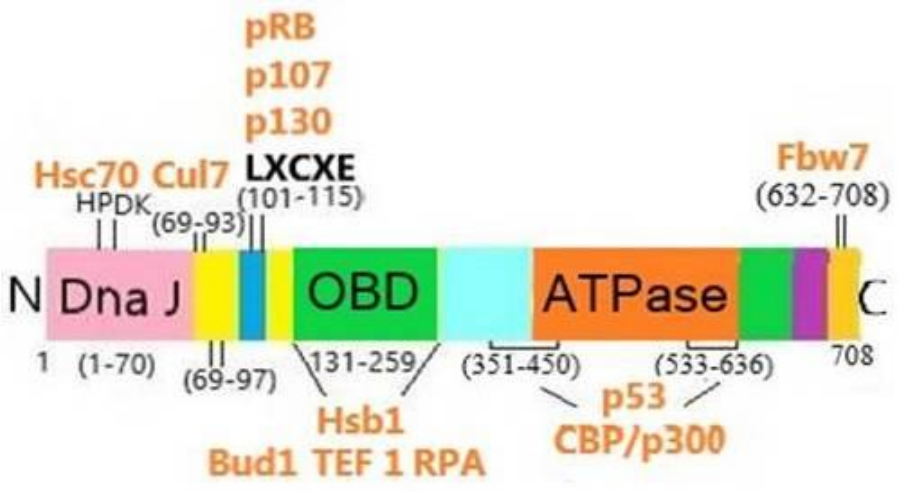


**Figure 1.6** Schematic of binding domains and interacting partners of SV40 Large T antigen. (*from Gjoerup and Chang, Adv Cancer Res 2010*).

The nuclear phosphoprotein LTAg is multifunctional, which is seen in its modular structure. LTAg has discrete regions corresponding to the binding domains of various interaction partners. Some of these interaction partners include pRB, p53, p107, p130, Hsc70, Cul7, p300/CBP, and FBW7 (Figure 1.6) (*Sullivan et al. 2002; Ahujaet al. 2004; Ali et al. 2004; Cotsiki et al. 2004; Fei et al. 1995; Srinivasan et al. 1997; Stubdal et al. 1997; Stubdal et al. 1996; Yaciuk et al. 1991; Lill et al. 1997; DeCaprio et al. 1988; Lane et al. 1979; Linzer et al. 1979*). Two of the most important tumor suppressor genes, p53 and the Retinoblastoma protein (pRB), were either discovered or functionally dissected as a result of their interaction with SV40 LTAg (*Dilworth 2002; Pipas 1992; Butel et al. 1999*).

### 1.4.8 Interaction with pRB family of proteins

Today, we know that most tumor viruses target memberts of the pRB pathway for inactivation. Polyomavirus LTAgs share a highly conserved LXCXE motif, which binds to RB family proteins (*DeCaprio et al. 1988; DeCaprio 2009; Chen et al. 1990; Dyson et al. 1989; Munger et al. 1989; Whyte et al. 1988*). The majority of cancers (viral and non-viral) contain alterations in the regulation of the pRB pathway (*Burkhart, et al. 2008*). This shows a common mechanism shared between viruses in targeting specific cellular proteins and proves the importance of this protein family in tumorigenesis.

Knudson and collaborators first identified the pRb gene in 1971. They performed a genetic study demonstrating that childhood retinoblastoma had a hereditary element, and concluded that two separate mutation events were responsible for development of the disease. In hereditary retinoblastoma, the child inherited a mutated gene and obtained a second mutation in a somatic cell. In contrast, two independent mutations in the same somatic cell (later found to be two alleles of the same gene (*Godbout et al. 1983; Comings 1973*) led to the development of sporadic retinoblastoma (*Knudson Jr. 1971*). The gene was then mapped to chromosome 13q14 and cloned. The gene encodes for a nuclear

phosphoprotein of 110kDa (*Lee et al. 1987*). The fact that pRB undergoes phosphorylation in a cell cycle-dependent manner provided an important insight into its function. pRb protein is hypo-phosphorylated, in the G0 phase of quiescent or differentiated non-cycling cells and in the G1 phase of cycling cells. In this state, pRb binds to E2F transcription factors and inhibits the transcriptional activity of genes having E2F-dependent regulatory elements. pRb is hyper- phosphorylated by cyclin dependent kinases, and phosphorylated pRb then releases the E2Fs, allowing them to stimulate the transcription of their target genes, which normally occurs as cells enter the S-phase of the cell cycle. The products of these genes then usher the cell from late G1-phase into S-phase. Therefore, the hyposphosphorylated form of pRb functions as a tumor suppressor by preventing cells from entering S phase.

pRb has been shown to mediate the transcriptional regulation of numerous target genes and has been reported to bind to over a hundred protein partners (*Morris et al. 2001*). The various cellular functions regulated by pRb include temporary and permanent cell cycle arrest, differentiation, genome stability and apoptosis.

The first proof of a viral oncogene targeting a known tumor suppressor was the discovery that pRB is a target of the adenovirus E1A protein (*Whyte et al. 1988*). Subsequencet to this, Decaprio and collaborators showed that SV40 LTAg binds pRB and more intriguingly LXCXE mutants that are unable to bind pRB, failed to transform cells in a variety of cell types and assay systems (*DeCaprio 2009; DeCaprio et al. 1988*). To activate cell-cycle-regulated genes, thus driving the cell into S-phase and increasing cell proliferation, DNA viruses must bind and sequester the hypophosphorylated form of pRb and free E2F transcription factors (Figure 1.7) (*Reety Arora, Thesis Submitted for the PhD degree, University of Pittsburgh, USA 2012*). The Retinoblastoma protein is composed of two domains, A and B, forming a pocket crucial for tumor suppression and is thus often referred to as a pocket protein (*Burkhart et al. 2008*). This region constitutes the binding site for the LXCXE motif and mutations in human malignancies usually map to this region. Despite,

the binding sites for both viral T antigens and E2F mapping to the pocket domain, they are distinct and pRB can bind both simultaneously.

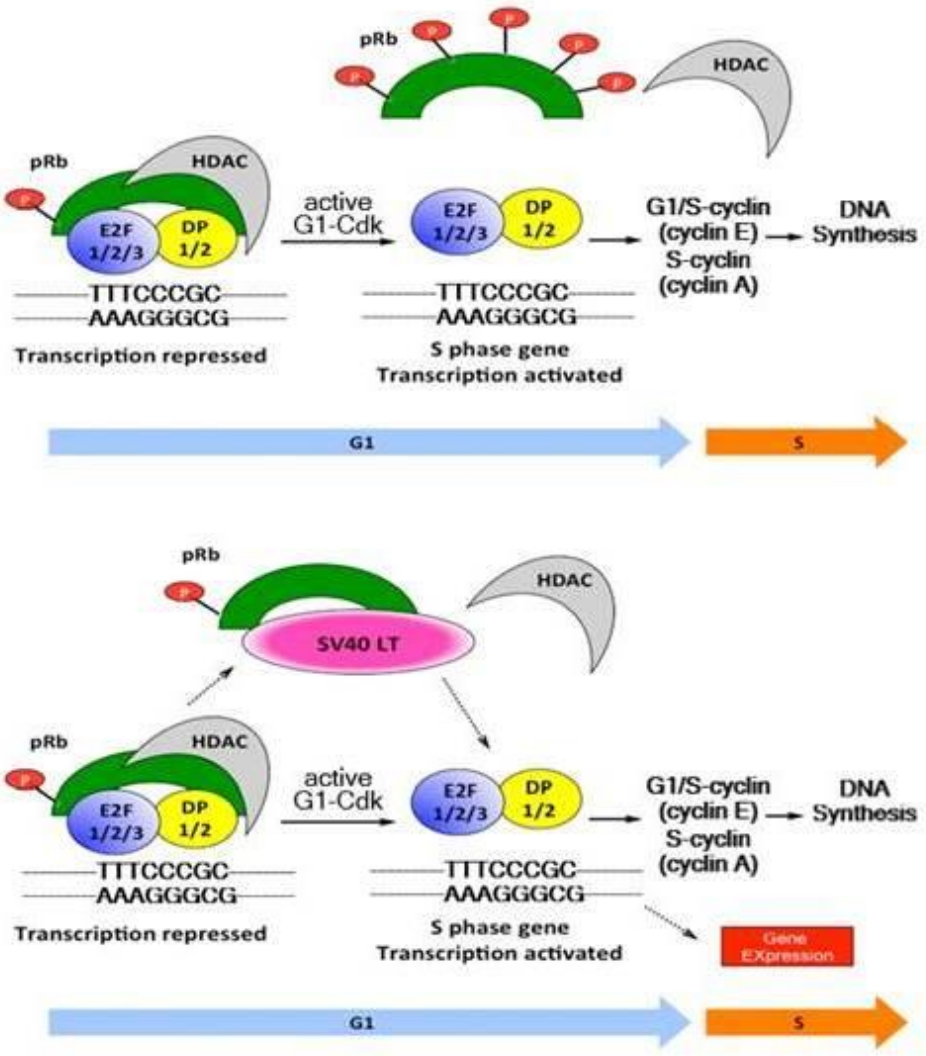


**Figure 1.7** Model for SV40 LT mediated sequesteration of Rb and subsequent S phase related gene expression. Hypo phosphorylated pRb (green) binds to the transcription factor E2F (which bound to a DP1 protein (blue and yellow)) and prevents transcription of several S phase related genes by attracting histone deacetylase (gray) enzymes inhibiting them. When the cell enters the S phase in normal cells, pRb becomes hyper phosphorylated and is released from the complex, releaseing E2F to transactivate and regulate gene expression (top). SV40 LT binds and sequesters pRb and is able release E2F independent of the cell cycle phase. This helps activate cell cycle S phase related genes and progression (bottom). (Modified from Reety Arora, Thesis Submitted for the PhD degree, University of Pittsburgh, USA 2012).

Additional pocket proteins have been identified, such as p107 and p130 that also bind to the LXCXE domain of SV40 LTAg (*Dyson et al. 1989; Ewen et al. 1989; Hannon et.al. 1993; Mayol et al. 1993*). There are a number of properties that distinguish the three proteins and there is a central spacer domain in p107 and p130 that binds to CDK2: cyclin complexes and different Rb family members are responsible for binding to different E2F family members. For example, pRB targets E2F1-3 (the "activating" E2Fs), in contrast p107/p130 targets E2F4/5 (the "repressing" E2Fs) (*DeCaprio 2009*).

The importance of the LTAg HPDKGG/J domain in the inactivation of pRb was revealed by studies of SV40 LTAg. The model is that LTAg binds to the hypo-phosphorylated form of pRb and then recruits Hsc70 via this HPDKGG/J domain. The Rb-E2F complex first binds to LTAg and then it interacts with the substrate-binding domain of Hsc70. ATP hydrolysis provides energy to Hsc70 that changes the conformation of the bound pRB, resulting in the release of E2F. (*Kim et al. 2001; Zalvide et al. 1998*).

### 1.4.9 Interaction with p53

The p53 tumor suppressor protein was discovered in 1979 as a cellular protein that binds to SV40 LTAg, both in SV40 transformed cells and infected cells (*Lane et al. 1979; Linzer et al. 1979*). It is now recognized that p53 is one of the most commonly mutated tumor suppressors and is found to be mutated in ~50% of human cancers (Hollstein et al. 1994). p53 is a DNA damage and cellular stress responsive transcription factor that regulates DNA synthesis and repair, induces cell cycle arrest, activates apoptosis and cellular senescence and is also known as the "guardian of the genome" (*Lane 1992*). p53 is inactivated by most DNA viruses. Two well-known examples are adenovirus E1B 55k which binds and inactivates p53; together with E4orf6 that targets p53 for degradation, and human papillomavirus E6 protein, which also targets p53 for proteasomal degradation (*Yew et al. 1992; Scheffner et al. 1990*).

Within SV40 LTAg, the binding site of p53 is bipartite and is found at residues 351-450 and 533-626 (*Kierstead et al. 1993*). The co-crystal structure of the LTAg ATPase domain bound to p53 revealed a region within the core DNA binding domain of p53 as interacting with LTAg (*Lilyestrom et al. 2006*). The interaction between T antigen and p53 blocks p53- dependent gene expression by blocking p53 from binding to DNA (*Lilyestrom et al. 2006; Bargonetti, et al. 1992*). The ability of LTAg to bind p53 is not sufficient in many cases for transformation (*Kierstead et al. 1993; Conzen et al. 1995*). While one of the results of the interaction between LTAg and p53 is the prevention of a DNA damage response, the effects of this interaction are now known to be more complex. It is becoming clear that the effects of the LTAg and p53 interaction are not completely understood. Some studies found that the interaction between LTAg and p53 also blocked LTAg replicative functions. Studies of growth phenotypes in the presence or absence of p53, or p53 mutants in assays of LTAg transformation led to the idea that LTAg stabilizes p53 and may induce it to acquire an unknown function (*Hermannstadter et al. 2009; Tiemann et al. 1994; Deppert et al. 1989*). The finding that wild-type p53 promotes tumor formation in LTAg transgenic mice is consistent with a gain of function phenotype (*Herzig et al. 1999*). One explanation may be that LTAg stabilizes p53 in order to gain access to p300/CBP, which then acts on promoters, or other LTAg bound proteins (*Borger et al. 2006*). p53 mutants seen in cancers sometimes show a similar gain of function mutation (*Brosh et al. 2009; Dittmer et al. 1993*) and certain mutations in p53 may turn it into an oncogene.

### 1.4.10 Other interactions DnaJ Domain

A common region shared in LTAg and sTAg, the HPDKGG motif, has been implicated in transformation (*Campbell et al. 1997*). This N terminal region of the two T antigens exhibits sequence and structural homology to DnaJ (*Campbell et al. 1997*). The chaperone DnaJ, also known as Hsp40, recruits other heat shock family proteins, the DnaK family members, for protein folding and protein transport. LTAg DnaJ domains bind to the constitutively expressed Hsc70 chaperone and stimulates its ATPase activity (*Sullivan et al. 2002; Srinivasan et al. 1997; Campbell et al. 1997*). The D44N and H42Q mutants break up this interaction and have been used to show the importance of the T antigen DnaJ domain in viral replication and in oncogenic transformation (by functional inactivation of pRB family members) (*Sullivan et al. 2002; Srinivasan et al. 1997; Campbell et al. 1997; Stubdal et al. 1997; Zalvide et al. 1998; Stubdal et al. 1996*). The DnaJ domain's contribution to LTAg mediated cellular transformation is limited to a subset of phenotypes. The D44N mutant affects the ability of LTAg to promote anchorage independent growth. (*Stubdal et al. 1997*) and the DnaJ domain is required, along with the LXCXE motif, to disrupt the pRb/p107/p130 and E2F complexes and to promote growth in low serum, as well as allowing growth to a high saturation density (*Stubdal et al. 1997; Sullivan et al. 2000; Zalvide et al. 1998*).

### 1.4.11 p300/CBP and p400

Cyclic-AMP Response Element Binding (CREB)-protein and p300 are large scaffold proteins involved in transcriptional regulation. They act as co-activators, in part via their intrinsic histone acetylase (HAT) activity and mediate a number of biological processes, including cell growth and transformation and are thus considered tumor suppressors (*Iyer*

*et al. 2004*). Adenovirus E1A was first shown to bind p300/CBP and this binding was linked to adenovirus transformation and cellular DNA synthesis (*Howe et al. 1990; Wang et al. 1993*). Yaciuk and collaborators showed that pRB binding-deficient SV40 LTAg, but not DnaJ domain mutants, complemented p300/CBP binding- defective mutants of E1A to re-estabilish transformation in primary baby rat kidney cells (*Yaciuk et al. 1991*). While early studies suggested LTAg's CR1-like sequence as a binding site for p300/CBP, it was subsequently demonstrated that LTAg C terminal residues 251- 708 are responsible for the interaction (*Lill et al. 1997; Eckner et al. 1996*). Importantly, it was found that p53 supported the binding of p300/CBP in a cooperative manner. The LTAg-CBP interaction results in the acetylation of LTAg on K697 and this acetylation also required p53 (*Borger et al. 2006; Poulin et al. 2004*). Work based on structure-guided mutational analysis of LTAg, indicated a direct binding of LTAg and p300/CBP proteins that is essential for oncogenic transformation (*Ahuja et al. 2009*). SV40 LTAg also binds to the p400 protein across its C terminal 251-708 segment, but the meaning of this interaction in LTAg-mediated transformation is not clear (*Lill 1997; Barbeau et al. 1994*). p400 belongs to the SWI2/SNF2 family of chromatin remodeling proteins, it also interacts with a c-myc binding protein called TRRAP and is likely to be involved in the p53-p21 cellular senescence pathway and p53-dependent apoptosis (*Fuchs et al. 2001; Samuelson et al. 2005; Chan et al. 2005*).

### 1.4.12 Small tumor antigen (sTAg)

The small tumor antigen (sTAg) is a protein expressed early in the infectious cycle and is usually not essential for viral proliferation. The sTAg protein is 174 amino acids long and its gene overlaps with the gene for LTAg. The two T antigens share the first 82 amino acids, which includes the DnaJ-like domain (*Srinivasan et al. 1997*). Although LTAg is a nuclear protein, sTAg is found both in the nucleus and cytoplasm. The C-terminus of

sTAg has two CXCXXC clusters that bind Zinc and confer conformational stability (figure 1.8) (*Turk et al. 1993*). sTAg is known to interact with host cell proteins, including phosphatase 2A (PP2A), and may activate the expression of cellular proteins associated with the cell cycle transition to S-phase. In SV40, sTAg is unable to induce neoplastic transformation in the host cell, but its presence may increase the transforming efficiency of LTAg. In Merkel cell polyomavirus, sTAg seem to be important for replication and appears to be the principle oncoprotein in MCPyV.

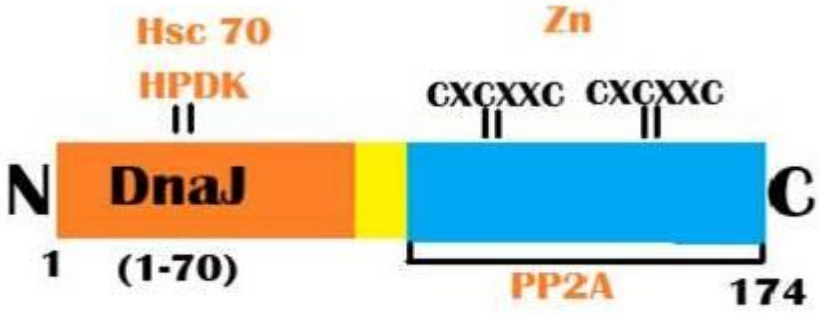


**Figure 1.8** Schematic of binding domains and interacting partners of SV40 Small T antigen. (*from Gjoerup & Chang, Adv Cancer Res 2010*)

### 1.4.13 PP2A

The heterotrimeric protein phosphatase or Protein phosphatase 2 (PP2), known as PP2A, is a ubiquitously enzyme expressed in eukaryotic cells. It is a serine/threonine specific phosphatase and has a large substrate specificity and diverse cellular functions. PP2A is composed of an A scaffold subunit, a B regulatory subunit and a C catalytic subunit. There are two different A subunits, two different C subunits and 17 known B subunits that can assemble together, in various combinations, into more than 100 different holoenzyme complexes (*Sablina et al. 2008; Sontag 2001*). Several oncogenic signaling molecules, such as Raf, MEK, and AKT, are PP2A targets. Since the replication of the polyomavirus

genome is based on the DNA replication mechanism of the host cell, the host cell must be in S phase in order to provide the necessary molecular machinery for replication of viral DNA. The viral proteins promote entry into the S phase of the host cell cycle and this function is mainly provided by LTAg, through its interactions with pRb and the p53 protein (*Topalis et al. 2013; An Ping et al. 2012*). The sTAg contributes to this process through its interaction with protein phosphatase 2A (PP2A). The functional role of sTAg changes among the polyomaviruses, for example in the SV40, sTAg has a small role in cellular transformation (*Khalili et al. 2008*). While in the Merkel cell poliomavirus, it appears to play a significant role in oncogenesis, a function performed primarily by LTAg in other polyomaviruses (*Tsang et al. 2016*).

## 1.5 Merkel Cell Carcinoma

### 1.5.1 Origin and pathology

Merkel cell carcinoma (MCC) is a rare and highly aggressive skin cancer, which, in most cases, is caused by the Merkel cell polyomavirus (MCPyV) (*Agelli et al. 2003; Hodgson 2005*). Initially named trabecular carcinoma of the skin, it was first described by Toker in 1972 (*Toker 1972*). MCC was thought to derive from mechanoreceptor Merkel cells located at the basal layer of the epidermis (Figure 1.9). The Merkel cells play a role in the sensory system of the skin (*Pearse 1980; Halata et al. 2003; Lucarz et al. 2007; Van Keymeulen et al. 2009; Haeberle et al. 2004; Maricich et al. 2009*). Most common sites of MCC occur in sun-exposed areas such as the head and neck, followed by the lower and upper extremities and the trunk region.

### 1.5.2 Risk factors and clinical features

The incidence of MCC, increases in elderly populations (median age = 65 years) (Heath et al. 2008) and in the immunosuppressed, for example following transplantation, immune-related cancers, or AIDS, are other recognized risk factors (*Agelli et al. 2010; Agelli et al. 2003*). MCC, like melanoma, shows a strong correlation to UV exposure (*Miller et al. 1999*). The majority of the patients with MCC are fair skinned and MCC typically occurs in sun exposed areas of the skin (*Agelli et al. 2003; Hodgson 2005; Allen et al. 2005*).

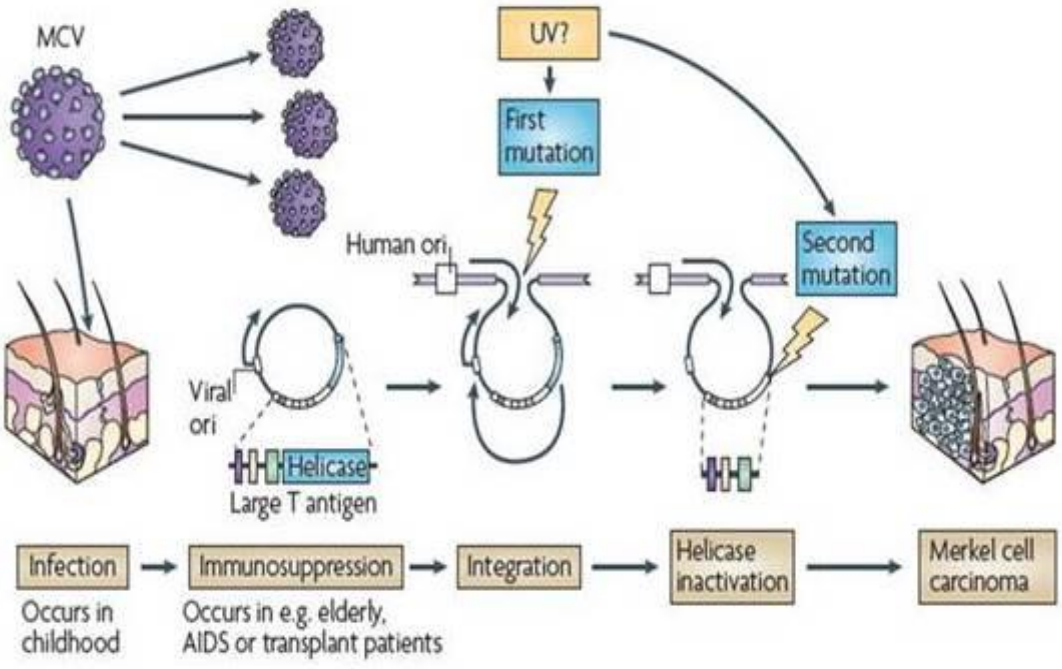


**Figure 1.9** Development of MCPyV-MCC. *Reprinted from Moore et al. 2012.*

### 1.5.3 Natural infection of HPyV and associated diseases

All described HPyV, including MCPyV, are highly prevalent in the human population and infection starts during infancy. Seroprevalence is measured by IgG antibodies specific to the major capsid protein VP1. The seroprevalence peaks at 98% for WUPyV, 92% for BKPyV, 80% for JCPyV, 67% for KIPyV, 69% for HPyV-6, 35% for HPyV-7, more than 60% for MCPyV, about 70% for TSPyV and 47% for HPyV-9 (*Chen et al. 2011; Faust et al. 2011; Kean et al. 2009; Knowles 2006; Neske et al. 2010; Van der Meijden et al. 2011; Viscidi et al. 2011; Trusch et al. 2012*).

Faecal-oral, oral and respiratory routes of transmission have been the suggested mechanisms of viral spread (*Gjoerup et al. 2010*) and this is supported by the finding that JCPyV and BKPyV can be found in sewage samples and rivers. DNA of HPyVs has been detected in tonsillar tissue, indicating a possible point of entry (*Gjoerup et al. 2010*). The mode of MCPyV transmission is unclear. Intrauterine transmission does not appear to occur, as no MCPyV DNA is detectable in miscarried or aborted fetuses (*Sadeghi et al. 2010*). However, it is clear that MCPyV infection occurs in early infancy (*Kean et al. 2009; Chen et al. 2011; Tolstov et al. 2009*). MCPyV DNA is common on the human skin (*Schowalter et al. 2010; Foulongne et al. 2010*). In a study of 60 environmental surface samples, 45 (75.0%) were positive for MCPyV DNA and in a few of these samples the viral DNA was even protected from DNase degradation, suggesting that it was viral DNA encapsidated inside infectious virus particles (*Foulongne et al. 2011*). As well as the skin, MCPyV DNA has also been found in the upper aerodigestive tract, in the digestive system and in the saliva, but was less frequently found in lung and genitourinary system samples (*Loyo et al. 2010*). MCPyV has also been found in the lower respiratory tract (*Babakir-Mina et al. 2010*) and on the tonsils (*Chen et al. 2011*). The age distribution of samples from immunocompetent or immunocompromised patients indicates that Merkel cell virus

DNA is more frequent in adults (8.5%) than in young children (0.6%). The notable age difference of MCPyV possibly reflects a major dissimilarity in the lifecycles of this virus (*Kantola et al. 2009*). MCPyV can also persist in inflammatory monocytes and is spread along monocyte migration routes (*Mertz et al. 2010*). MCPyV has also been found in the lymphatic system (*Toracchio et al. 2010*).

BKPyV is a nephrotropic virus and is associated with urinary tract pathologies in transplant patients (*Jiang M, et al. 2009*). BKPyV- associated nephropathy occurs in 2-5% of renal transplant patients. Viral reactivation during these complications is robust (*Bonvoisin et al. 2008; O'Donnell et al. 2009*). JCPyV is neurotrophic and is the etiological agent of progressive multifocal leukoencephalophaty (PML) in immunosupressed patients (*Jiang et al. 2009*). PML is a disease caused by JCPyV reactivation in the central nervous system and JCPyV can be detected in the cerebral spinal fluid (*Drews et al. 2000*). Recently, JCPyV was associated with male infertility as semen from infertile men contained JCPyV DNA in 25% of the cases compared to 11% in controls (*Comar et al. 2012*). So far, it has not been possible to associate BKPyV or JCPyV with human cancers (*Gjoerup et al. 2010*). Recently, a high prevalence and a high viral load of TSPyV DNA has been found in TS lesions, implying a causal relationship between TSPyV infection and TS disease (*Kazem et al. 2012*). Importantly, the vast majority of HPyVs have not been associated with any human disease. This is true even for KIPyV and WUPyV, which were originally detected in respiratory samples of symptomatic children (*Norja et al. 2007*).

### 1.6 Merkel Cell Polyomavirus (MCPyV)

Merkel cell polyomavirus (MCPyV) was discovered at the University of Pittsburgh in 2008, similar to other polyomaviruses, it is a non-enveloped, icosahedron shaped, small, double stranded DNA virus that is phylogenetically classified into the mammalian Orthopolyomavirus genera (*Johne et al. 2011*). Polyomavirus ability to induce neoplastic

transformation in cell culture and neoplasias in vivo have been well documented (*Cheng et al. 2009*) however none had been consistently and convincingly linked with human cancer until the discovery of MCPyV and the discovery of MCPyV, as an integrated part of MCC, represents the first accepted association of a specific human cancer with the presence of a polyomavirus genome. About 80% of Merkel-cell carcinomas contain the MCPyV genome. The virus is clonally integrated into the cancerous cells and it has a characteristic set of mutations only found in cancer cells, but not when it is detected in healthy skin cells. Direct proof for this oncogenetic mechanism comes from studies showing that inhibition of production of MCPyV proteins causes MCPyV-infected Merkel carcinoma cells to die but has no effect on malignant Merkel cells that are not infected with this virus. MCC that do not contain MCPyV genomes, - which account for about 20% of Merkel-cell carcinomas, appear to have a separate and as-yet unknown cause.

### 1.6.1 MCPyV discovery

Merkel cell polyomavirus (MCPyV) was discovered using a technique called Digital Transcriptome Subtraction (DTS) (*Feng et al. 2007*). DTS became a practical approach to detect new viral agents associated with human diseases. cDNA from MCC tumor tissues were exhaustively sequenced to generate a high fidelity transcriptome database of MCC tumors. An in silico subtraction of known human sequences from RefSeq, mitochondria, assembled chromosomes, and immunoglobulin sequences in NCBI databases removed the majority of human sequences resulting in the identification of candidate nonhuman, suspect pathogen sequences for further examination. 2395 sequences were identified as non-human candidates and these candidates were then analyzed using low-stringency alignment to viral databases. This analysis resulted in the discovery of a new member of the polyoma virus family.

### 1.6.2 Genomic organization of MCPyV

MCPyV is a typical polyoma virus in many ways. It is a non-enveloped, double-stranded DNA viruses and has a ~5.4kb (5.2-5.4kb) genome that is divided into early (ER) and late (LR) coding regions by a noncoding regulatory region (NCRR). The early region (ER) encodes a large T antigen (LTAg), a small T antigen (sTAg) and a 57kT antigen (analogous to the SV40 17-kT antigen (*Zerrahn et al. 1993*), all of which share a 78 amino acid stretch in the N-terminus. These three proteins are expressed from a multiply spliced mRNA with frame changes as shown in Figure 1.10. The late region (LR) encodes 3 capsid proteins (VP1, VP2 and VP3) that are expressed after the start of viral DNA replication. These structural proteins self-assemble into ~55 nm diameter icosahedron viral particles (Tolstov et al. 2009; Pastrana et al. 2009). Unlike the other polyomaviruses, MCPyV does not encode an agnoprotein (*Sariyer et al. 2011; Jay et al. 1981*) or VP4 (*Fischer et al. 1972*). Little is known about the kinetics and regulation of MCPyV late gene expression because virus replication studies have been limited.

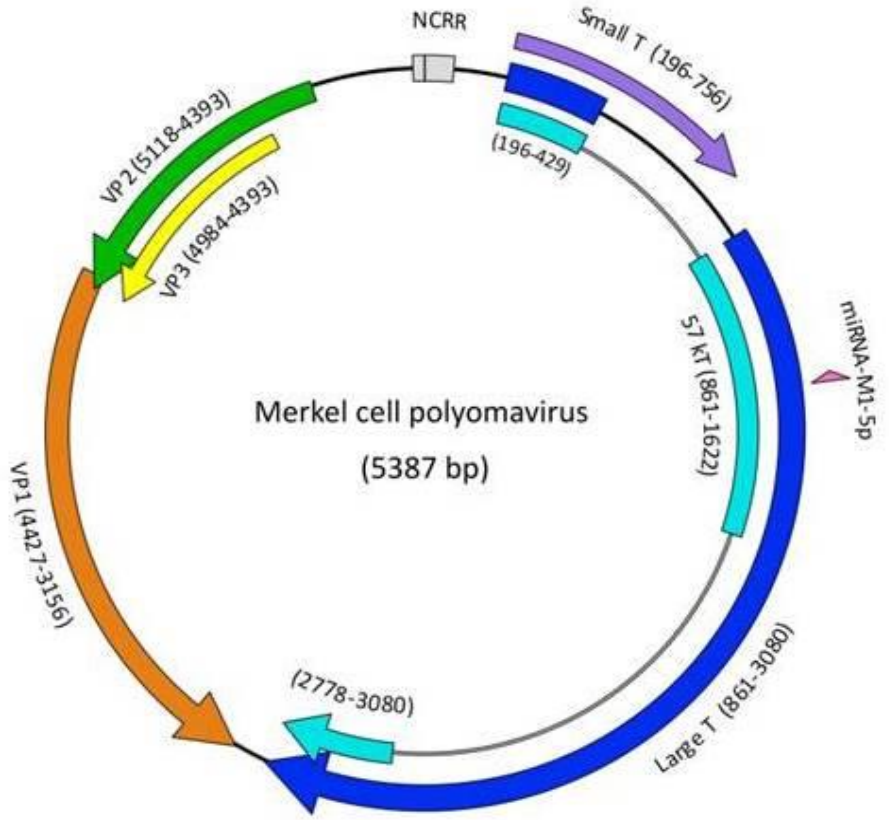


**Figure 1.10** Genome organization of Merkel cell polyomavirus. Merkel cell polyomavirus has a circular, 5387 bp genome divided into two halves by the noncoding regulatory region (NCCR). This NCCR contains the origin of replication (ori) of the virus as well as the promoters and regulatory elements to bidirectionally encode early (ER) and late (LR) viral proteins. The early region (ER) encoded proteins comprise the Large T, small T and the 57kT antigens. Viral protein 1, 2 and 3 (VP1, VP2 and VP3) constitute the gene products of the late region.

The MCPyV NCRR region contains a 71 bp viral origin of replication (ori). This sequence includes an AT-rich tract (helps in DNA melting) and 8 GAGGC pentanucleotide sequences that bind MCPyV LTAg. The NCRR also contains bidirectional transcriptional promoters and regulatory elements for early and late viral gene expression. Additional studies have identified an MCPyV encoded miRNA-MCPyV-mir-M1 (Seo et al. 2009). Further studies in MCPyV encoded miRNAs and their potential targets in normal and MCC tumor tissues are needed to understand their function.

### 1.6.3 Tumor specific signature mutations

The MCPyV large T antigen contatins the canonical LTAg domains that are present in other polyomavirus family members (*Pipas 1992; Ahuja et al. 2005*). As shown in Fig. 1.11, LTAg also encodes origin binding and helicase/ATPase regions needed for viral replication (*Shuda et al. 2008*).

However, the LTAg found in MCC has a premature stop codon that truncates the LTAg protein, eliminating its C-terminal domains (*Shuda et al. 2008; Martel-Jantin et al. 2012*), including the orgin binding and helicase domains. Despite these truncation mutations removing the replication functions of MCPyV LTAg, they occur after the LXCXE retinoblastoma-binding motif and do not appear to interfere with other N-terminal LTAg domains (*Shuda et al. 2008*). These two independent mutation events: viral integration and T antigen truncation appear to play a mechanistic role in the development of MCC. Both events are suspected to be relatively rare and this may be why MCC occurs so infrequently. Importantly, as MCC occurs most commonly in sun exposed areas, UV exposure may promote one of both of these mutations.

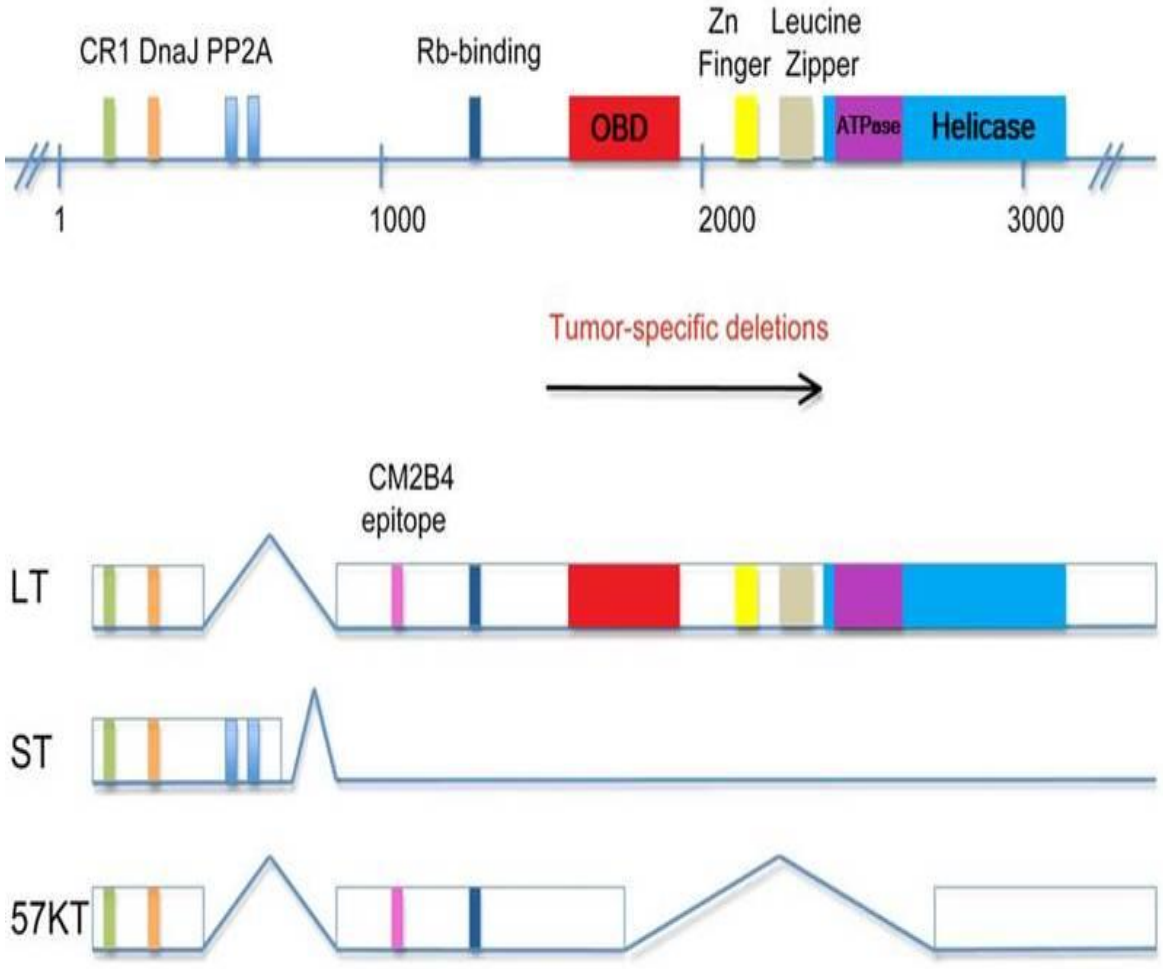


**Figure 1.11** Transcript mapping of multiply spliced MCPyV antigen locus. Three TAg's are identified as Large T, small T and 57kt. All four transcripts encode CR1 (green LXXLL) and DNAJ (orange, HPDKGG) domain. sTAg proteins contains two PP2A bindings motifs (blue, CXCXXC). Rb binding (dark blue, LXCXE) domain are conserved in large T and 57KT. Large T contains unique domain including origin binding (red) zinc finger (yellow), leucine zipper (blue) and helicase (cyan)/ATPase (purple). (*Shude et al. Int J Cancer 2009*).

## 1.7 Virus-like particles

Virus-like particles (VLPs) are similar to viral particles except that VLPs lack viral genomes. They are non-infectious, but have similar morphologies and cell tropism as the natural virus from which they are derived. They still show comparable cellular uptake and intracellular trafficking as the natural virus (*Petry et al. 2003*). VLPs are typically formed by expressing the structural genes of the virus and allowing particles to assemble. VLPs have been used as a model to understand viral entry and other process related to infection and cell tropism. Most importantly, VLPs have been shown to be useful in vaccine development or for gene therapy.

### 1.7.1 History

When Crawford and collaborators in 1962 were purifying MPyV by CsCl density gradients, they found two bands with different densities. The band with the lower density was shown to consist of empty capsids without any genes (*Crawford et al. 1962*). Later Michel et al (*Michel et al. 1967*) and Winicour (Winocour 1968) infected mouse kidney cells in culture with MPyV, and they found that the cells were not only producing virions with MPyV DNA, but also produced particles carrying host DNA, and they called these latter particles pseudovirus. They also realized that these particles could be of potential therapeutic value (*Michel et al. 1967; Winocour 1968*).

Viral capsid proteins can be expressed in bacteria or eukaryotic cells, where they self-assemble into virus-like particles (VLPs), also known as pseudo capsids. Already in 1978, the MPyV major capsid protein VP1, was chromatographically purified and formed pentamers that appeared similar to native virus pentamers (*Brady et al. 1978*). In 1986 Salunke and collaborators showed that VP1 pentamers subsequently self-assembled into

capsid-like structures of the same size and shape as native virus particles (*Salunke et al. 1986*). They concluded that the minor capsid proteins VP2 and VP3 were not required for capsid formation. Montross later produced VLPs by expressing the VP1 gene in insect cells by baculovirus expression (*Montross et al. 1991*). VLPs that lack viral DNA and RNA have been produced from different viruses, such as HPV (*Rose et al. 1993*), hepatitis B (*Miyanohara et al. 1986*), HIV (*Gheysen et al. 1989; Delchambre et al. 1989*) and bluetongue virus (*French et al. 1990*). VLPs can be used to vaccinate against the analogous virus. VLPs can also be used as carriers for other molecules, for example foreign DNA in gene therapy or proteins in immunotherapy.

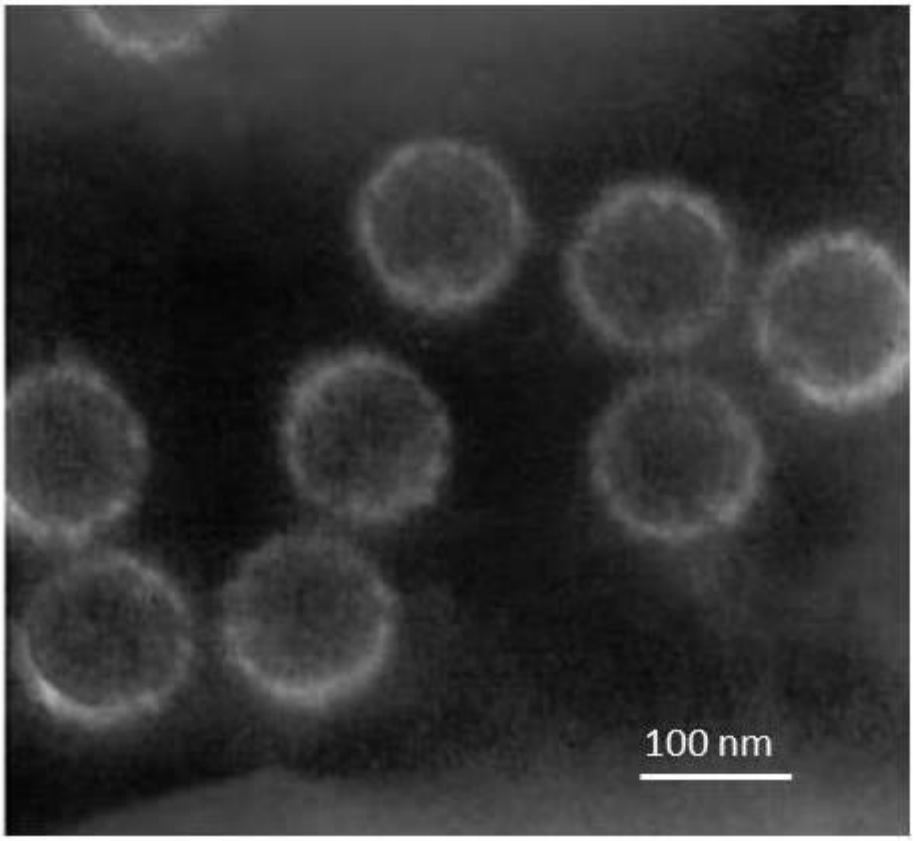


**Figure 1.12** Purified VLPs demonstrated with electron microscopy (*Tegerstedt et al. 2003*).

## 1.8 Proteomics

The human genome project opened new frontiers in medical research, but genome sequences are not sufficient to fully describe the biological characteristics and molecular processes that take place in the sequenced organisms. In recent years, genomic research has given way to a new discipline, proteomics, which has the potential to revolutionize the study of molecular and cellular processes. Proteomics represents the systematic study of the different properties of proteins, using a variety of approaches with the aim of providing a detailed description of the structure, function and control mechanisms of biological systems.

If we consider proteomics, based on the classical definition, the simultaneous study of a large number of proteins of a particular cell line or organism, the term can be traced back to 1975 (*O'Farrel 1975, Klose 1975, Scheele 1975*) which was applied to the mapping of the proteins obtained from Escherichia coli, the mouse and from the guinea pig by 2-dimensional electrophoresis. These researchers aimed to construct databases of proteins of a given species, so as to be able to compare different patterns of protein expression. However, this idea was not completely realized because, even high resolution gel electrophoresis does not provide the identity to any of the separated proteins. Furthermore, biological samples are often limited in quantity and in gel electrophoresis separation techniques many proteins are not visualized or are obscured by the presence of neighboring abundant proteins. One of the first methods used for protein identification was sequencing by Edman degradation (*Edman 1949*), which allows for the identification of numerous proteins by providing short amino acid sequences from the N-terminus of the protein, or later from peptides. Around the 1990's, the application of mass spectrometry (MS) to protein characterization has supplanted many of these techniques, because it provides a sensitive and rapid analysis of proteins. Initially, the analysis of

proteins by mass spectrometry still relied on the separation of proteins by gel electrophoresis, followed by digestion with sequence specific proteases, such as trypsin. The principle reason why peptides are analyzed rather than proteins is because peptides represent an information rich set of fragments of the same protein that more easily gives sufficient information to uniquely identify a protein. The introduction of this powerful analytical method was also accompanied by the availability of the entire sequence of the principle experimental model systems, as well as the human genetic code in public databases.

The development of proteomics is a direct consequence of the progress achieved in the large-scale sequencing of genomic DNA. Without this information, it is particularly difficult to identify proteins using mass spectrometry.

It is in this historical context that in 1994, at the first meeting on two-dimensional electrophoresis in Siena, the term proteome was coined. The proteome is defined as the protein complement to the genome and consequently its study is referred to as "proteomics" (*Wilkins et al, 1996*).

### 1.8.1 From the genome to the proteome

With the accumulation of large numbers of DNA sequence databases, the researchers found that much information on the biological functions of cells could not be obtained solely from the study of genes. The transcriptome analysis (the entire set of mRNAs transcribed from the genome of a cell) provides an indication of which genes are active in a particular cell, but does not give indications about the proteins that are expressed or their functions. In fact the knowledge of the sequence of a gene within the DNA molecule does not give us information on whether, or when, that particular gene will be transcribed and translated, and what the final gene product will be or what will be its localization or its role within the cell. In addition, in response to external or internal

stimuli, proteins can be modified, which can have a profound impact on their function, The proteome is also dynamic and varies in response to external factors and differs substantially between the different cell types of the same organism. Finally, it is important to think about how proteins, not genes, determine the phenotype of a cell, because it is the proteins that are responsible for performing and regulating cellular functions. Therefore, proteomic studies are important for connecting the link between the genomic information and the biochemical properties of the cell. The characterization of the proteomes of different cells is important to understanding how alterations in genomic activity can cause different phenotypes and pathological conditions.

### 1.8.2 The applications of proteomics

Initially, proteomics focused on the development of a series of methods to study the proteome and obtain a more complete picture of the protein content of the cell. With the eventual goal of being able to study all the protein products expressed in a cell, including all isoforms, all post-translational modifications, mapping protein interactions, etc. (Figure 1.13).

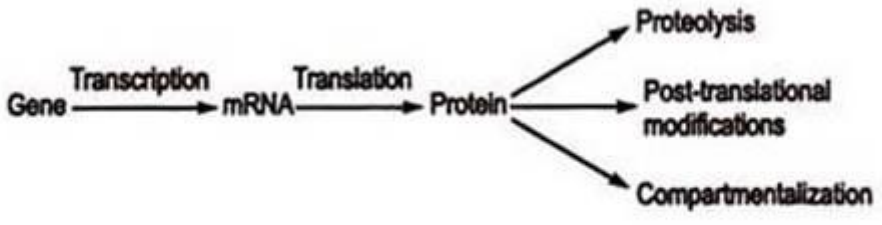


**Figure 1.13** Schematic representation of the "central dogma of molecular biology" adapted from the original by Crick in 1958 and modified according to current knowledge.

Through the use of mass spectrometry techniques, proteomics can be used to address three relevant types of biological problems:

a. The identification of proteins;

b. Quantification and expression analysis of protein profiles;

c. The study of post-translational modifications (PTMs) of gene products (*Aebersold, Mann 2003*).

Traditionally, three types of application to proteomics are considered: expression proteomics, which consists of qualitative and quantitative analysis of protein expression; structural proteomics, which aims to map the structure of protein complexes or proteins; and finally functional proteomics, whose goal is to study the protein profile in a given biological sample to better understand the functional organization at the molecular level (Figure 1.14).

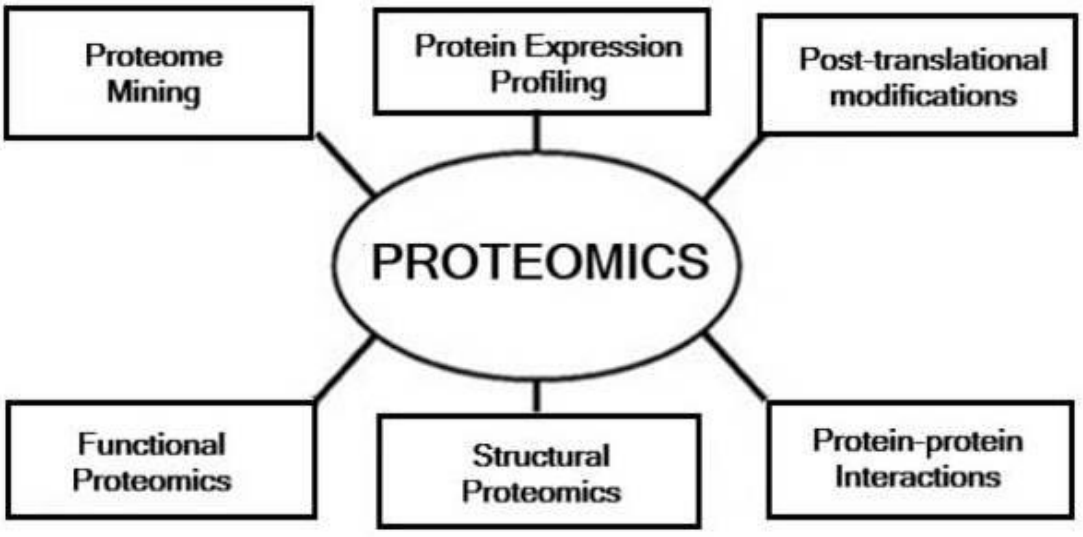


**Figure1.14** Understanding the application of Proteomics (*Graves and Haysted, 2002*).

### 1.8.3 Expression proteomics

Studies on RNA expression levels in mammalian systems have demonstrated that there is only a poor correlation between the protein expression of a given cell and mRNA levels. This lack of a strong correlation can be explained by the different stabilities of a particular mRNA and the protein it produces (*Vogel, Marcotte 2012*). In addition, the transcriptome varies from one cell to another in response to numerous physiological signals including: stress, changes in the surrounding environment, disease, stage in cell cycle, etc.

RNA transcription is just the beginning of a cascade of events that leads to the synthesis of a protein. The mRNA can undergo alternative splicing, editing and polyadenylation processes, which result in the creation different mRNA and protein isoforms. Finally, proteins are subjected to more than 300 naturally occurring post-translational modifications including proteolysis, phosphorylation, glycosylation, acetylation (*Patterson, Aebersold 2003*).

### 1.8.4 Structural proteomics

The goal of structural proteomics is to predict the three-dimensional structure of all proteins. Determining the structure of proteins and how they organize themselves to form complexes is important for understanding the behavior of a particular protein. The definition of the structure of a protein is required to understand the functional relationships between proteins, ligands or other cofactors, and is important for rational drug design.

### 1.8.5 Functional proteomics

The objective of functional proteomics is to define the biological function of proteins whose role is still unknown, and to identify protein-protein interactions in vivo, in order to describe the biological network.

### 1.8.6 The study of post-translational modifications

Post-translational modifications (PTMs) can be any modification to a protein. These modifications alter the primary structure of a protein and can have profound effects on its functionality. We know that typically more than one protein is generated from a single gene. Indeed, one of the most striking discoveries of this new post-genomic era is that the old paradigm of "one gene-one protein" is usually not valid.

Some PTMs, such as phosphorylation or methylation, are reversible, while others remain as a permanent mark until the protein is degraded. Of all the post-translational modifications known today (*Krishna, Wold 1993*), only a few have been studied systematically (*Mann, Jensen 2003*). So far, the most studied modification is phosphorylation, which is estimated to modify ~80% of all proteins. It is possible to analyze virtually all PTMs through mass spectrometry. This approach is based on the fact that the modifications give rise to specific fragments with altered masses, which forms a characteristic pattern that can be used to identify the modification itself.

### 1.8.7 Proteomics techniques

A typical proteomics experiment begins with sample preparation. The goal of sample preparation is to produce a sample that can be analyzed by mass spectrometry that still

represents the original sample. Typically this involves cell lysis or other extraction procedures and efficient lysis typically requires the presence of detergents or other agents that are incompatible wiyh the downstream analysis. Downstream steps, such as filtration or electrophoresis, are typically used to remove these agents. The proteins are subjected to digestion with sequence specific proteases to create a complex mixture of peptides. Importantly, each unique protein, including those generated by alternative splicing or post-translational modifications, produce a unique set of peptides. Mass spectrometry is used to analyze these peptides, which can then be mapped back to proteins in the sample.

A mass spectrometer can be split into two parts, the ionization source and the mass analyzer. Importantly, a mass spectrometer can only measure charged molecules, which is why an ionization source is required. For biological samples, Electrospray Ionization is the most commonly used source. The major advantage of ESI, or electrospray ionization, is in its ability to produce charged gaseous ions directly from a liquid solvent system by creating a fine spray of highly charged droplets in the presence of a strong electric field (Figure 1.15).

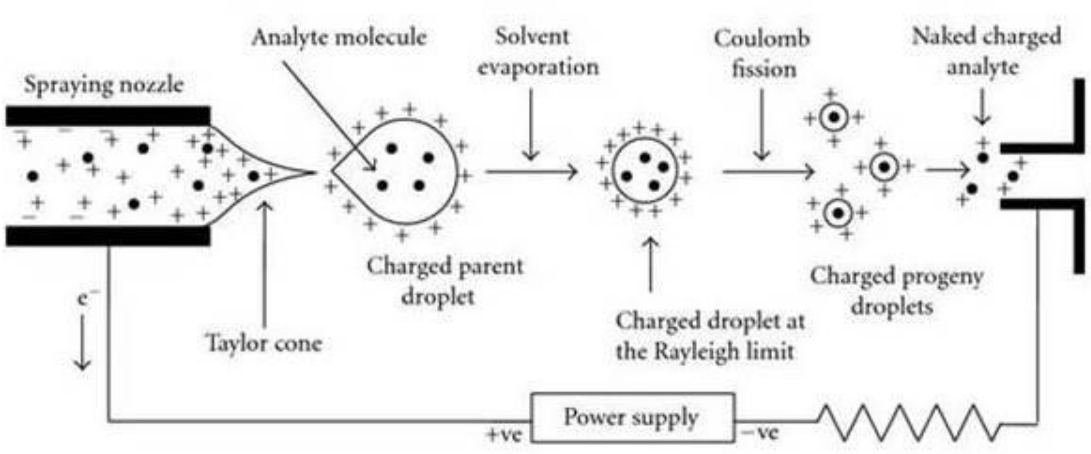


**Figure 1.15** Schematic picture of electrospray ionization (ESI). The high voltage applied to the source causes the formation of small charged droplets which undergo rapid evaporation and the ionized species are directed to a mass analyzer, which allows for differentiation and detection of the ions according to their mass-to-charge ratios (m/z). (*Banerjee et al. 2012*)

The sample solution is typically sprayed from the tip at high voltage and evaporation causes the droplet size to rapidly decrease, while the surface charge density rapidly increases. Ions are transferred to the gas phase as a result of their Coulombic expulsion from the droplet and are then directed into a mass spectrometer through a series of ion lenses. Importantly, ESI allows the convenient coupling of the mass analyzer to chromatography systems, such as HPLC, which allows for the easy analysis of complex mixtures of peptides.

The most widely used analyzers are quadrupole mass filters, quadrupole ion traps, Fourier transform ion cyclotron resonance spectrometers, and time-of-flight mass analyzers. The time-of-flight instruments are the simplest: the ions are periodically accelerated by an electric field and then passed into a field free drift tube. The time it takes for an ion to pass through the drift tube is directly related to its mass and charge. The other mass analyzers typically use an oscilating electric field for determining the mass to charge ratio. For example, in an ion trap, an oscillating electric field is used to "trap" ions in a stable orbit inside the mass analyzer. The amplitude or frequency of the electric field is altered to successively eject, and detect, molecules based on their mass to charge ratio. In any case, a mass spectrum is created in which the mass to charge ratio is plotted vs the intensity of the detected signal.

In tandem mass spectrometry a single ion is selected and then fragmented inside the mass spectrometer. Typically the sample is collided with an inert gas between two mass analyzers, which results in their fragmentation by collision-induced dissociation (CID) (*Hoffmann et al. 2007 Mass Spectrometry: Principles and Applications*). Often used combinations of analyzers are the triple quadrupole or quadrupole-TOF combinations. Following this round of fragmentation, a second mass spectrum is collected, which is referred to as the MS/MS spectrum. It is possible to select an ion in an MS/MS spectra and subject it to another round of CID, which would produce an MS/MS/MS spectrum, and this process can repeated upto about 10 times which would result in an MS10 spectrum.

In a typical proteomics experiment, the masses of a group of tryptic peptides is measured and then one peptide is subjected to CID and the masses of the fragments are analyzed by the second mass analyzer (Figure 1.16).

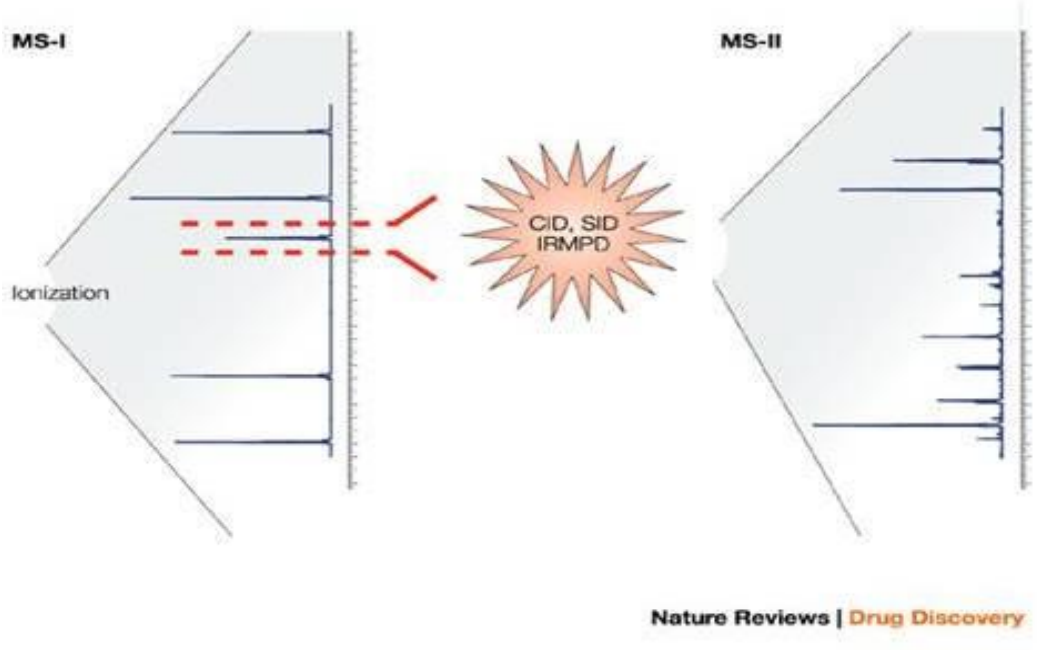


**Figure 1.16** Schematic diagram of tandem mass spectrometry. In tandem mass spectrometry (or MS/MS) ions with the mass-to-charge (m/z) ratio of interest (precursor ion) are selectively fragmented and a mass spectrum of product ions. is generated (*Glish et al. 2003*).

Performing MS/MS increases the amount of information in a peptide digest and results in many more protein identifications and allows for the efficient identification of PTMs. For example, a protein can be unambiguously identified by just one or two peptide MS/MS spectra. When the analysis is coupled to chromatography, especially HPLC, the MS/MS workflow can handle mixtures of 1000s of unique proteins and can map post-translational modifications at the amino acid level (*Yates et al. 1996*). Currently, it is possible to identify >4000 proteins from a single microgram of whole cell lysate in less than 60 minutes.

The MS/MS spectra generated by peptides are typically analyzed by a process called

spectral matching, in which the MS/MS spectra are compared to theoretical spectra generated from sequence databases. This comparison is made more efficient by using sequence specific proteases, which limits the number of theoretical spectra that need to be created, and by only comparing experimental and theoretical spectra that have a matching mass. Importantly, PTMs must be accounted for at this stage, as they will affect the mass of the peptides as well as the masses of the fragments in the MS/MS spectra. Typically, only a few PTMs can be searched at a time, but a growing number of algorithms are being developed that can perform the global analysis of PTMs (*Bern et al. 2012*).

## 1.9 Aim of the project

The principal objective of my project is the proteomic analysis of the MCPyV viral particle and the capsid proteins. Importantly, host proteins associated with the capsid were discovered and a number of post-translational modifications of the capsid proteins were also identified. Assays for transformation and for viral production will be important for determining the relevance of these interactions.

# 2. MATERIAL AND METHOD

## 2.1 Materials

### 2.1.1 Suppliers

General laboratory chemicals were of analytical grade and obtained from *Sigma-Aldrich Company Ltd*. or *Merck Chemicals Ltd*. General disposable plasticware was supplied by *Sterilin Ltd*., *Sarstedt Ltd*, *VWR International Ltd.* and *Eppendorf Ltd.* All tissue culture plasticware was obtained from *Falcon™ Gilson Inc* and *Sarstedt Ltd.*

### 2.1.2 Bacterial Strains

Strain: SIG10 ULTRA Electrocompetent Cells

Genotype: F-mcrAΔ(mrr-hsdRMS-mcrBC)endA1recA1Φ80dlacZΔM15ΔlacX74araD139 Δ(ara,leu)7697galU galK rpsL nupG λ-tonA (StrR)

Source: *Sigma-Aldrich*

### 2.1.3 Preparation of competent prokaryotic cells

The SIG10 E. coli were plated on LB Agar (Luria-Bertani) without antibiotic and grown at 37°C overnight. A single colony was 5 mL of LB (Luria-Bertani) liquid medium and grown at 37°C while shaking overnight. The overnight growth of E. coli was diluted 1:100 into prewarmed LB (Luria-Bertani) broth and grown at 37°C in a shaker until the optical density (OD600) was between 0.4 and 0.5. The growth flask is placed on ice for 30 minutes and the bacteria harvested by centrifugation. The supernatant is removed and the

cells resupended in 250 mLs of sterile ice cold water. The cells are centrifuged and the water removed. The cells are resuspended in 3 mL of ice cold 10% glycerol in water and single use aliquots frozen at -80°C.

### 2.1.4 Transformation of Bacteria

Thaw 50 µL of Electrocompetent Cells in an ice bath and add 1–2 µL of the transforming DNA solution directly into the thawed cell suspension. Mix gently to ensure even distribution and subsequent incubation on ice for 30 minutes. Transfer the mixture of cells and DNA to a cold 0.1 cm electroporation cuvette (*Sigma-Aldrich*), applies an exponential decay wave pulse using an ECM 399 electroporation system (BTX). Immediately add 1 mL of LB (Luria-Bertani) medium (precooled in an ice bath), then transfer the mixture to another tube. Incubate by shaking (160–250 rpm) for 1hr at 37°C. Plate an appropriate amount of culture on selective medium and Incubate overnight at 37°C. Single colonies were isolated. Each colony was used to inoculate 5 mL of LB containing antibiotics and incubated in the orbital shaker overnight.

## 2.1.5 Antibodies

**Table 2.1A**: Primary Antibodies used for western blots

| | | | | |
|---|---|---|---|---|
| **Primary** | Ubiquitin (P4D1) mouse Cell Signaling #3936 | anti-AAV VP1/VP2/VP3 mouse B1 #61058 Progen | Monoclonal Anti-β-Actin−Peroxidase mouse #A3854 Sigma | Anti-acetyl Lysine antibody-ChIP Grade #ab21623 abcam |
| **Dilution/Assay** | 1/1,000 Western blot | 1/500 Western blot | 1/30,000 Western blot | 1/1,000 Western blot |

**Table 2.1B:** Secondary Antibodies used for western blots

| | | | | |
|---|---|---|---|---|
| **Secondary** | Anti-mouse IgG, HRP-linked Cell Signaling #7076 | Anti-mouse IgG, HRP-linked Cell Signaling #7076 | -------- | Anti-rabbit IgG, HRP-linked Cell Signaling #7074 |
| **Dilution/Assay** | 1:1,000–1:3,000 Western blot | 1:1,000–1:3,000 Western blot | -------- | 1:1,000–1:3,000 Western blot |

### 2.1.6 Plasmid DNA

- pwM2m (VP1 and VP2 dual expression) (*Pastrana et al. 2010*).
- ph2m (high VP2 expression) (*Tolstov et al 2009*).
- pEGFP-N3 is an expression vector that allows the expression of EGFP (Green Fluorescein Protein) (Addgene)

### 2.1.7 Cell Lines

#### 2.1.7.1 HEK 293TT

HEK 293TT (Human Embryonic Kidney cells) cells, a gift from Dr. Lawrence Banks Tumor Virology lab ICGEB (*Buck et al. 2004*). HEK 293TT cells were grown in DMEM media (*Sigma-Aldrich*) supplemented with 10% fetal bovine serum (*Gibco*), 50 U/mL penicillin (*Sigma-Aldrich*), 100 ng/mL streptomycin (*Sigma-Aldrich*).

## 2.2 Molecular biology techniques

### 2.2.1 DNA digestion

Restriction enzyme digests were performed on plasmid DNA for clonal analysis or isolation of DNA fragments. Restriction enzymes were purchased from NEB and DNA digestion was performed in the buffer suggested by the Double Digest Finder tool in NEB website (*www.neb.com*). Reactions were conducted in a reaction volume of 50 µL and 1 µg of DNA was cut in preparative digestions.

### 2.2.2 Plasmid DNA Purification (Mini and Maxi-Prep)

Plasmid DNA from bacteria cells was purified using the GenElute Plasmid Miniprep Kit (Sigma-Aldrich) using the manufacturer instructions. Breifly, cells from a 5Ml LB overnight culture were pelleted by centrifugation at 7,000 rpm for 5 minutes and lysed using the provided buffers. The DNA was bound to the GenElute columns and the purified DNA was eluted in 50 µL $ddH_20$ and stored at -20°C. The high scale plasmid DNA purification (Maxi-prep) started from 100 mL of overnight culture. The cells were pelleted by centrifugation and plasmid DNA was extracted and purified using the GenElute™HP Plasmid Maxiprep Kit (*Sigma-Aldrich*) according to the manufacturer's instructions. The purified DNA (a typical yield is 100 µg) is eluted in 200 µL of $ddH_20$ and stored at -20°C. The concentration of purified DNA was determined using a nanodrop spectrophotometer.

### 2.2.3 SDS-PAGE Gel Electrophoresis and Western Blot

Protein samples were supplemented with 6X Laemmli sample buffer (*Sigma-Aldrich*) and boiled for 10 minutes. The samples were separated by 10% bis-Tris SDS-PAGE (https://openwetware.org/wiki/Sauer:bis-Tris_SDS-PAGE,_the_very), with 0.5% Chloroform or Trichloromethane $CH_3Cl$ (*Sigma-Aldrich*) for stain-free detection. The gels were run for 1 hr at 110/125 mA/gel (start) to 70/80 mA/gel (end) and then electro-blotted onto PVDF membranes (*Millipore*). The transfer was performed at 200 mA for 2hrs. The membranes were blocked at room temperature for 2hrs in PBS buffer supplemented with 0.1% Tween-20 (*Sigma-Aldrich*) and 5% skim milk (w/v) (*Sigma-Aldrich*) or Bløk-CH Noise Cancelling Reagents for Chemiluminescence Detection (*Millipore*). The blocked membranes were then incubated with the appropriate primary antibodies (Table

2.1A), diluted in the blocking buffer and incubated with the membranes overnight at 4°C. The membranes were washed extensively with PBS supplemented with 0.1% Tween-20 (*Sigma-Aldrich*), and then incubated for 1h with a horseradish peroxidase (HRP)-conjugated secondary antibodies (Table 2.1B). After extensive washing, the blots were developed with enhanced chemi-luminescence reagents (ECL+) (*Biorad*) following the manufacturer's instructions. The membranes were visualized on a ChemiDoc™ Imaging Systems (*Biorad*).

### 2.2.4 Colloidal Blue Coomassie G-250 Staining

To visualize proteins after SDS-PAGE, the gels were washed once with $ddH_2O$ and incubated for one hour at room temperature with Colloidal Blue G-250 Coomassie solution (10% (w/v) $(NH_4)_2SO_4$ (*Sigma-Aldrich*), 20% $C_2H_5OH$ (*Sigma-Aldrich*), 0.4% (w/v) Coomassie Brilliant Blue G-250 (*Biorad*) and 3% $H_3PO_4$ (*Sigma-Aldrich*)). The gels were washed with $ddH_2O$ in order to remove the background staining and to enhance the visualization of protein bands (*Modified protocol from Kang et al. 2002*).

## 2.3 Pseudovirions (PsV)

### 2.3.1 Production

For MCPyV pseudovirus (PsV) production, 10 x 10 cm tissue culture dishes with $3\text{-}4x10^6$ HEK 293TT cells in 10 mL growth medium were prepared and incubated at 37°C, 5% $CO_2$ for 24 hrs to allow attachment of the cells to the dish. The cells were co-transfected using the corresponding plasmid DNAs, encoding the MCPyV late proteins VP1 and VP2 at a 1:3 ratio and the Gaussia luciferase or pEGFP-N3 plasmid reporter using calcium phosphate transfection. For the calcium phosphate transfections, HEK 293TT cells were

grown to 50%-70% confluence and a reaction mixture, made up of 445 µL sterile $H_2O$, 50 µL of 2.5 M $CaCl_2$ (*Sigma-Aldrich*), 8 µL of specific plasmid DNA and 2 µL of pEGFP-N3 plasmid, were added to 500 µL of 2X BBS reagent while bubbling. The mixture was immediately added to the growth media of the cells and incubated at 37°C. Efficiency of transfection was visualized 48 hrs after transfection using an inverted fluorescent microscope using the GFP filter set and then the cells were harvested. The cells were harvested by resuspension in growth medium and centrifugation at 1,900 rpm for 5 minutes. The pellet was washed with 1 mL DPBS, and the cell suspension was transferred to a siliconized 2 mL screw-top tube and centrifuged at 1,900 rpm for 5 minutes at 4°C. The pellet was resuspended in lysis buffer, at 100 million of cells per mL of lysis buffer, and incubated at 37°C for 24 hrs to allow capsid formation. The cell suspension was incubated on ice for 5 minutes before adding 0.17 volumes 5 M NaCl. Cell debris were removed by centrifugation at 10,000 rpm for 5 minutes at 4°C and the clarified supernatant was transferred to a fresh 1.5 mL siliconized tube. The pellet was resuspended in 300 µL DPBS/0.8 M NaCl and centrifuged for a second time at 10,000 rpm for 10 minutes at 4°C. The supernatants were combined and 1 µL benzonase (100 units) was added and incubated at 37°C for 1h. The crude extract was harvested by centrifugation (10,000 rpm / 10 minutes / 4°C) and collected in a new 1.5mL siliconized tube. A small aliquot of the crude extract was taken and analyzed by SDS-PAGE. The remaining crude extract was used for VLP purification.

### 2.3.2 Purification of pseudovirions

Pseudovirions were purified on an Iodixanol (*OptiPrep TM*) density gradient. 27%, 33% and 39% Iodixanol solution in DPBS / 0.8 M NaCl was prepared from the 60% (w/v) Iodixanol stock solution and layered into Ultra-clear centrifuge tubes (1/2x2 in.) (*Beckman*). The tubes were covered with Parafilm and incubated for 3 hrs at room temperature to allow softening of the inter-phases. Approximately 0.5 mL of the crude extract was gently overlayed onto the top of the gradient and centrifuged in SW-55Ti rotor (*Beckman*) at 55,000 rpm (234,000 g) for 210 minutes at 16°C. After centrifugation, the VLP band was visible as a light grey layer a little over a third of the way up the gradient. The VLPs were harvested by puncturing the bottom of the tube slightly off center with a syringe needle. An initial 1 mL fraction was collected followed by 250 µL fractions. The collected fractions were put on ice immediately. The MCPyV VLPs are usually found in fractions 3-5. Fraction screening is performed by silver staining or Coomassie staining of SDS-PAGE gels. The fractions were stored at -80°C.

### 2.3.3 Pseudovirus Infection

To test of the purified PsV fractions for PsV infection activity, purified fractions were tested in constant 1: 1,000 dilutions. HEK 293TT cells were infected at 70-80% confluency with pseudo virus. After 24 hrs the infection media was replaced with fresh warmed maintenance media. Viral titer was visualized directly using an inverted fluorescent microscope and the GFP filters.

## 2.4. Mass spectrometry sample preparation

### 2.4.1 In-solution Digestion

Dithiothreitol (DTT) (*Sigma-Aldrich*) was added to a final concentration of 5 mM and the sample was heated to 55°C for 10 minutes. Iodoacetamide or Chloroacetamide (*Sigma-Aldrich*) was added to 15 mM and the reaction was allowed to proceed for 1 hr at room temperature. Trypsin (*Promega*) was then added at a ratio of ~1:20 followed by digestion for overnight at 42°C. The digested sample is desalted and concentrated using STAGE tips (*Rappsilber et al. 2007*).

### 2.4.2 In-gel Digestion

Samples separated by SDS-PAGE were stained with Commassie Blue as previously described. Visualized bands, or discrete areas of the gel, were excised using a scalpel and chopped into ~1 $mm^3$ pieces. Reduction and alkylation steps are performed similarly to the in-solution digest protocol and then subjected to extensive washing with 20 mM Triethyl Ammonium Bicarbonate (*Sigma-Aldrich*), pH 8.5 in 50% Acetonitrile (ACN) (*Sigma-Aldrich*). The gel pieces were dehydrated with 100% Acetonitrile (*Sigma-Aldrich*) and then 20 ng/µL trypsin (*Promega*) was added to completely cover the gel pieces and the digestion was allowed to proceed overnight at 42°C. The supernatant was harvested and any remaining peptides were extracted from the gel by sonicating for 20 minutes with 0.1% Formic acid (FA) (*Sigma-Aldrich*). Recovered tryptic peptides are then purified using filter tips as described.

### 2.4.3 Acetylation protocol

The MCPyV pseudoviruses Optiprep gradient fractions were incubated for 1hr at 25°C with 50mM Acetic Anhydride (*Sigma-Aldrich*) (final 5mM) The reaction was stopped with 100mM $NH_4HCO_3$ (*Sigma-Aldrich*) (final 10mM). Once the incubation was performed, the loading buffer was added to the sample and boiled for 5 minutes, then centrifuged and loaded into SDS-PAGE.

### 2.4.4 Stage Tips

Stage tips were prepared with reverse phase filters (*Empore$^{TM}$ 3M*). The volume of the filter disk and the tips are determined based on the amount of sample used. A small core of the reverse phase filter is punched out of the filter using a 2.5 mL combi-tip (*Sarstedt Ltd*) and then lodged near the end of a 20 or 200 µL pipette tip (*Gilson Inc*). Loading, washing and elution steps are performed by pushing the appropriate solvent over the tip.

### 2.4.5 LC/MS-MS Analysis

Chromatographic separation was accomplished using 3 µm C12 resin (*Phenomenex*) packed into a 75 µm x 15 cm fused silica capillaries (*Polymicro*) using an EASY-nLC II system (*Bruker Daltonics*) at a flow rate of 500 nL/min. 90 minutes gradients from 100% buffer A (99.9% water with 0.1% FA) to 60% buffer B (100% Acetonitrile) were used to develop the column. The column effluent was sprayed directly into an AmaZon ETD Iontrap mass spectrometer (*Bruker Daltonics*) using a custom electrospray interface.

Data collection was controlled by the HyStar program (*Bruker Daltonics*) using a data-dependent acquisition mode. MS spectra were acquired in the range of m/z 380 –1600

followed by maximum of five MS/MS analyses. The typical duty cycle was approximately 2 seconds. The precursor selection was based on peak intensity and all charge states were selected except for 1+, which was excluded. Dynamic exclusion was set to allow each peak to be analyzed 3 times in a 1 minute window.

## 2.5 Data Analysis

### 2.5.1 X!Tandem

Data analysis was performed on 3 independent replicates for each experimental condition. Data from each experiment was merged and the searches were performed on both merged data and on individual experimental runs using the X!Tandem search engine (*Fenyö et al., 2003).* Data was searched against the UniProt human database (forward and decoy). Trypsin was selected as the protease with a maximum of one missed cleavage allowed. Carbamidomethyl was set as a complete modification and partial oxidation of methionine and partial deamidation of glutamine and asparagines were also allowed in the search parameters. MS tolerance was set to 0.5 Da while MS/MS tolerance was set to 0.3 Da.

## 3. RESULTS

The main objective of my project is the proteomic analysis of the MCPyV viral particle and of the capsid proteins. I produced MCPyV VLPs in tissue culture cells, purified the VLPs and analyzed the VLPs by mass spectrometry. I was able to identify a number of PTMs on the viral capsid proteins as well as >90 host proteins that co-purified with the VLPs. VLPs were produced using two plasmids provided by Christopher B. Buck (Figures 3.1 A and B), which are needed to produce Virions in mammalian cells.

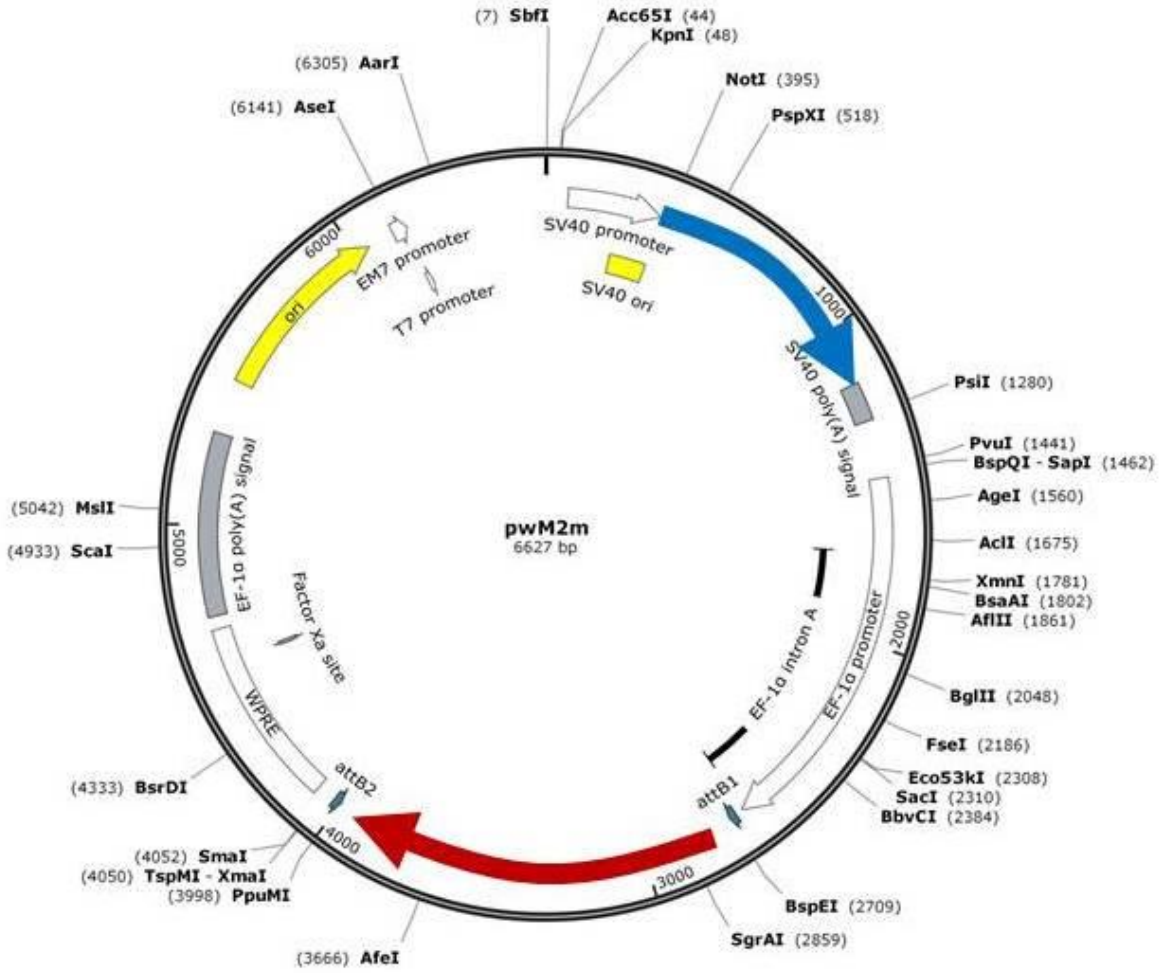


**Figure 3.1 A Diagram of pwM2m for production of MCPyV virions.** The VP1 ORF is denoted by the red arrow and the VP2 ORF is denoted by the blue arrow, was a gift from Christopher Buck (Pastrana et al, 2010)

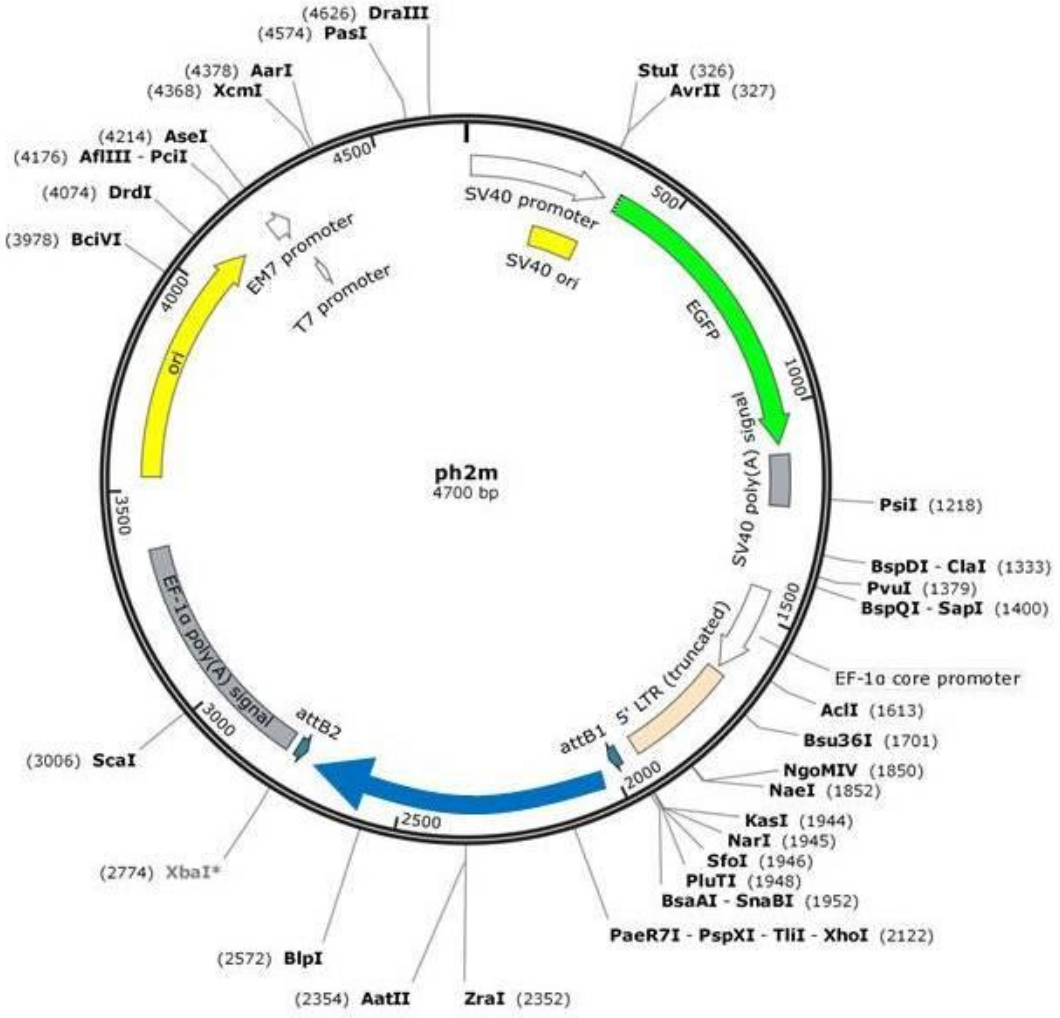


**Figure 3.1 B Diagram of ph2M for over expression of MCPyV VP2**. The VP2 ORF is denoted by the blue arrow., was a gift from Christopher Buck (Addgene plasmid 22518) (Pastrana et al, 2009).

Transfection of HEK293-TT with the two plasmids results in the expression of VP1 and VP2 and the production of VLPs. Initially, I attempted to produce viral capsids using just the pwM2m (*Eash el al 2004*) plasmid, since it encodes both VP1 and VP2. However, there was very low VP2 expression. Therefore, I included the plasmid ph2m in the transfection to improve the ratios of VP1 and VP2 (*Schowalter et al, 2013*). HEK293-TT cells were transfected using a modified calcium phosphate transfection protocol (Figure 3.2) with the ratio of plasmids favoring VP1 expression (3:1). In addition a plasmid expressing GFP (Figure 3.1 B) was used to estimate transfection efficiency and for other studies, as the GFP plasmid is efficiently packaged into the VLPs. The expression of the capsid proteins was allowed to proceed for 48 hours and the virus like particles were purified. The virions were liberated from the cells by hypotonic lysis and the virions matured for 16-24 hours. Following maturation, the virions were purified using an Optiprep gradient and 12 fractions were collected. 20 µL of the resulting fractions were analyzed by SDS-PAGE stained with Coomassie (Figure 3.3) and Silver (Figure 3.4).

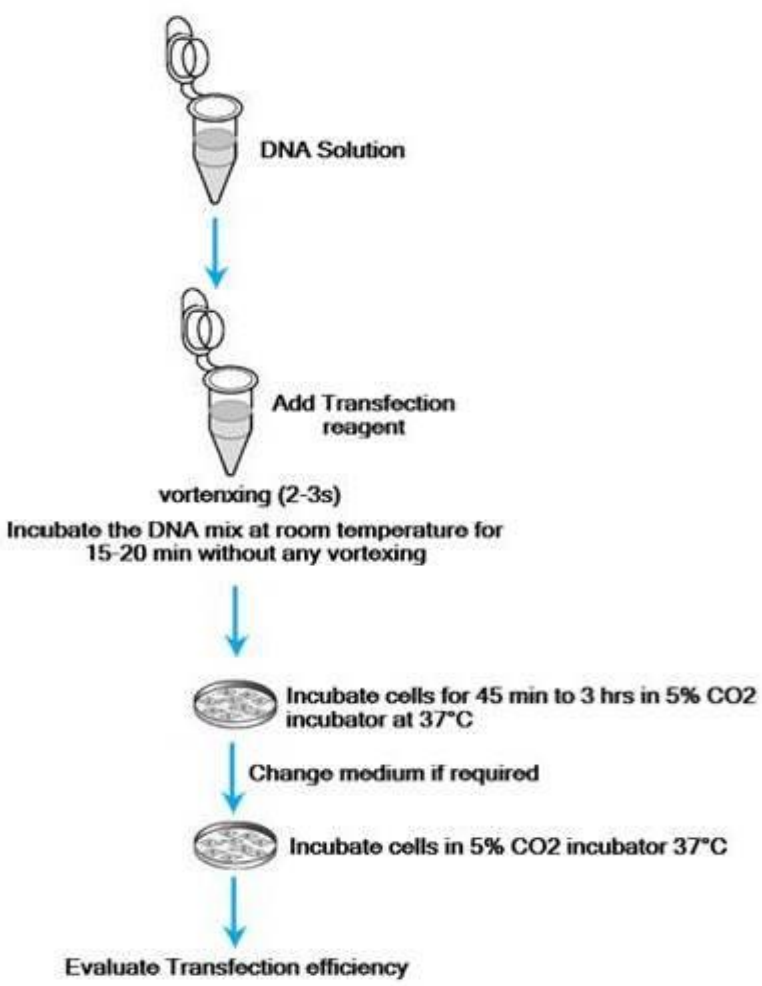


**Figure 3.2** Calcium phosphate transfections

The qualitative characteristics of the protein extracts were evaluated by observing the electrophoretic separation by SDS-PAGE, which allowed the visualization of the proteins. The gels, shown in figures 3.3 and 3.4, represent the proteins fractionated by Optiprep gradient.

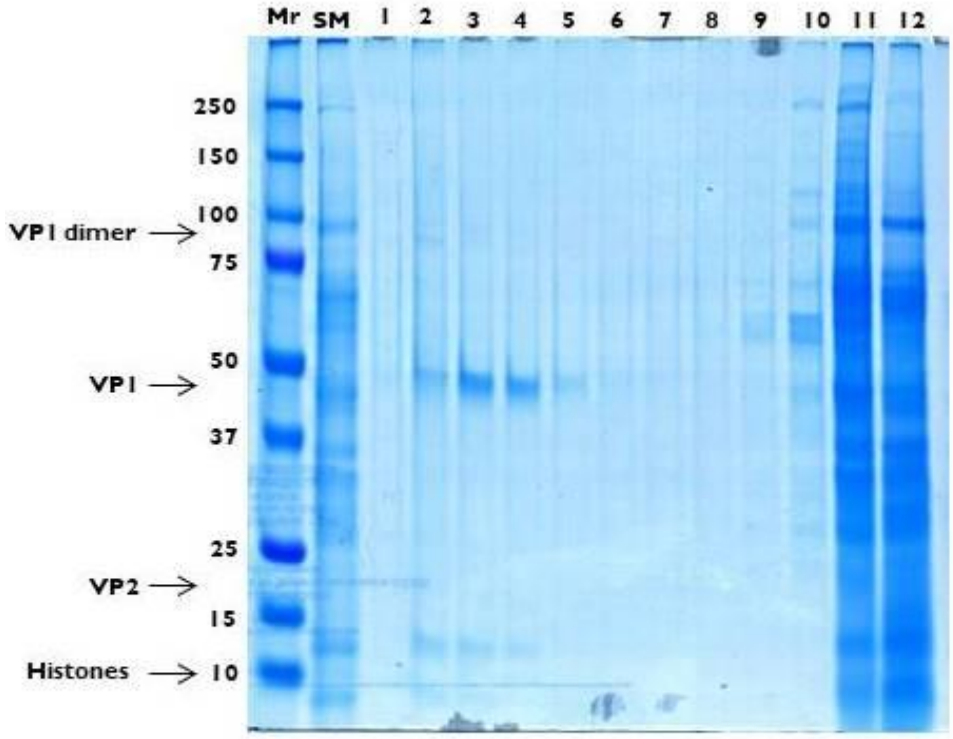


**Figure 3.3** Purified MCPyV pseudoviruses were ultracentrifuged on Optiprep gradients, fractions were collected from the bottom of the tube, run on SDSPAGE, and the gel was stained with Coomassie. Mr is protein ladder markers Thermo #26619; SM is Starting material

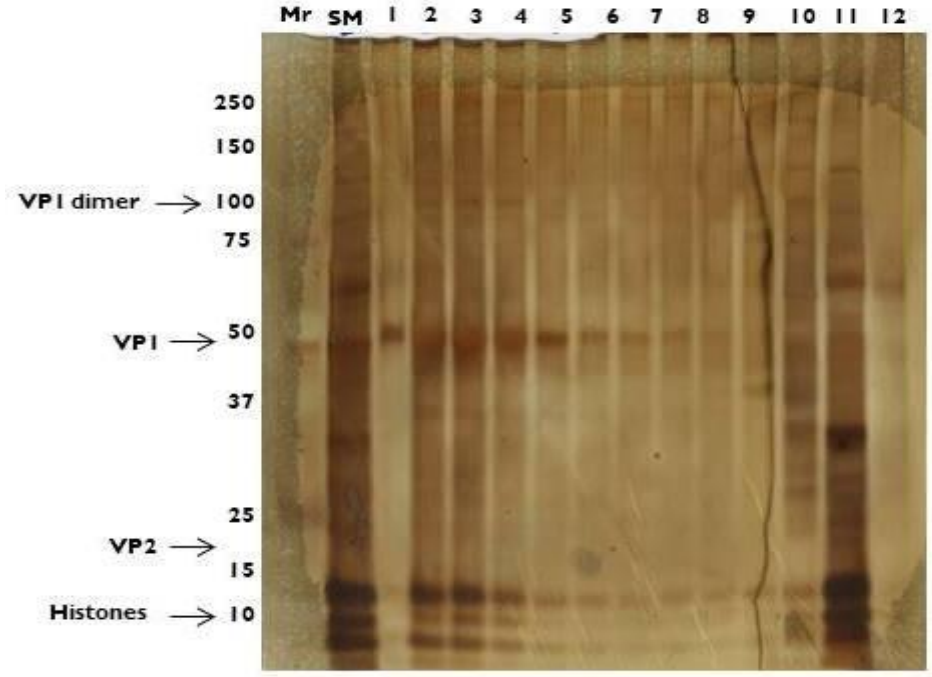


**Figure 3.4** Purified MCPyV pseudoviruses were ultracentrifuged on Optiprep gradients, fractions were collected from the bottom of the tube, run on SDSPAGE, and the gel was stained with Silver. Mr is protein ladder markers Thermo #26619; SM is Starting material.

The fractions containing virions were identified by the presence of VP1 and were typically found in the higher density fractions. The fractions containg mature virions, as well as the bands corresponding to VP1 and VP2 were analyzed by mass spectrometry (Figure 3.7), which verified the presence of MCPyV capsids. Importantly, the mass spectrometry of purified virus revealed the presence of a number of cellular proteins, including the core set of 4 histones and a number of other proteins involved in DNA metabolism or transcription.

Western blotting was used to analyze the separation on the Optiprep gradients produced from cells that were making VLPs GFP. These samples were blotted using an αGFP antibody (αGFP-HRP 1:500) to test the relative amount of contaminating cellular proteins in the VLP fractions. GFP immunoreactivity was found at the beginning and end of the Optiprep gradient but was not found in any of the fractions containing VLPs. These results indicate that the Optiprep gradient efficiently purified the VLPs from the majority of cellular proteins (Figures 3.5 and 3.6).

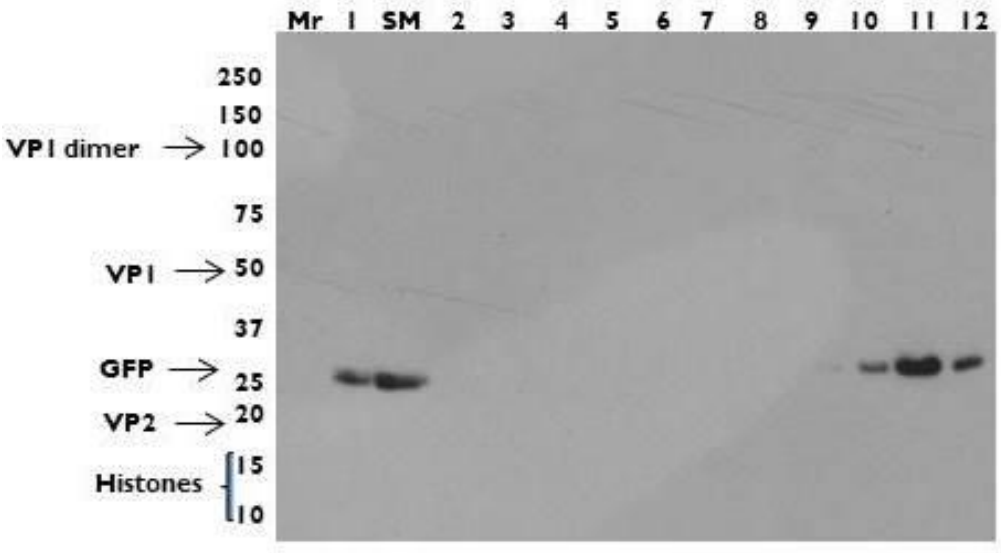


Figure 3.5 Purified MCPyV pseudoviruses Optiprep gradient fractions were analyzed by SDSPAGE and western blot with anti-GFP antibody. Mr is protein ladder markers Thermo #26619; SM is Starting material.

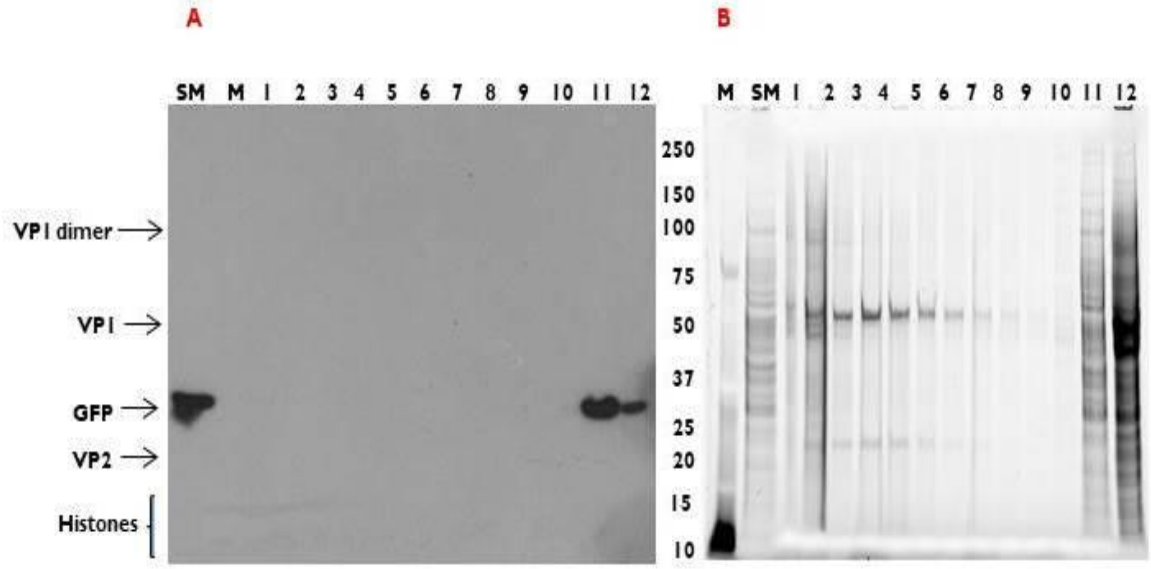


**Figure 3.6** Second Purified MCPyV pseudoviruses Optiprep gradient fractions were analyzed by two SDSPAGE gels A was stained with Trihalo system (0.5%TCE) and B by western blot with anti-GFP antibody. Mr is protein ladder markers Thermo #26619; SM is Starting material.

In order to test the presence of higher order complexes, I used ultrafiltration to fractionate the sample based on size and the resulting fractions were analyzed by SDS-PAGE (Figure 3.8).

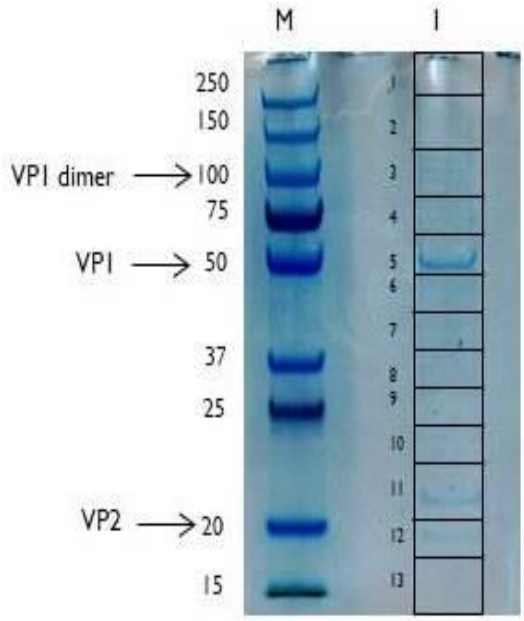


**Figure 3.7** Mass spectrometry identifies proteins from SDSPAGE Coomassie stained of pool purified MCPyV pseudoviruses Optiprep gradient fractions. Mr is protein ladder markers Thermo #26619; Line 1 was cut and each piece was digested and analysed by MS

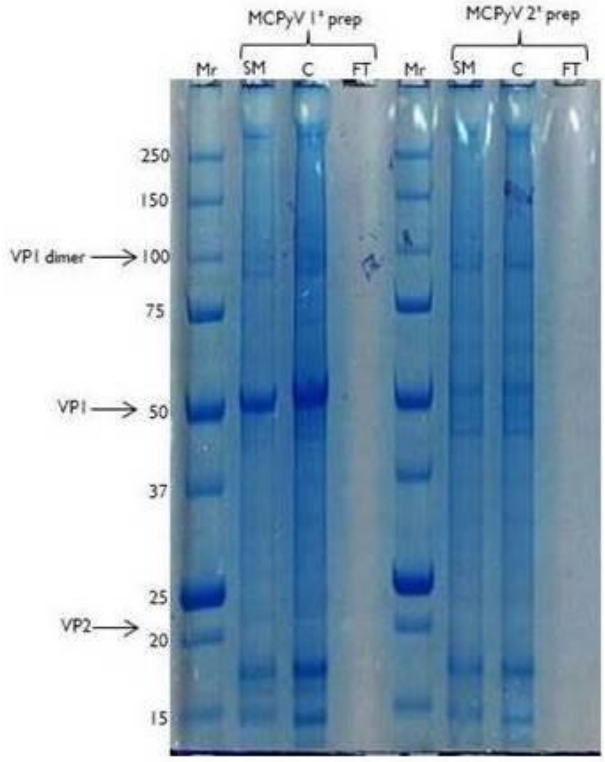


**Figure 3.8** Two Pools of gradient fractions (2to5) were ultrafiltered with a 100kD membrane, concentrate and flow through samples were analyzed by SDSPAGE and the gel was stained with Coomassie. Mr is protein ladder markers Thermo #26619; SM is Starting material.

Virtually all the proteins in these fractions remained in the concentrate, indicating that they are part of higher order complexes greater than 100 kDa and further indicate that the VLP preparation is not contaminated by free cellular proteins.

MS analysis was performed on the VLP containing fractions, either by in solution digest or on individual bands that were cut from the gel. The bands were proteolytic digested with trypsin and the resulting peptides were extracted from the gel. Protein identification was performed by nano LC-MS/MS and the resulting spectra were searched using the X!Tandem search engine.

Analysis of these samples by mass spectrometry identified 93 proteins. Gene ontology analysis reveals that many of these proteins are involved in the life cycle of other viruses, transcription, DNA replication and repair, protein folding, homeostasis and other types of nucleic acid binding proteins (Table 3.1). Table 3.2 contains the results from the LC-MS/MS analysis containing the most reproducible proteins.

**Table 3.1** Detailed information of the protein pathways identified with GO analysis from the GPM. The results were filtered based on p-value rate and only those results with a p-value < 0.05 are shown.

| pathway ID | pathway description | p-value |
|---|---|---|
| GO:0016032 | viral process | 3.42e-16 |
| GO:0071822 | protein complex subunit organization | 2.41e-15 |
| GO:0019058 | viral life cycle | 3.08e-14 |
| GO:0019083 | viral transcription | 9.59e-14 |
| GO:0019080 | viral gene expression | 2.73e-13 |
| GO:0043933 | macromolecular complex subunit organization | 4.38e-13 |
| GO:0006605 | protein targeting | 6.19e-13 |
| GO:0051084 | de novo posttranslational protein folding | 5.7e-12 |
| GO:0006457 | protein folding | 7.39e-12 |
| GO:0034655 | nucleobase-containing compound catabolic process | 5.12e-10 |
| GO:0015031 | protein transport | 3.82e-06 |
| GO:0010467 | gene expression | 6.09e-06 |
| GO:0090304 | nucleic acid metabolic process | 6.1e-06 |
| GO:0006461 | protein complex assembly | 6.28e-05 |
| GO:0070271 | protein complex biogenesis | 6.28e-05 |
| GO:0042981 | regulation of apoptotic process | 0.000105 |
| GO:0006259 | DNA metabolic process | 0.000841 |
| GO:0006310 | DNA recombination | 0.00245 |
| GO:0006974 | cellular response to DNA damage stimulus | 0.00347 |
| GO:0071158 | positive regulation of cell cycle arrest | 0.0045 |
| GO:0032508 | DNA duplex unwinding | 0.00797 |
| GO:0044774 | mitotic DNA integrity checkpoint | 0.00974 |
| GO:0006977 | DNA damage response, signal transduction by p53 class mediator resulting in cell cycle arrest | 0.0177 |
| GO:0072331 | signal transduction by p53 class mediator | 0.0202 |
| GO:0075733 | intracellular transport of virus | 0.0226 |
| GO:0031571 | mitotic G1 DNA damage checkpoint | 0.0248 |
| GO:0042769 | DNA damage response, detection of DNA damage | 0.0303 |

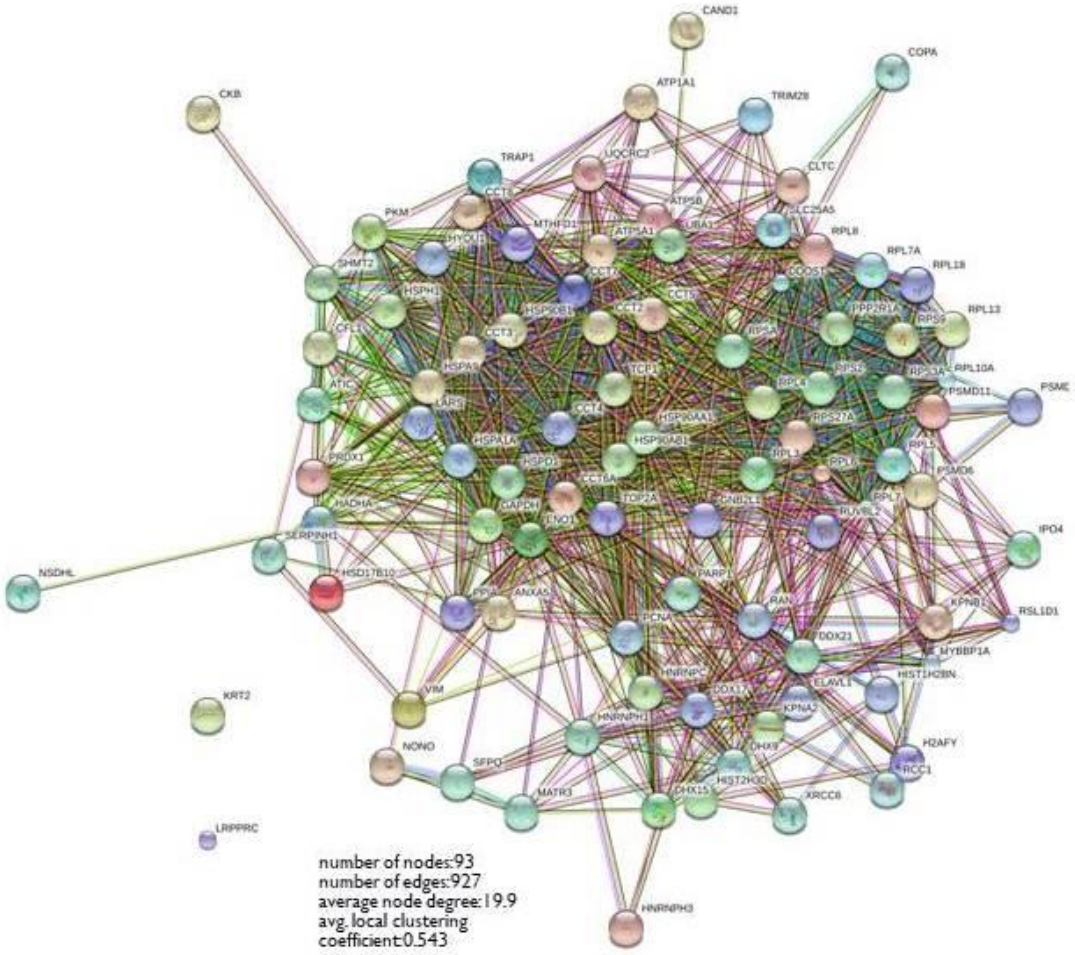


**Figure 3.9** Network Graph of the MCPyV VP1 protein Interactions involved in some way with the life cycle of the virus.

STRING was used to map the known interactions between these 93 proteins and 91 of these proteins are known to form interactions with each other (Figure 3.9).

In addition, the mass spectrometry data was searched for the PTMs of VP1. The search focused on phosphorylation, ubiquitinylation and acetylation as these are the most common PTMs (Figure 3.10). This resulted in the identification of 14 of phosphorylation sites, 6 acetylation site, and 7 of ubiquitinylation sites. Analysis by scan site indicated that a number of kinases are likely to phosphorylate VP1, and although a prevalence of proline directed sites were found by mass spectrometry, none of these were identified as potential sites of known proline directed kinases, such as the cdks. Importantly, there is

an antagonistic relationship between acetylation and ubiquitinylation as these two modifications target lysine residues. In fact, we find some lysine residues that carried the ubiquitin mark or the acetyl mark, while 5 of the residues could carry either mark (Figure 3.10). The function of these modifications is currently unclear.


**Figure 3.10** Summary of PTM identification and sequence coverage of VP1 protein based on combined mass spectrometric analyses. The grey highlighted amino acids were not found in LC-MS/MS. The red highlighted amino acids as phosphorylated. The blue highlighted amino acids were ubiquitinylated. The yellow highlighted amino acids were acetylated. The green highlighted amino acids were found to be either acetylated or ubiquitinylated.

**Table 3.2** Identification of proteins co-purified through Optiprep gradient and analyzed by mass spectrometry ESI-IonTrap with the most relevant proteins are highlighted in red.

| % measured | % corrected | unique | total | Description |
|---|---|---|---|---|
| 79 | 100+ | 41 | 689 | VP1 [Merkel cell polyomavirus] |
| 37 | 54 | 25 | 133 | HSP90AB1:p , heat shock protein 90 alpha family class B member 1 [Source:HGNC Symbol;Acc: HGNC:5258 ] |
| 56 | 64 | 23 | 248 | ACTG1:p , actin gamma 1 [Source:HGNC Symbol;Acc: HGNC:144 ] |
| 17 | 25 | 13 | 43 | HSP90AA1:p , heat shock protein 90kDa alpha (cytosolic), class A member 1 [ Source: HGNC 5253 ] |
| 48 | 58 | 17 | 56 | ATP5B:p , ATP synthase F1 subunit beta [Source:HGNC Symbol;Acc: HGNC:830 ] |
| 29 | 40 | 19 | 51 | EEF2:p , eukaryotic translation elongation factor 2 [Source:HGNC Symbol;Acc: HGNC:3214 ] |
| 40 | 60 | 15 | 121 | TUBB:p , tubulin beta class 1 [Source:HGNC Symbol;Acc: HGNC:20778 ] |
| 37 | 53 | 14 | 54 | EIF4A1:p , |
| 12 | 18 | 15 | 39 | DHX9:p , DExH-box helicase 9 [Source:HGNC Symbol;Acc: HGNC:2750 ] |
| 31 | 58 | 15 | 92 | EEF1A1:p , eukaryotic translation elongation factor 1 alpha 1 [Source:HGNC Symbol;Acc: HGNC:3189 ] |
| 15 | 20 | 11 | 42 | UBA1:p , ubiquitin like modifier activating enzyme 1 [Source:HGNC Symbol;Acc: HGNC:12469 ] |
| 14 | 21 | 11 | 19 | HSP90B1:p , |
| 29 | 37 | 10 | 49 | ENO1:p , enolase 1 [Source:HGNC Symbol;Acc: HGNC:3350 ] |
| 23 | 31 | 12 | 23 | HNRNPM:p , heterogeneous nuclear ribonucleoprotein M [Source:HGNC Symbol;Acc: HGNC:5046 ] |
| 19 | 25 | 10 | 28 | EEF1G:p , |
| 13 | 18 | 8 | 20 | HSPA1A:p , heat shock protein family A (Hsp70) member 1A [Source:HGNC Symbol;Acc: HGNC:5232 ] |
| 7.1 | 10 | 2 | 2 | HIST1H2BG:p , histone cluster 1 H2B family member j [Source:HGNC Symbol;Acc: HGNC:4761 ] |
| 7.7 | 11 | 6 | 21 | PARP1:p , poly(ADP-ribose) polymerase 1 [Source:HGNC Symbol;Acc: HGNC:270 ] |
| 16 | 19 | 4 | 6 | PCNA:p , proliferating cell nuclear antigen [Source:HGNC Symbol;Acc: HGNC:8729 ] |
| 6.5 | 9 | 4 | 5 | HSPH1:p , heat shock protein family H (Hsp110) member 1 [Source:HGNC Symbol;Acc: HGNC:16969 ] |
| 8.7 | 30 | 3 | 22 | VP2 [Merkel cell polyomavirus] |
| 3.9 | 6 | 2 | 3 | HSPA8:p , heat shock protein family A (Hsp70) member 8 [Source:HGNC Symbol;Acc: HGNC:5241 ] |
| 7.3 | 10 | 3 | 3 | HSPD1:p , heat shock protein family D (Hsp60) member 1 [Source:HGNC Symbol;Acc: HGNC:5261 ] |
| 4.8 | 8 | 2 | 2 | H2AFY2:p , H2A histone family member Y2 [Source:HGNC Symbol;Acc: HGNC:14453 ] |
| 2.7 | 4 | 2 | 2 | DDX3X:p , DEAD (Asp-Glu-Ala-Asp) box helicase 3, X-linked [ Source: HGNC 2745 ] |
| 2.2 | 3 | 2 | 2 | COL6A2:p , collagen type VI alpha 2 chain [Source:HGNC Symbol;Acc: HGNC:2212 ] |

In order to begin testing if any of the identified proteins are packaged inside the capsid, I treated the purified VLPs with acetic anhydride. This results in the non-specific acetylation of surface exposed lysine residues, which can then be detected using an anti-acetyl-lysine

antibodies (Figure 3.11). VP1 is acetylated upon acetic anhydride treatment and no acetylated proteins were detected in the absence of acetic anhydride treatment. Importantly, the histones are not acetylated regardless of the treatment indicating that the capsid is able to exclude acetic anhydride under the conditions used and that the histones packaged into the capsid do not carry an acetyl mark and are probably not transcriptionally active. Analyzing these acetic anhydride treated samples by mass spectrometry is one of my future aims, as this should allow me to determine which proteins are inside and outside the capsids, as those inside the capsids will not become acetylated in response to acetic anhydride.

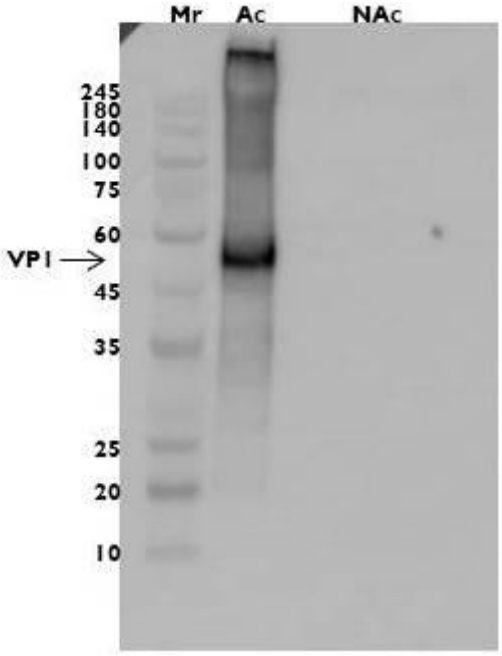


**Figure 3.11 Acetylation of MCPyV pseudovirus.** Optiprep gradient fractions were pooled and blotted with Anti-acetyl lysine antibodies. Mr is the protein ladder SMOBIO #PM2610, AC is sample treated with Acetic Anhydride and NAc is the untreated sample.

## 4. CONCLUSIONS

Viruses are under tremendous evolutionary pressure and there are a number of ways that organisms use to combat viral infection. However, once the virus enters the cell, which is not so obvious as there are more defense mechanisms of the cell to prevent it, it begins to exploit the cellular structures and processes to decompress their genetic load and start production replication and these processes depend on a variety of interactions between viral and host proteins.

While, the interactions of viral proteins with cellular proteins are clearly important, our understanding of these interactions, especially outside the replicative life cycle, is typically incomplete. Many viruses dramatically remodel the host's cellular pathways to their own aims, and it is often not clear why certain pathways are targeted, especially in cases like HIV, where there can be a long period of dormancy, or in cases such as polyomavirus, where there is usually very little pathology until the host's immune system is compromised. In addition, there are several unanswered questions on the mechanism of virus assembly and packaging, including uncovering the cellular proteins that participate in these process and whether or not the cellular proteins that are packaged inside the virions play a role in the next infective cycle.

I produced VLPs of MCPyV by transfecting HEK293TT cells with plasmids that overexpress two viral proteins: VP1 and VP2. This results in the self assembly of capsids that behave similarly to the infective virions. The VLPs were purified with Optiprep gradients, which separate proteins by their apparent densities. The VLPs were analyzed by ultrafiltration, SDS-PAGE, and western blotting, which revealed that the VLPs were highly purified and that most proteins were part of higher order complexes. Mass spectrometry (MS) was exploited to identify the viral and cellular proteins in the VLP preparation. Only two MCPyV proteins were identified, VP1 and VP2, and a number of PTMs were identified on VP1. The role that these modifications play in the MCPyV lifecycle is not

clear, but they may increase the functions of VP1 as I also usually found the corresponding unmodified residue.

The VLPs also contained as many as 93 cellular proteins. This data set is enriched GO terms relating to the viral lifecycle and a database of protein : protein interactions revealed that 91 of these proteins can be found as part of the same network. Of these 91 proteins, I have chosen three possible cellular proteins that could interact with the protein VP1, namely PARP1, Histone and HSP90, for further discussion.

PARP-1 is a nuclear protein, whose main role is to identify DNA single-strand breaks (SSB) and signal to the enzymatic apparatus involved in SSB repair. PARP-1 modifies itself as well as the chromatin proteins involved in the repair process. PARP-1 attaches a string of ADP-ribose molecules to the target protein. Viral chromatin is enclosed in an icosahedral capsid of 72 pentamers of the main capsid protein VP1, with each pentamer associated with one VP2 protein (*Eckhart 1990*). Furthermore, VP1 interacts with the entire viral genome in mature particles, (*Carbone et al. 2004*) suggesting that VP1 can contribute to modulating or maintaining the compaction of chromatin of the encapsulated viral DNA. The condensation of the minichromosome is initially promoted by the histone linker H1 until it is removed by VP1 during the final maturation of the viral particles (*Yuen, Consigli 1985*). A possible role played by PARP-1 could be the remodeling of chromatin through the modification of histone and transcription factors and in the modulation of viral gene expression (*Carbone et al. 2006*).

Early viral transcription has been shown to be reduced by competitive PARP inhibitors in 3T3 cells and almost abolished in PARP-1 knockout fibroblasts and wild-type fibroblasts when PARP-1 was silenced by RNA interference. (*Carbone et al. 2006*). Carbone and collaborators have seen that from in vitro experiments the viral protein VP1 stimulates the enzymatic activity of PARP-1 and binds non-covalently. (*Carbone et al. 2006*). Then it could be that PARP-1 packs inside the virion, so that it is already present when it is needed to promote viral transcription.

Histones are basic proteins that make up the structural component of chromatin. The large number of basic residues in Histones promotes the interaction between Histones and the negatively charged DNA, which forms structures called nucleosomes. Histones are among the most conserved eukaryotic proteins during the course of evolution, in fact most changes to their sequence are lethal, which confirms their fundamental role in chromatin compaction. However, unlike cellular chromatin, polyomavirus minichromosomes do not have histone H1 (*Fang et al. 2010*). Histone H2A is one of the five major histone proteins involved in chromatin structure in eukaryotic cells and was identified by mass analysis. To date, five families of histones are known; which are called H1 / H5, H2A, H2B, H3 and H4 (*Cox et al. 2005*). The histone H2A is composed of non-allelic variants (*Bosch et al. 1995*). The term "histone H2A" is intentionally non-specific and refers to a variety of closely related proteins that often vary only by some amino acids. The variant that resulted from the mass analysis is MacroH2A a variant similar to H2A and is encoded by the H2AFY gene. This variant differs from H2A due to the addition of a fold domain in its C-terminal queue. The MacroH2A variant is expressed in the X chromosome inactive in females (*Costanzi et al. 1998*). This last statement allows us to speculate on the fact that there is a correlation between the incidence of MCC on male patients compared to female patients, explaining the fact that the histone protein is transported by the virion. We know that the modification of histone proteins can lead to a change in function, such as phosphorylation that occurs due to rupture of the dsDNA (*Talbert et al. 2010*) or acetylation, however the modification of H2A is currently underway of research.

Histones are also cationic proteins involved in antimicrobial activities. In vertebrates and invertebrates, the histone H2A variant is involved in the host immune response acting as an antimicrobial peptide (AMP) (*Arockiaraj et al. 2013*). It could be that the virus, by encapsulating this protein for example by preventing its acetylation, prevents it from acting as an antimicrobial agent. In fact, in treating the virion sample with acetic anhydride

it was found that the histone protein does not acetylated, presumably because it is protected by the capsid itself.

Hsp90 is an abundant cellular chaperone that interacts with many proteins, including transcription factors, kinases, ligases, structural proteins, ribosomal components and metabolic enzymes (*Zuehlke et al. 2015*). Hsp90 is also known to be involved in the lifecycle of many viruses. Hsp90 participates in virus replication, the folding of structural proteins and assembly of virions (*Geller et al. 2012*). Given that Hsp90 is known to be a protein that binds microtubules (*Giustinian et al. 2009; Fostinis et al. 1992; Echeverria & Picard 2010*), it would be interesting to know if this chaperone mediates the interaction between VP1 and microtubules. The role of the HSP90 protein is not clear, it could simply be trapped in the virion after being involved in the assembly of the virion, or since it is used by estrogens to control the interaction of the estrogen receptor transcription factor to be involved in the life cycle of the virus or in the formation of the MCC. Estrogens are present in significant amounts in both men and women and in women are present in high quantities at the beginning of menstrual periods and puberty and then decrease with age. The primary function of estrogens is the development of female secondary sex characteristics, while in men estrogen helps in sperm maturation. Estrogen helps in protein synthesis and increases platelet adhesiveness and decreases antithrombin III, increases HDL and triglycerides while decreasing LDL, helps fetal development. The reduction of estrogen causes a significant lowering of mood and may predispose to depression. Estrogens improve collagen content and quality, increase skin thickness and improve interface blood supply by acting through estrogen receptors. The number of receptors varies in different parts of the body. The parts of the body with the greatest number of receptors are found on the face, above the thigh and the chest. This allows us to hypothesize that the HSP90 protein closely related to estrogen is somehow involved with MCC and would justify the fact that HSP90 is transported by the virion. Males also

have estrogen receptors but, to a lesser extent than women, estrogen levels in the male's blood are greater than those in post-menopausal women.

There are a number of questions that remain about the proteins that interact with the VLPs. The most important question is whether they play a role in the lifespan of the virus. It is possible that these proteins do not play a role in the lifecycle. However, if they do play a role, it seems likely that they either function early in the infective cycle, to promote a successful infection, or they are involved in the very late stages of capsid formation and packaging. The functions of these proteins are best determined in the background of a wild type virus, so these experiments should be repeated using a native virus. The function of the associated proteins can be determined by disrupting their expression, using siRNA or CRISPR/Cas9, in the packaging cell lines and then assessing various properties of the resulting virions. For example, the yield of viral particles and their infectivity will give a good indication of whether the knocked down protein is required during the late stages or the early stages of the MCPyV life cycle.

In addition, I currently do not know if the identified proteins are packaged inside the virion or if they are associated with the outside of the VLP. I have already begun to address this question by treating the purified VLPs with acetic anhydride. The acetic anhydride will covalently modify accessible lysine residues and proteins within the virion appear to be resistant to this modification, as the histones were not modified when the VLPs were treated with acetic anhydride. Importantly, another round of MS will be required to identify which proteins are modified by acetic anhydride treatment, and are on the outside of the particle, and which proteins are not, and are on the inside of the particle. I initially hoped that labeling with trihalo compounds could also be used for this purpose (appendix 1), but this modification is always incomplete and would not be suitable for these experiments.

# 5. APPENDIX Development of Trihalo Labeling for Protein Analysis

## 5.1 Abstract

Protein electrophoresis and western blotting are important techniques for protein detection and quantification. However, these techniques are long and labor-intensive processes and traditional protocols require approximately 2 days to complete. In addition to the many steps, such as sample preparation, gel casting, protein electrophoresis and transfer, membrane blocking followed by antibody incubation, etc., there is often a need to repeat parts of the process to ensure equal protein loading and to collect data that can be quantitated. Therefore, I investigated the performance of a "stain-free" procedure to confirm that the stain-free technology provides an easy and rapid protein visualization that can be used for the normalization of protein loading and the verification of transfer efficiency. The stain-free procedure is based on the UV-induced reactions of *Trihalo organic compounds* with tryptophan residues in proteins. The reaction of *Trihalo* compounds with tryptophan residues results in the creation of a new fluorophore that can be detected using a suitable imager. This chapter presents an optimized protocol that allows the proteins on a polyacrylamide gel to be viewed both before and after protein transfer. Finally, I adapted the *TriHalo* labeling to in solution reactions so that it may be useful for gaining structural information about protein complexes. There are many advantages of using *TriHalo*-based analysis including high sensitivity, wide linear dynamic range for quantitative accuracy, reproducibility, cost-efficiency, timesaving, ease of use, and compatibility with downstream protein identification such as western blotting and *mass spectrometry* (MS).

## 5.2 Introduction

### 5.2.1 Stain-free detection, basics of the UV light induced reaction

In *stain-free* detection a *trihalo compound* is used to induce the fluorescence of tryptophan amino acids when irradiated under UV light. Examples of suitable Trihalo compounds include: Trichloromethane (*Chloroform TCM), 2, 2, 2-trichloroethanol (TCE), trichloroacetic acid (TCA), 2, 2, 2-tribromoethanol (TBE), 2, 2, 2-trifluoroethanol (TFA),* These and other similar *trihalo compound* react with *indole* containing compounds, such as tryptophan in the presence of UV light. The characterization of indole derivatives reacting with *chloroform*, and other *trihalo* and *dihalo compounds* in photoreactions were reported by Ladner and co-workers (*Ladner et al. 2004*). For example, the two principal products formed in a photochemical reaction between *chloroform* and *tryptophan* are derivatives at carbon positions 4 (4-imido tryptophan) and 6 (6-formyl tryptophan) (Figure 5.1). Importantly, the reaction with trihalo compounds results in enhanced fluorescence from the modified tryptophan which can be easily detected (Figure 5.2).

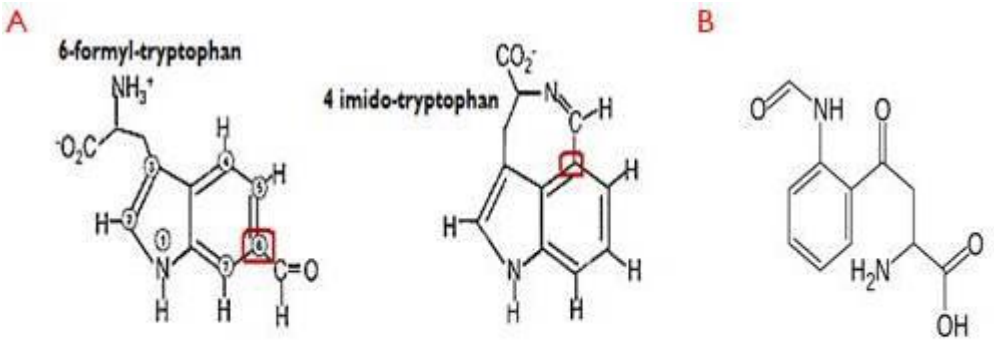


**Figure 5.1 UV-dependent modifications of tryptophan using chloroform:** The figure shows A: The structure of the two derivatives, in position 6 (left) and in position 4 (right) of the indole chromophore in tryptophan (*modified from Ladner et al. 2014*); B: N-formyl-kynurine forms upon UV exposure in the absence of trihalo compounds.

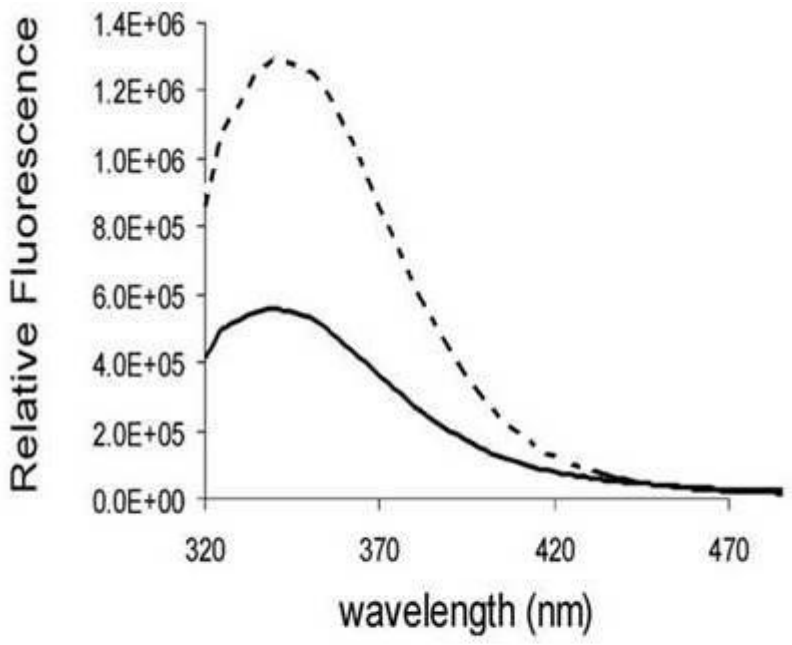


**Figure 5.2: TCE modified KWK products.** The figure shows a fluorescence emission spectra of tripeptide KWK (lysyltryptophanyllysine) reacted with TCE before (solid line) and after (dashed line) 10 min of irradiation at 280 nm with 40 mM TCE. (*modified from Ladner et al. 2006*).

The presence of *chloroform* in the reaction adds a *formyl group* (or *Aldehyde group −CHO*) to the aromatic chromophore (Figures 5.1 and 5.3) *(modified from Ladner et al. 2006).* In contrast, when no *trihalo compound* is present, N-formyl-kynurenine (NFK) (Figure 5.1B) is the only photoreaction product. After an initial photoreaction of *indole* with a *trihalo compound*, further reactions with water result in the complete release of the halogen atoms (Figure 5.4). Although the modifications added by other trihalo compounds are different from chloroform, for most of the compounds tested, the fluorescence excitation and emission wavelengths are similar to those obtained from reactions with chloroform. Trichloroethanol (TCE) reacts more quickly than chloroform, but in an analogous way it adds the halo compound carbon skeleton to the *indole ring*, modifying the *indole ring carbon atom* of the reactant to a carbonyl. *Trichloroacetate* (TCA) mass addition (*+44 AMU*) implies that a *carboxyl group* (C (=O)OH )is added (*Ladner et al. 2007*). In particular, this product has nearly the same fluorescence properties as the *formyl* products

mentioned above, but has much less intensity. The photoreaction with *trihalo compounds* makes a significant change: it enlarges the conjugated system in the *indole* chromophore, which is not the case with *mono halo compounds* (Figure 5.3).

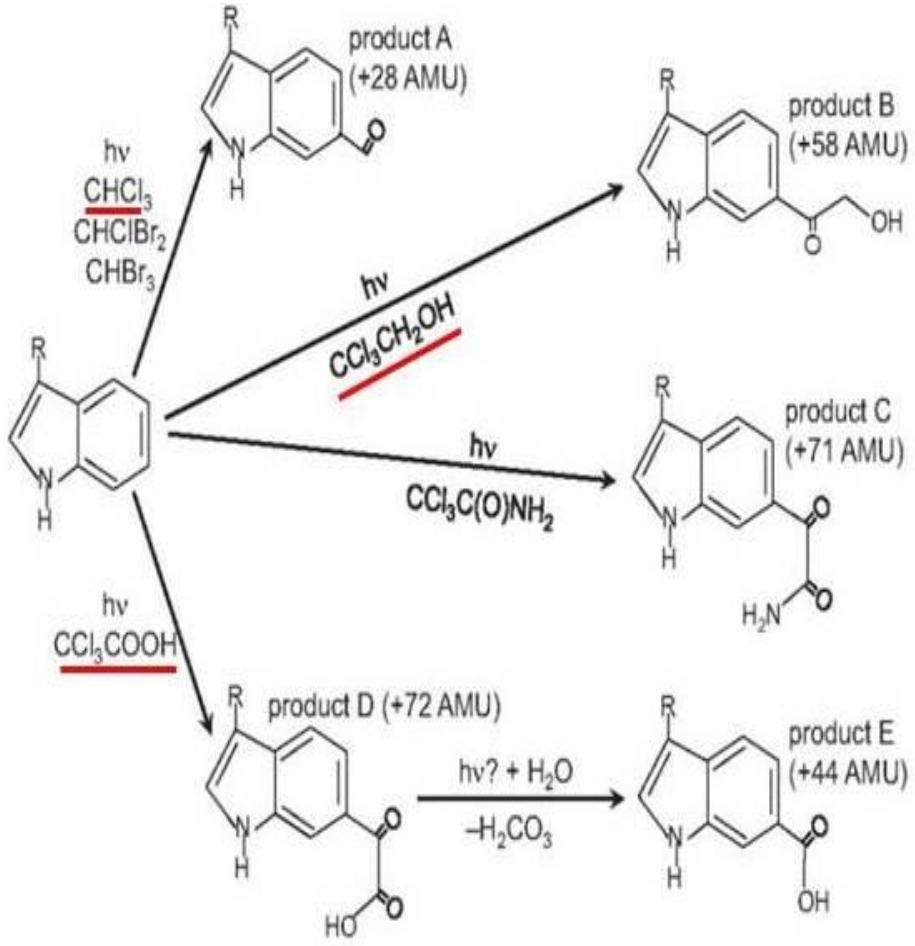


**Figure 5.3 Photoreactions of the indole chromophore with different trihalo compounds.** The mass additions reported after reactions with both lysyltryptophanyllysine and leucyltryptophanylleucine are shown. With trichloroacetic acid a hydrolysis product that modifies product D to product E with a decrease of 28 AMU, is also shown (three trihalo compounds of our interest are underlined in red: chloroform ($CHCl_3$), 2, 2, 2-trichloroethanol ($CCl_3CH_2OH$) and trichloroacetic acid ($CCl_3COOH$)) (*Ladner et al. 2014*).

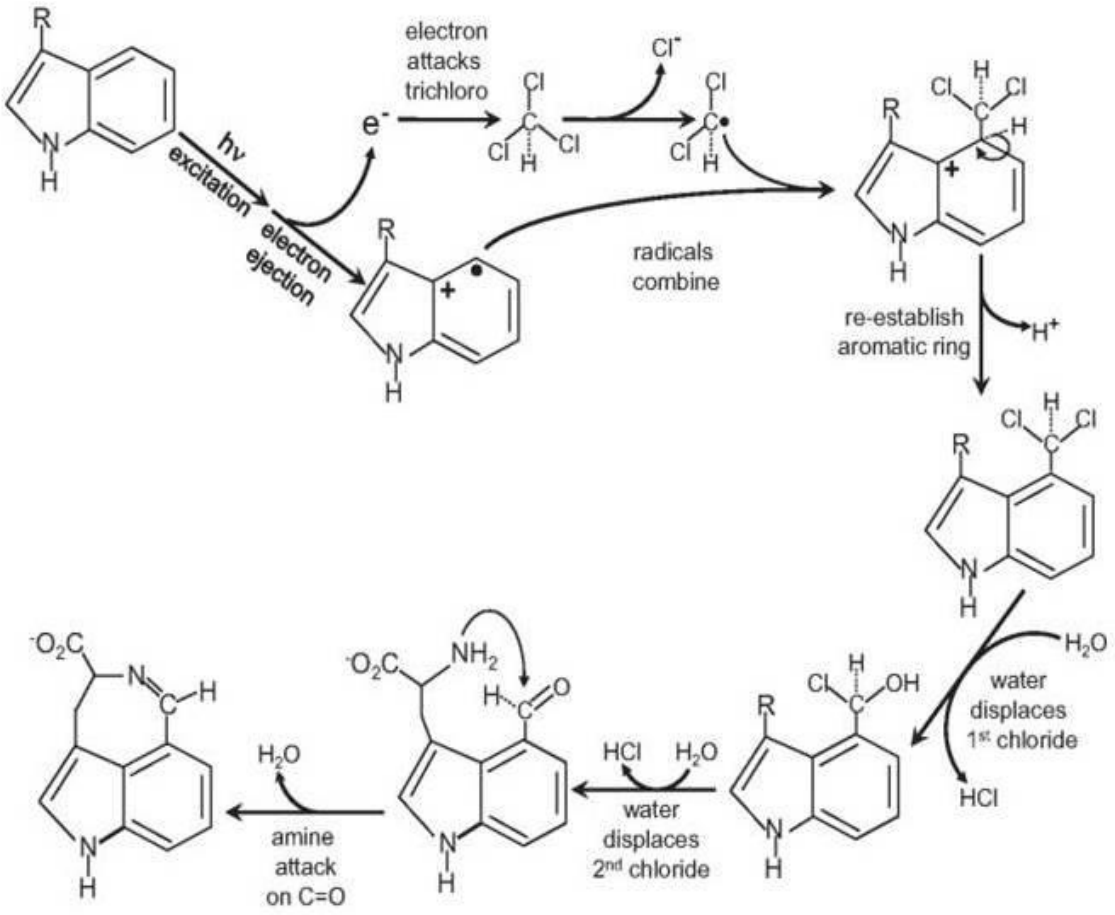


**Figure 5.4 Proposed mechanism for the photoreaction of an indole ring with chloroform** Proposed mechanism for the photoreaction of an indole chromophore with chloroform after ejection of an electron from the excited indole. The ejection of the electron produces a radical cation which can combine with the dichloromethane radical to produce the addition product. Reestablishment of the aromatic ring leads to a dichloro-intermediate which rapidly reacts with water to form the formyl derivative. If there are amine groups (as in tryptophan) which are sterically able to react with the carbonyl group, then in the final step an imine can be formed. (*Ladner et al. 2014*).

In stain-free polyacrylamide gels, after protein sample loading, the UV light induces release of an electron from the indole ring of tryptophan, this electron reacts with the trihalo compound, resulting in the covalent binding of the trihalo compound to the light-activated tryptophan residue, due to the high sensitivity of fluorescent detection, this chemistry allows for the detection of proteins down to 20–50ng per band. The UV dependent addition does not appear to interfere with downstream steps, such as immunoblotting. Addition of the trihalo compound enhances the rate of the photochemical reaction that produces fluorescence. In fact, chloroform increases the rate of photobleaching of the indole fluorophore nine-fold over when no trihalo compound is present, making the rate

of the background reaction without trihalo compounds inconsequential (*Ladner et al. 2014*).

A method to fluorescently visualize proteins in polyacrylamide gels using chloroform and trichloroacetic acid (TCA) was reported (*Kazmin et al. 2002*). It consists of soaking the gel in TCA, followed by a 300nm UV light illumination in order to obtain a fluorescent product. This process depends on tryptophan content. If tryptophan residues are lacking in a protein, this protein is not detected; however, in most organisms, at least one tryptophan is contained in 90% of proteins and the majority of the proteins lacking in tryptophan are less than 10kD in size (Table 5.I).

**Table 5.1:** Tryptophan (W) content of the predicted proteomes of several model organisms (from UniProt database modified from BioRad).

| Species | Total # of proteins | # of proteins lacking W | % of proteins lacking W | # of proteins > 10kD | # of proteins > 10kD lacking W | % of proteins >10kD lacking W | # of proteins < 10kD lacking W | % of proteins <10kD lacking W |
|---|---|---|---|---|---|---|---|---|
| *Homo sapiens* | 40,827 | 4,209 | 10.31 | 37,548 | 2,754 | 7.33 | 1455 | 3.56 |
| *Escherichia coli O:K1 / APEC* | 4,865 | 458 | 9.41 | 4,754 | 408 | 8.58 | 50 | 1.03 |
| *Escherichia coli (strain K12)* | 4,181 | 456 | 10.91 | 3,879 | 325 | 8.38 | 131 | 3.13 |
| *Rattus norvegicus* | 12,022 | 1,081 | 8.99 | 11,421 | 745 | 6.52 | 327 | 2.72 |
| *Mus musculus* | 35,344 | 3,435 | 9.72 | 33,262 | 2,480 | 7.46 | 955 | 2.70 |
| *Saccharomyces cerevisiae* | 5,815 | 648 | 11.14 | 5,563 | 491 | 8.83 | 157 | 2.70 |

After *stain-free* it is possible to proceed with CBB (*Coomassie Brilliant Blue*) staining and visualization (*Ladner et al 2004*).

### 5.2.2 Stain-free method as a reliable total protein loading control

Western blotting is a biochemical technique that allows the identification of a specific protein from complex mixtures of proteins, via the recognition by specific antibodies. In general, the protein mixture is first separated using a polyacrylamide gel, which is subsequently transferred onto a membrane support, such as nitrocellulose.

Western blot analysis is routinely employed for quantifying differences in protein levels between samples. To control equal loading and compensate loading differences, immunodetection of "housekeeping" proteins (HKPs) is commonly used. HKPs may show inconsistency in their expressional level under modifications in experimental conditions, for example actin is a frequently used housekeeping gene, but its levels change during the cell cycle (*Rubin et al. 1978*). On the other hand, total protein normalization (TPN) makes use of the signal intensity from the entire lane of the sample loaded as a loading control for the respective target protein. TPN resolves issues related to stripping and reprobing of the membrane, where it is important to ensure that the primary antibody previously used is totally removed, leaving no residual signals. Total protein stains, such as Ponceau S, Sypro Ruby, Amido Black, have been used for TPN but they can negatively affect downstream applications and/or are difficult to image. At the same time, a proper verification tool that can also be used for a reliable quantitation would be of a major interest for western blot experiments. With *trihalo labeling*, reprobing steps can be avoided, as it does not require HKP immunodetection for normalization, and trihalo labeling validates differences in the level of the protein of interest using total protein measurement as the loading control (*Posch 2013*).

## 5.3 Aim of the Appendix

Light dependent reactions with *trihalo compounds* allows for the rapid fluorescent detection of proteins without the need for additional staining or destaining steps. Currently, trihalo labeling is only available in commercial precast gels, and I set out to optimize trihalo labeling for both qualitative and quantitative analysis of western blots with laboratory-made gels. In addition, I adapted the triHalo labeling technique to solutions of proteins, rather than being limited to only gel based labeling. This increases the versatility of the technique so that it can be used for protein visualization in gels and directly on blots and as a tryptophan specific label for the mass spectrometry analysis of proteins. These studies show that labeling with *trihalo compaunds* gels does not interference with the analysis of protein samples by mass spectrometry and or western blotting.

## 5.4 Materials and Methods

### 5.4.1 Materials

**Table 5.2:** List of chemicals, kits and consumables used.

| ***Product*** | ***Description; Manufacturer*** |
|---|---|
| Chloroform, TCA, TCE, DCM, TFE, TBE, TFA | Standard chemicals were obtained from Sigma-Aldrich with analytical grade (>99%) |
| Bradeford-Protein determination | Bio-Rad Laboratories |
| Luminol reagent | Clarity™ Western ECL Blotting Substrate Bio-Rad Laboratories |
| Mini-PROTEAN TGX Precast Gels | Bio-Rad Laboratories |
| Protein standard | PageRuler Plus Prestained (*cat. # 1610374*) Bio-Rad Laboratories and Thermo (*cat. #26619*) and PageRuler Unstained (*cat. #1610363*) Bio-Rad Laboratories |
| PVDF-Membrane | Immobilon; Millipore GmbH |

### 5.4.1.3 Buffers and solutions

**Table 5.3:** List of buffers and solutions used.

| ***Description*** | ***Composition*** |
|---|---|
| Laemmli sample buffer (6x) | 7mL 4xTris/SDS pH 6.8 (3.02g Tris; 0.2g SDS; 50mL $ddH_2O$; pH 6.8); 3.6mL Glycerin; 1g SDS; 0.93g DTT; 1.2mg Bromophenol blue; 10mL $ddH_2O$ |
| Bloking solution | 5% milk powder in TBS-T or 1% BSA in TBS-T |
| PBS | Dulbecco´s Phosphate Buffered Saline; Sigma Aldrich |
| MOPS Running buffer (10X) | 60.6g Tris base, 104.63g MOPS, 3.8g EDTA powder (MW 372.24), 10g of SDS powder. |
| bis-Tris (3.5X Stock) | 1.25M bis-Tris HCl pH 6.8 (65.40g add $ddH_2O$ (200mL) adjust pH with HCl 37% and bring the volume to 250mL with $ddH_2O$). |

### 5.4.1.4 Software and databases used

**Table 5.4:** Software used.

| ***Software*** | ***Manufacturer*** | ***Use*** |
|---|---|---|
| Image Lab | Bio-Rad Laboratories | Western blot- and agarose gel analyses Stain-free detection activation, visualization and analyses |
| The GPM | The Global Proteome Machine Organization | Proteomics data analysis |
| Data analysis Bruker | Bruker Daltonics | Mass spectrometry Analysis |

**Table 5.5:** List of antibodies used

| Antigen | Origin | Animal | MW | Type | Epitope |
|---|---|---|---|---|---|
| β-actin | Cell Signalling #3700 | Mouse Monoclonal | 45 | primary | Product with synthetic peptide corresponding N-Term of human β-actin |
| p53 | Cell Signalling #9282S | Rabbit Polyclonal | 53 | primary | Product with full length human p53 |
| H3(1B1B2) | Cell Signalling #14269S | Mouse Monoclonal | 17 | primary | Product with peptide C-Term of human H3 |
| PTEN | Cell Signalling #9188S | Rabbit Monoclonal | 54 | primary | Product with peptide C-Term of human PTEN |
| p21 | Santa Cruz #sc-397 | Rabbit Polyclonal | 21 | primary | Product with peptide C-Term of human p21 |
| Cofilin (D59) | Cell Signalling #3318S | Rabbit Polyclonal | 19 | primary | Product with synthetic peptide surrounding Asp (D) 59 |
| PCNA | Santa Cruz #sc-25280 | Mouse Monoclonal | 36 | primary | Product with linear peptide corresponding to aa 1-261 of human PCNA |
| ACE_H3 | Millipore #06599 | Rabbit Polyclonal | 17 | primary | Product with linear peptide corresponding to human H3 acetylated of N-Term |
| p84 | AbCam #ab487 | Mouse Monoclonal | 84 | primary | Product with fusion protein containing aa 15-574 of human p84 |
| GFP | Santa Cruz #sc-9996 | Mouse Monoclonal | 27 | primary | Product with synthetic peptide aa 1-238 of GFP protein |
| Actinin | Santa Cruz #sc-17829 | Mouse Polyclonal | 100 | primary | Product with peptide aa 593-892 of human actinin |
| mouse IgG HRP-conjugated | Santa Cruz #sc-17829 | goat | | secondary | |
| rabbit IgG HRP-conjugated | Santa Cruz #sc-17829 | goat | | secondary | |

### 5.4.2 Methods

#### 5.4.2.1 Protein quantification by the Bradford method

The assay was performed as described by the manufacturer and a standard curve was generated using BSA as a standard. Dilutions of the protein samples were prepared to fit the linear range of the calibration curve.

#### 5.4.2.2 MOPS SDS-PAGE

To prepare *stain-free* handcast mini-gels, 10mL of the gel mix stock was mixed with 50µL of one of the *trihalo compound* (*Chloroform* (TCM), *2, 2, 2-trichloroethanol* (TCE), trichloroacetic acid (TCA), *2, 2, 2-tribromoethanol* (TBE), *2, 2, 2-trifluoroethanol* (TFE); *Dichloromethane* (DCM) and *2-Chloro Acetamide* (2ClAA) then 100µL APS (10%) and 3µL TEMED were added to initiate the polymerization. Prior to loading, the protein samples were heat denaturized for 5 min at 95°C.

#### 5.4.2.3 Activation of trihalo-based SDS gel

After electrophoresis, the gel was carefully removed from the cassette and placed on the tray of a ChemiDocTM Touch (*Bio-Rad Laboratories GmbH*) to activate the photochemical reaction of the trihalo compound with tryptophan. Activation was done for 45 – 300 seconds at wavelength 300 nm.

#### 5.4.2.4 Western blot

#### 5.4.2.5 Semi-Dry blot protein transfer

Protein transfer from the gel to a nitrocellulose membrane was carried out using the semi-dry blotting procedure (*Kyhse-Andersen 1984*). Briefly, a transfer membrane and filter sheets were cut to fit the measurement of the gel, the filter papers and membrane were equilibrated in the transfer buffer for at least 1 minute. A transfer sandwich between two electrodes was prepared. The air bubbles were removed from the transfer sandwich and the transfer was performed at 60 mA per gel (0.8 mA / $cm^2$) for 90 min.

Prior to transfer, UV irradiation of the gel is necessary to modify the tryptophan residues in the separated proteins (*Ladner et al 2004*). UV irradiation was performed on the Chemidoc MP System (*Bio-Rad Laboratories GmbH*), as stated above. Activation of the gel is necessary only once as the reaction is covalent and further imaging of the gels or membranes is done without another activation step. Afterwards the membranes can be imaged on Chemidoc MP System, which verifies the efficiency of protein transfer.

#### 5.4.2.6 Blocking, immunodetection and evaluation

Nonspecific protein binding was blocked by incubating the membrane for 2 h in nonfat dried milk powder (5%) in 1x TBS-T or BSA (1%) in 1x TBS-T at RT. After three washing steps with 1x TBS-T for 5 min, the membrane was incubated with the corresponding primary antibody diluted in blocking buffer on the rotatory mixer (5 rpm, 4°C, O/N). The following day, the membrane was washed three times in TBS-T and then incubated with the respective secondary antibody in blocking buffer for 1h at RT. In Table 6.6, the antibodies used in this work are listed, with the name, type, the producer, host animal, dilution and epitope. After a final set of washing steps, the blot was developed with ECL reagents (*Bio-Rad Laboratories GmbH*). The resulting signal was visualized using the ChemiDoc MP system and evaluated in the Image Lab program (*Bio-Rad Laboratories GmbH*).

## 5.5 Results

### 5.5.1 Trihalo labeling technology

Reliable loading controls are required for the proper interpretation of western blots. It is important that the blots do not show saturation or inconsistent expression level in different samples or experimental conditions. Influenced by these concerns that could potentially produce data artifacts, scientific journals are requiring stricter controls and imaging methods for quantitative comparisons (https://www.nature.com/nature-research/editorial-policies/image-integrity). Instead of using an HKP, which results in single band loading controls, total protein signals in each lane can be used as a loading control as an alternative solution. *Trihalo* labeling offers a rapid protein visualization method on polyacrylamide gels and transfer membranes, and is an ideal alternative to other total protein stains such as Ponceau S or Amido Black. In a typical application, trihalo labeling only adds an additional 5 minutes of time to the western blotting workflow.

### 5.5.2 Testing different halo compounds and concentrations

#### 5.5.2.1 Investigation of the optimal halo compound for in-gel visualization method.

In this study I explored pre electrophoresis, post electrophoresis and in gel labeling protocols and a number of different protocols for trihalo labeling. Initially, I included different *trihalo compounds* into the gel before polymerization. Compounds were tested at 0.5% or 2% and compared to CBB staining. A mix of a constant amount of BSA (1 µg) and increasing concentrations of Lysozyme (2.5 - 600 ng) were analyzed to assess the

performance of trihalo labeling. Labeling with TCM and TCE allows for rapid protein detection, which is significantly more sensitive than the standard CBB (Figure 5.5). The in-gel method compared to CBB staining shows that TCE and TCM labeling are more sensitive than CBB staining with the minimal detectable limits being 40ng for TCM and 200ng for CBB. Furthermore, the increasing concentrations of Lysozyme indicated a linear relationship between protein amount and labeling strength. While DCM was roughly as sensitive as CBB and no proteins were visualized with TFE or TCA (Figure 5.8).

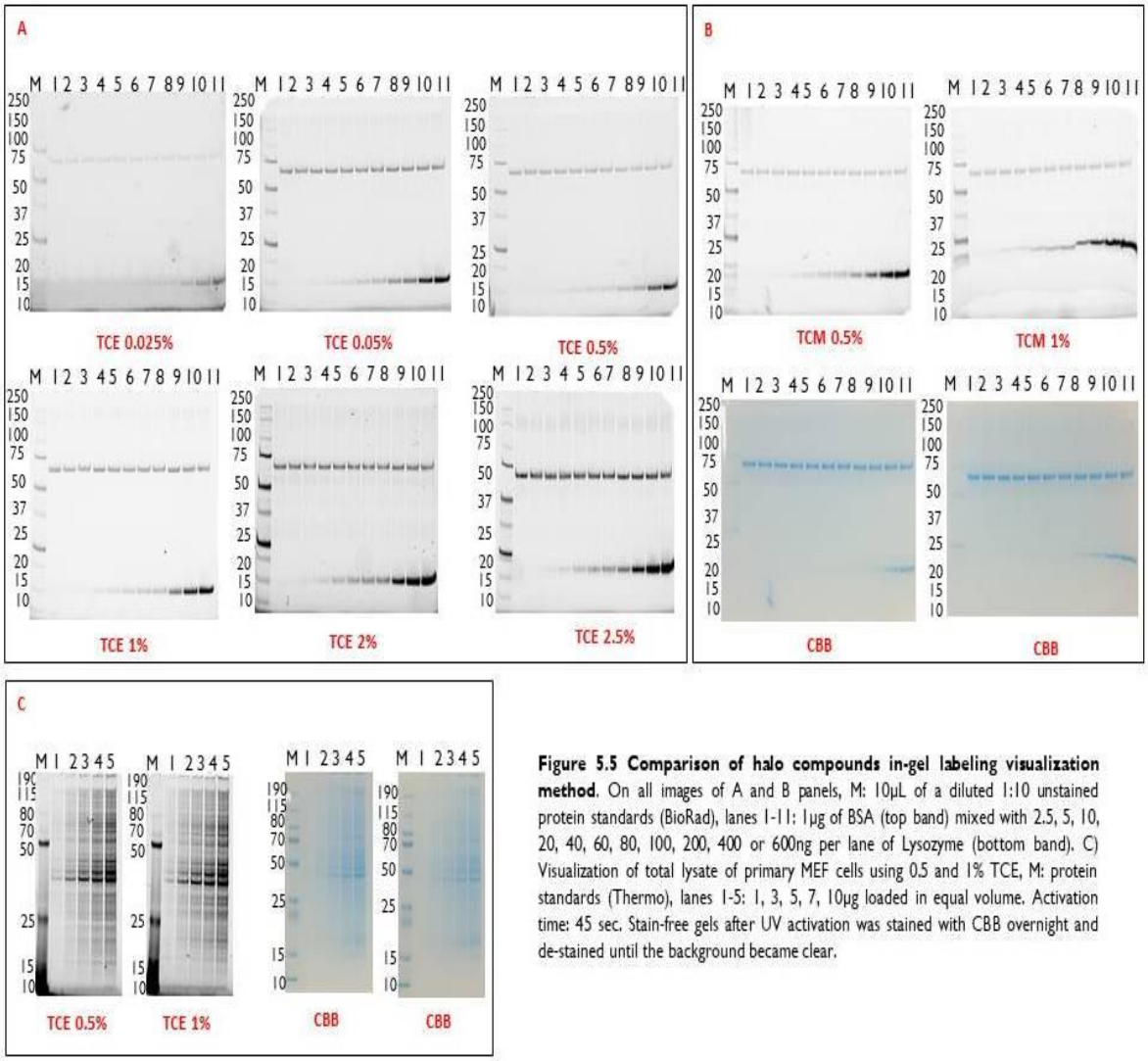


**Figure 5.5 Comparison of halo compounds in-gel labeling visualization method.** On all images of A and B panels, M: 10µL of a diluted 1:10 unstained protein standards (BioRad), lanes 1-11: 1µg of BSA (top band) mixed with 2.5, 5, 10, 20, 40, 60, 80, 100, 200, 400 or 600ng per lane of Lysozyme (bottom band). C) Visualization of total lysate of primary MEF cells using 0.5 and 1% TCE, M: protein standards (Thermo), lanes 1-5: 1, 3, 5, 7, 10µg loaded in equal volume. Activation time: 45 sec. Stain-free gels after UV activation was stained with CBB overnight and de-stained until the background became clear.

### 5.5.2.2 Comparison of using different concentration of *trihalo compounds* for in-gel visualization method.

I tested TCM and TCE compounds at different concentrations in the range from 0.025% to 2% in-gel visualization method and using the same mixture of BSA and Lysozyme or using total lysate of primary MEF cells as the sample. The TCE signal intensity increased proportionally with the concentration (Figures 5.5A and 5.5C). I found that TCM was problematic, in that it affected the quality of the electrophoresis when added at 1% (Figure 5.5B) or greater and that extra care had to be taken to keep the gel from heating during the run as this appeared to cause the outgassing of TCM.

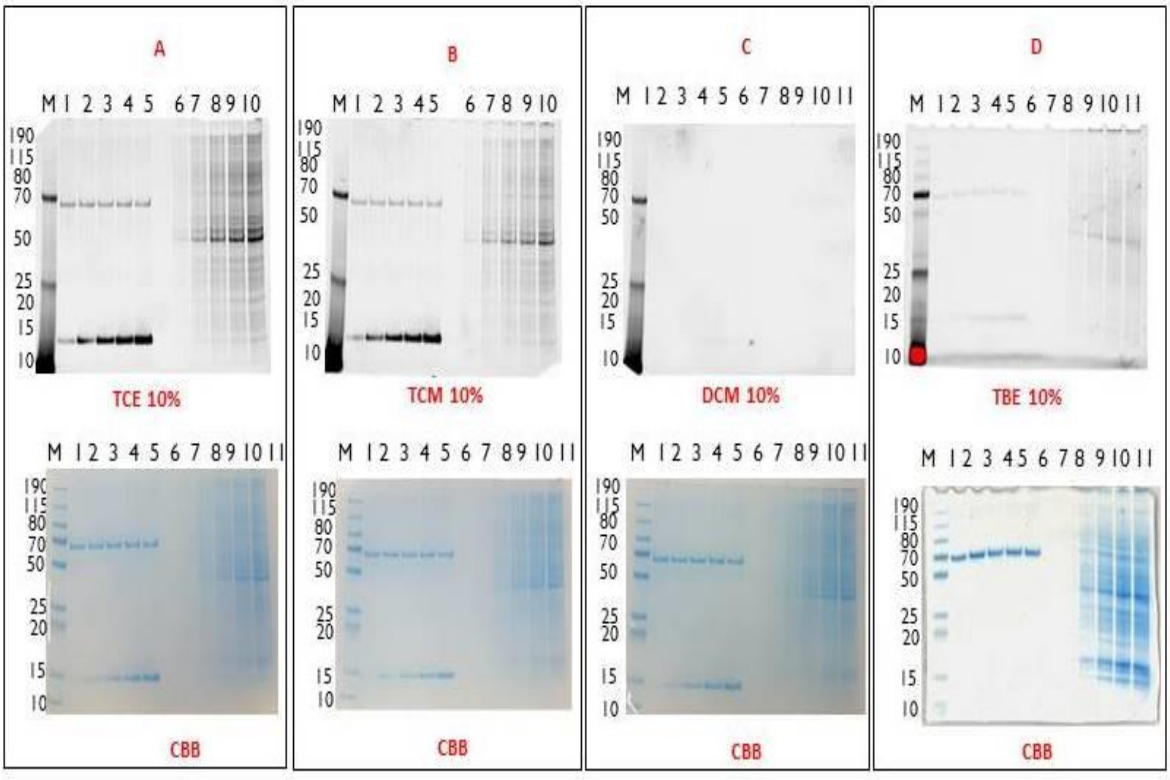


**Figure 5.6: Post-electrophoresis staining using trihalo compounds.** Following electrophoresis, each Stain free gel were incubated in a 10% solution of the indicated compound for 15 minutes and activated with UV for 45 seconds. Images were captured with 10 second exposures. On panels A-D: M; protein standards, lands 1-5: 1ug BSA mixed with 10, 30, 50, 70, or 100 ng lysozyme), lanes 6-10: 1, 3, 5, 7, 10 ug primary MEF total lysate. Gels were imaged using trihalo labeling (upper panels A-D) and CBB (lower panels A-D).

### 5.5.2.3 Using *trihalo compound* for post-electrophoresis staining

I also explored various trihalo compounds reactions with t TCM, TCE, DCM and TBE used for post-electrophoresis labeling. After electrophoresis, the gel was incubated in a 10% solution of one of the trihalo compounds for about ten minutes and Coomassie staining was used for comparison. The results show that both TCE and TCM give an excellent signal; TBE gave a poor signal, while DCM did not give any signal (Figure 5.6). It is unclear why DCM gives a signal when incorporated into the gel, but does not work when the gel is incubated in DCM following electrophoresis. The Coomassie blue staining of the same gels shows the same intensity all four gels.

### 5.5.2.4 Trihalo compound reactions in-sample buffer

To determine if the photochemical reaction of the trihalo compound with tryptophan can occur in sample buffer, I activated the photochemical reaction in sample buffer 1) before and 2) after boiling the sample. In the first case, before boiling the sample, activation of the photochemical reaction was achieved with UV light for 5 minutes followed by denaturing the samples at 95°C for 5 min, and loading onto the gel. In the second case, where the labeling was performed after boiling the samples, the samples were diluted with unmodified sample buffer, followed by boiling at 95°C for 5 min, the indicated trihalo compounds were added to the sample to 1% and activation of the photochemical reaction was also achieved with a 5 minute exposure to UV light. The images were captured with the ChemiDoc Touch. I used a sample of BSA treated with TCE 1% as a positive control while the different concentrations of lysozyme were treated with different trihalo compounds (TCM, TFE, DCM, TCA or TFA). Five trihaol compounds were used in this experiment and only TCE and TCM showed a clear and strong signal,

while TFE, DCM and TFA give no signal (Figure 5.7). Using TCE in-sample labeling showed a higher sensitivity than in-gel labeling as in the first lane of (Figure 5.7) 10 ng of lysozyme is clearly visible and indicates that the presence of the bromo-phenol blue does not inferfere with the photoreaction.

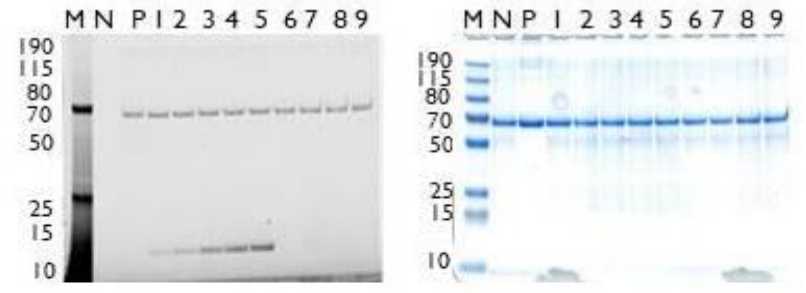


**Figure 5.7 Photoreaction with Trihalo compounds in sample buffer** Trihalo compound photoreaction using in-sample labeling: M: Protein Markers, N: No trihalo, P: BSA 1µg modified by 1% TCE, lanes 1-4: 10, 20, 30, and 40ng per lane of Lysozyme modified by TCE, lanes 5-9: 40ng of lysozyme modified by TCM, TFE, DCM, TCA and TFA, respectively. All lanes (except N) has 1µg BSA modified by 1% TCE. Gels were imaged using trihalo labeling (left panel) and CBB (right panel).

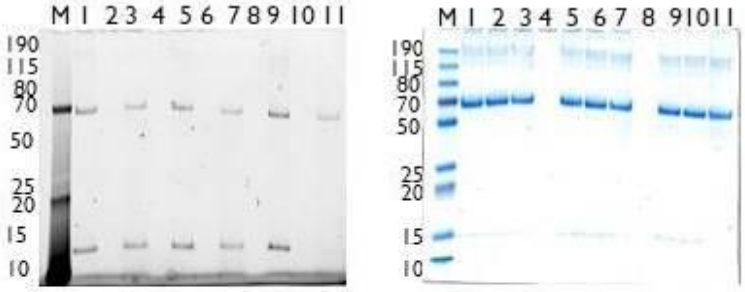


**Figure 5.8 Photoreaction with trihaloethanol with three different halogens**: Gel of three different trihalo compound with different halogens: M: standard protein; lanes 1-3: BSA 1µg and 80ng of Lysozyme modified by TCE, TFE, TBE at 0.05%, lanes 5-7: BSA 1µg and 80ng of Lysozyme modified by TCE, TFE, TBE at 0.1%. Lanes 9-11: BSA 1µg and 80ng per lane of Lysozyme modified by TCE, TFE, TBE at 0.5%. Gels were imaged using trihalo labeling (left panel) and CBB (right panel).

My results indicated that the organic compound can have a strong effect on labeling, as there are clear difference in the labeling, where the halogen is the same, but the organic carrier is different, for example TCE and TCM. Therefore, I wanted to test the same organic carrier, but with different halogens. TCE, TFE, and TBE, were chosen to test the effect of different halogens on the labeling (Figure 5.8). TFE resulted in no labeling and the photoreaction with TCE and TBE was very similar, except at the lowest concentrations of TBE and TCE, where TCE was clearly stronger.

I also tried in gel labeling experiments with TBE, which proved unsuitable, as the TBE promoted the polymerization of the gel prior to the addition of TEMED and APS. This suggested that TBE is a reactant during the polymerization of the gel and is most probably producing free radicals similar to APS. If this were the case, TEMED may be able to increase the trihalo labeling, as its main function during acrylamide polymerization is to stabilize free radicals. As seen in Figure 5.11, the addition of TEMED to an in solution reaction with TCE results in enhanced labeling. Importantly, APS was not able to potentiate labeling with TCE. In addition, TEMED or APS alone were also inefficient at inducing the fluorescence of tryptophan in the absence of a trihalo compound.

I also tested the ability of TEMED to increase the labeling with TFE or TBE, and TEMED was able to promote the labeling with TCE and TBE, but was not able to rescue the poor labeling with TFE (Figure 5.10).

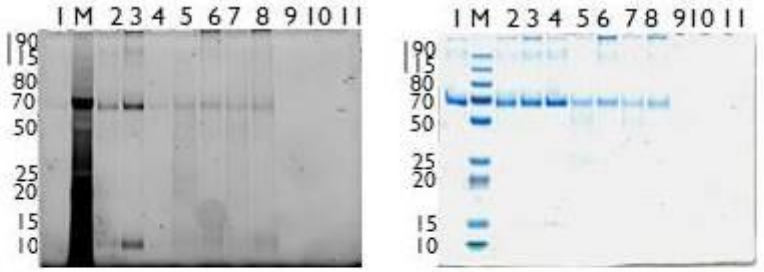


**Figure 5.9 Affect of APS and Temed on trihalo labeling:** Gel testing the components for gel polymerization. On the gel, M: standard protein (Thermofisher), lane 1 to 8: BSA1µg and 80 ng of Lysozyme lane 1: No Trihalo lane 2: TCE, at 0.5% lane 3: TCE, at 0.5% and Temed at 0.04% lane 4: Temed at 0.04% lane 5: APS at 0.1% lane 6: TBE at 0.5% and APS at 0.1% lane 7: TCE at 0.5% and APS at 0.1% lane 8: TBE at 0.5%. Gels were imaged using trihalo labeling (left panel) and CBB (right panel).

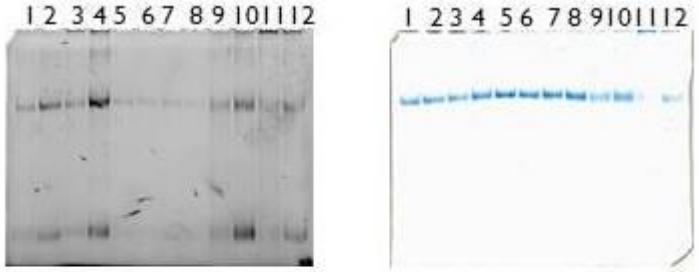


**Figure 5.10 Affect of Temed on signal amplification of Trihalo compounds:** lanes 1-12: BSA1µg and lysozyme 80ng; lane 1: 0.05% TCE lane 2: 0.05% TCE and 0.04% Temed; lane 3: 0.5% TCE, Lane 4: 0.05% TCE 0.04% Temed; lane 5: 0.05% TFE; lane 6: 0.05% TFE and 0.04% Temed; lane 7: 0.5% TFE; lane 8: 0.5% TFE and 0.04% Temed; lane 9: 0.05% TBE; lane 10: 0.05% TBE and 0.04% Temed; lane 11: 0.5% TBE; lane 12: 0.5% TBE and 0.04% Temed. Gels were imaged using trihalo labeling (left panel) and CBB (right panel).

### 5.5.2.5 Compatibility of TCE-based stain-free with western blot.

Western blotting is one of the most common techniques used in modern biological research. This method consists of several steps: sample preparation, casting the gel, protein electrophoresis and transfer, membrane blocking, incubation with antibodies, imaging and analysis. This may be followed by the stripping and reprobing of the same blot. Each of these steps plays a key role in the final detection of proteins and could be considered a limitation of this technique. In fact, errors can be made at every stage of this process. So, a more practical and reliable modification of this method would be of a major interest, for both qualitative protein verification and quantitative analysis. Many of these limitations such as sample loading, transfer efficiency and using the wrong loading control can be avoided by using trihalo gel labeling. The main step in western blotting is the recognition between the antibody and antigen. Therefore to investigate if the TCE-labeling has any effect on this step of western blot, several antibodies were used to confirm the compatibility of TCE-labeled proteins with western blot.

I tested cellular samples modified by trihaolo compaunds, and then analyzed them by Western blot using various types of antibodies and as can be seen from (Figure 6.12).

I initially tested the trihalo labeling on a crude MCPyV virion sample by running unpurified MCPyV preps onto two 10% gels, one with TCE at 0.5% and the other without any trihalo compound. Serial dilutions of the same crude preparation were run into both gels and the gels were activated for 5 minutes with UV light. The gels were transferred to PVDF membranes and subsequently analyzed using anti-GFP and anti-GAPDH antibodies. The following day the membranes were developed, acquiring the images of the various exposures with the ChemiDoc Touch. We proceeded with the analysis of the quantifications and the normalization of the results obtained through the ImageLab software. Importantly there was no impairment of either antibody signal following trihalo

labeling. In fact, trihalo labeling resulted in a slight increase in sensitivity. I followed this up by analyzing a panel of antibodies on different samples (Figure 5.11) and trihalo labeling did not result in the loss of signal from any of these antibodies.

## 5.6 Quantification and normalization

### 5.6.1 TriHalo labeling as a loading control

I also tested the trihalo labeling on a MCPyV virion sample by running crude, unpurified MCPyV preps onto two 10% gels, one with TCE at 0.5% and the other without any trihalo compound. Serial dilutions of the same crude preparation were run into both gels and the gels were activated for 5 minutes with UV light. The gels were transferred to PVDF membranes and subsequently analyzed using anti-GFP and anti-GAPDH antibodies. The following day the membranes were developed, acquiring the images of the various exposures with the ChemiDoc Touch. We proceeded with the analysis of the quantifications and the normalization of the results obtained through the ImageLab software (Figure 5.12) and this indicated that there was no loss of signal following the photoreaction with TCE.

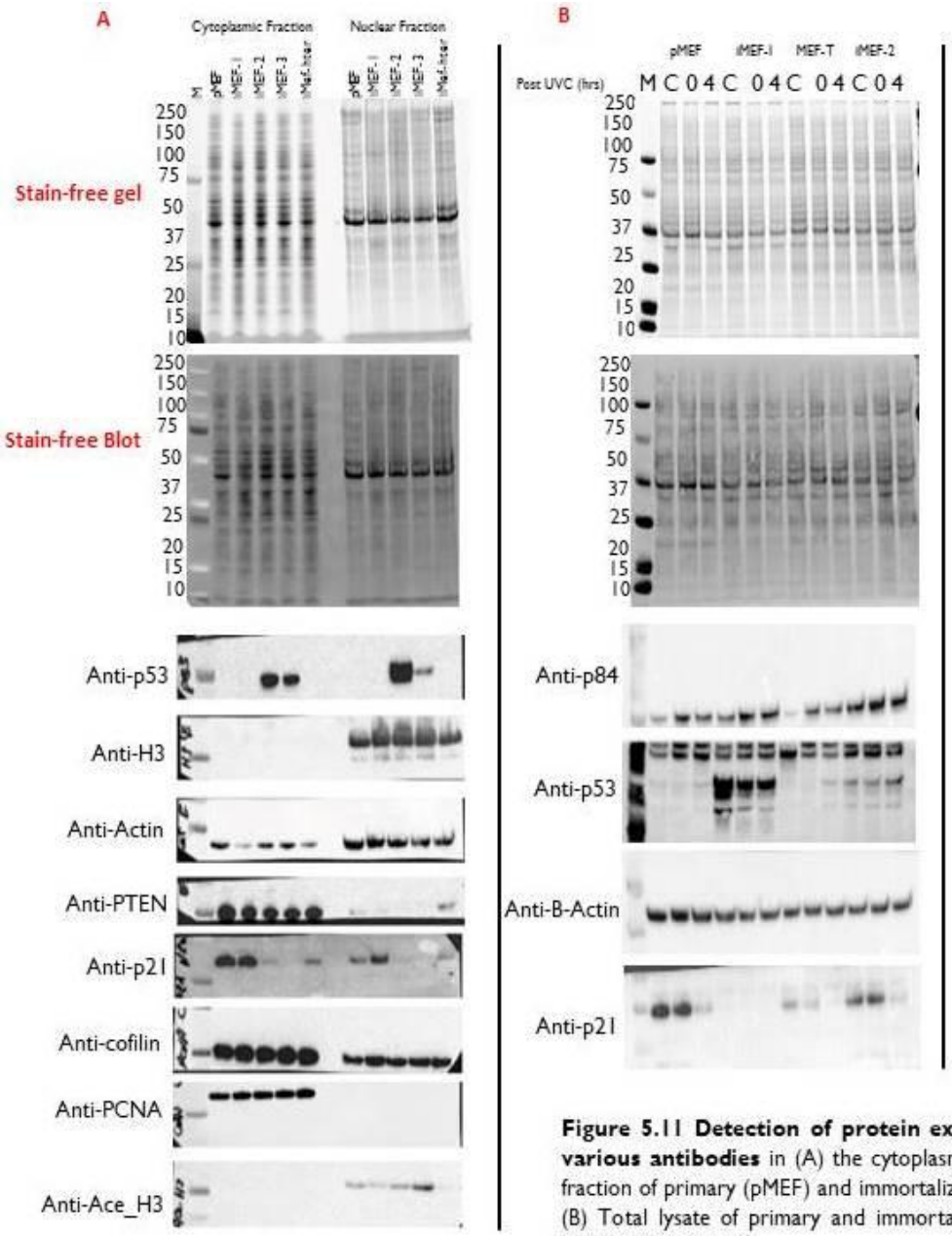


**Figure 5.11 Detection of protein expression with various antibodies** in (A) the cytoplasmic and nuclear fraction of primary (pMEF) and immortalized (iMEF) cells, (B) Total lysate of primary and immortalized MEF cells after UVS treatment.

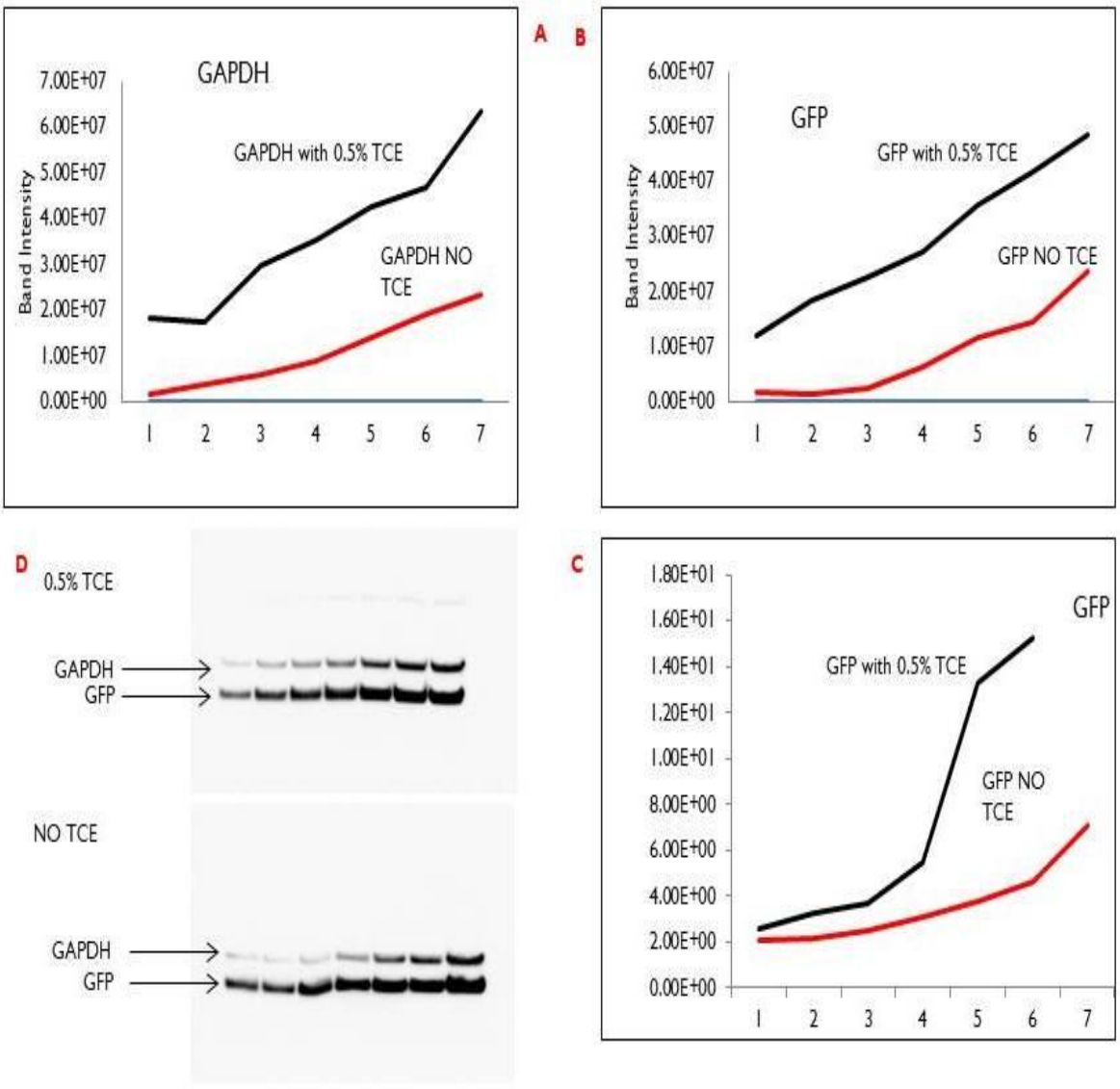


**Figure 5.12 Analysis of western blot detection following trihalo labeling** Western blot of Starting material of VLPs MCPyV production in different dilutions: (1) 1:11.40; (2) 1:7.60 ; (3) 1:5.06( 4) 1:3.37; (5) 1:2.25; (6) 1:1.5 and (7) not diluted in two different gels one with 0.5% TCE and one without TCE and blotted into PVDF and develop with Anti-GFP (1:1000) and Anti-GAPDH (1:7000). A) Intensity of GAPDH with and without 0.5% TCE by total protein normalization (TPN), the abundance of the GAPDH protein is normalized to the total amount of protein in each lane. B) Intensity of GFP with and without 0.5% TCE by total protein normalization (TPN), the abundance of the GFP protein is normalized to the total amount of protein in each lane. C) Intensity of GFP with and without 0.5% TCE by housekeeping protein normalization (GAPDH), D) Western Blots of GFP and GAPDH with and without 0.5% TCE .

## 5.7 MS analysis of the modifications formed from the photochemical reaction of lysozyme with trihalo compounds.

MS analysis of in-gel digested TCE or TCM labeled Lysozyme was performed to characterize the modifications formed by the photochemical reaction. I found that the photochemical reaction of lysozyme with TCM produced a mass addition of +28 to tryptophan, while the photochemical reaction of TCE produced a mass addition of +58 (Figure 5.13), these mass shifts are in agreement with Ladner et al. 2014. MS analysis was able to detect the trihalo modified tryptophan residues and no other trihalo modified residues were detected. In all cases tested, MS analysis revealed that the UV-dependent reaction of trihalo compounds with tryptophan is inefficient, as there was always unmodified or oxidized tryptophan residues. This is true even following the addition of Temed to enhance the reaction. Importantly, this indicates that the trihalo labeling is unlikely to inhibit antibody binding, even if the antibody-of-interest binds to tryptophan residues, because there will still be a pool of unreacted tryptophans to interact with the antibody.

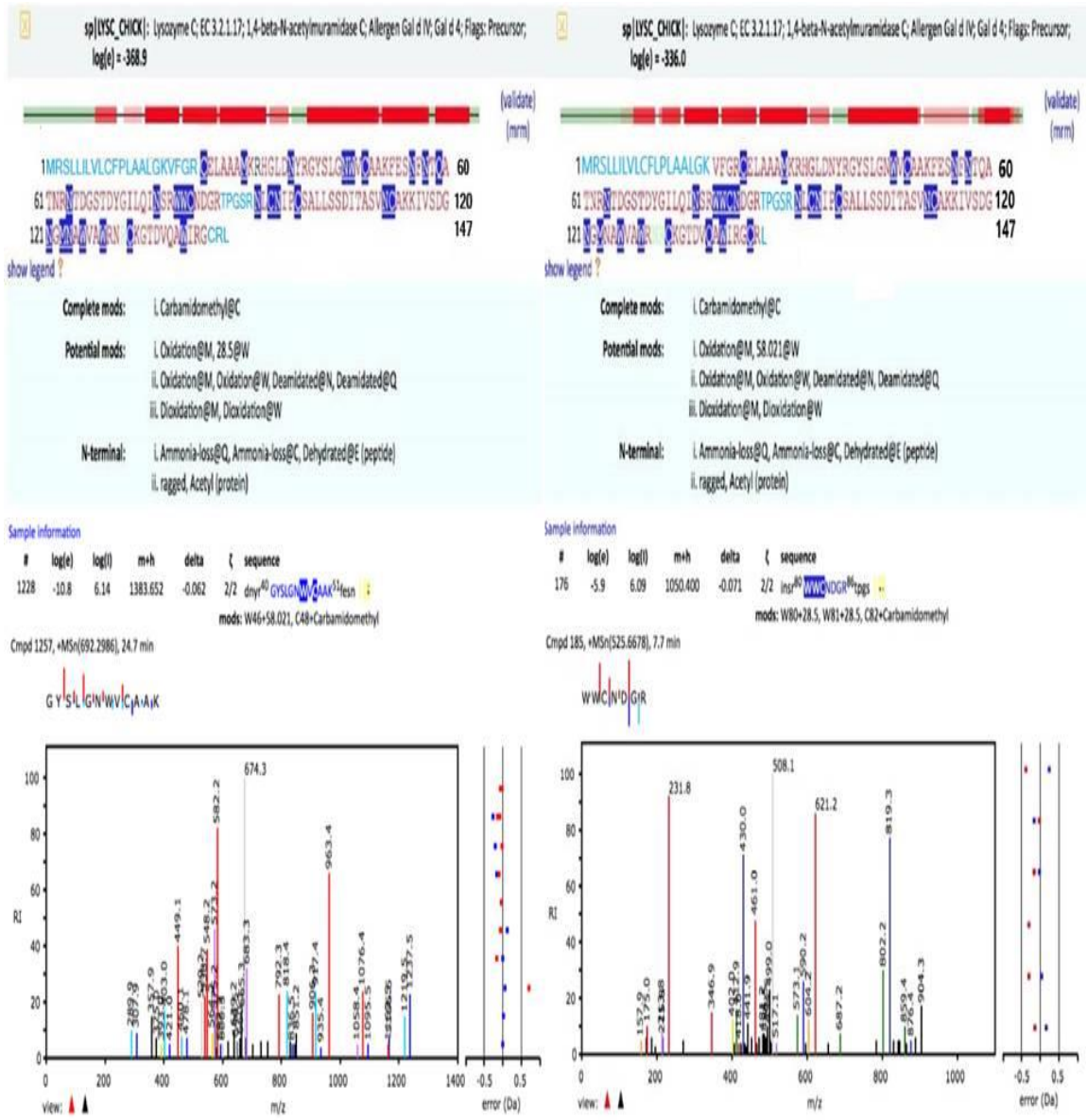


**Figure 5.13 MS analysis for the modification formed from the photochemical reaction of the lysozyme with TCE (A) or TCM (B).** The photochemical reaction of lysozyme with TCM yielded a mass addition of +28 to tryptophan, while TCE photochemical reaction yielded a mass addition of +58. A MS/MS spectrum of a peptide carry a modified tryptophan is shown for TCE and TCM derivatization.

## 5.8 Discussion

A fast stain-free protein visualization method based on the fluorescence of modified tryptophan is reported. Precast stain-free gels are already on the market, but the cost for routine laboratory use is prohibitively high, therefore I developed a hand casting procedure for in gel labeling. In addition, I also developed a post electrophoresis reaction where the trihalo compounds are added after electrophoresis is completed and I also developed an in solution procedure that can be used to label prior to electrophoresis, or other techniques, such as mass spectrometry. In fact, the pre electrophoresis and hand casted in gel versions of this technique have not yet been established, and several halo compounds differing in chemical properties and concentrations were examined to determine the best trihalo reagent.

Trihalo compounds, such as trichloroacetic acid (TCA) and trifluoroethanol (TFE) were not useful labeling reagents, as the Trp residues were poorly visible after UV irradiation (Data not show). In fact, Ladner reported that the TCA photoreaction has nearly the same fluorescence shift as the formyl products of mentioned trihalo compounds, but with much less intensity (*Ladner et al. 2014*). In addition, TCA has the added difficulty of strongly affecting the solubility of proteins in solution and the quality of the electrophoresis.

During the course of these experiments, I noticed that tribromoethanol (TBE) was able to initiate acrylamide polymerization prior to the addition of APS and TEMED. This suggests that the TBE was acting to provide the free radicals necessary to initiate the polymerization reaction. I tested if APS and Temed could replace or augment the ability of the trihalo compounds to modify tryptophan residues. Importantly, TEMED significantly increased the intensity of the labeling with trihalo compounds. In this regard, TEMED is most likely acting to stabilize the free radicals produced by UV irradiation, in much the

same way that it stabilizes the free radicals produced by APS during acrylamide polymerization.

In conclusion trichlormethane (TCM) and trichloroethanol (TCE) appear to be the most useful trihalo compounds. The main difference between them appears to be related to the water solubility of TCM vs TCE. TCM is a hydrophobic solvent, more commonly called chloroform, and has limited water solubility. 2% TCM negatively impacted the quality of the gels formed and even at lower concentrations of TCM, increased care had to be taken during the run, because TCM is also much more volatile than TCE, and heating of TCM containing gels creates bubbles in the gel. Therefore TCE was chosen as the most optimal trihalo compound.

In addition, a number of western blots were performed that indicate that trihalo labeling does not interfere with most antibody: antigen pairs. This will likely be true even in the cases where the epitope contains tryptophan residues, as the mass spectrometry data demonstrated that it is very difficult to drive the photoreaction to completion.

The inability to drive this reaction to completion suggests that this strategy cannot be used to gain structural information about a protein, as it will be difficult to relate incomplete labeling with solvent accessibility.

## 5.9 Conclusion

In this work the photoreaction between trihalo compounds and tryptophan residues was studied. Some aspects of the stain-free technology were highlighted and confirmed. Results indicated that 2, 2, 2-trichloroethanol (TCE) was the best reagent for in-gel visualization, in-sample or post electrophoresis labeling. This is largely because TCE is highly soluble in aqueous buffers. The protocols I developed are similar to the commercially available product and have the same advantages, such as providing convenient check-points at different points in the western blotting procedure. The stain-

free TCE-optimized protocol showed remarkable linearity in given samples. Given these points, stain-free detection method fits perfectly in the world of western blotting, offering a sensitive and convenient tool for everyday analysis. The TCE optimized approach should be integrated into immunoblotting workflows, as an affordable hand cast alternative to commercial precast stain-free gels.

## 6. REFERENCES


1. Aebersold R1, Mann M. Mass spectrometry-based proteomics. *Nature*. 2003 Mar 13;422 (6928):198-207.
2. Agelli M, Clegg LX, Becker JC, Rollison DE. The etiology and epidemiology of merkel cell carcinoma. *Curr. Probl. Cancer.* 2010 Jan-Feb; 34(1):14-37.
3. Agelli, M and Clegg LX, Epidemiology of primary Merkel cell carcinoma in the United States. *Journal of the American Academy of Dermatology*, 2003. 49(5): p. 832-41.
4. Ahuja D, Rathi AV, Greer AE, Chen XS, Pipas JM. A structure-guided mutational analysis of simian virus 40 large T antigen: identification of surface residues required for viral replication and transformation. *Journal of virology*, 2009. 83(17): p. 8781-8.
5. Ahuja D, Saenz-Robles MT and Pipas JM. SV40 large T antigen targets multiple cellular pathways to elicit cellular transformation. *Oncogene*, 2005. 24(52): p. 7729-45.
6. Albores-Saavedra J, Batich K, Chable-Montero F, Sagy N, Schwartz AM, Henson DE. Merkel cell carcinoma demographics, morphology, and survival based on 3870 cases: a population based study. *J. Cutan. Pathol.* 2010 Jan; 37(1):20-7.
7. Ali SH, , Kasper JS, Arai T, DeCaprio JA. Cul7/p185/p193 binding to simian virus 40 large T antigen has a role in cellular transformation. *Journal of virology*, 2004. 78(6): p. 2749-57.
8. Allander T, Andreasson K, Gupta S, Bjerkner A, Bogdanovic G, Persson MA, Dalianis T, Ramqvist T, Andersson B. Identification of a third human polyomavirus. *Journal of virology*, 2007. 81(8): p. 4130- 6.
9. Allen PJ, Bowne WB, Jaques DP, Brennan MF, Busam K, Coit DG. Merkel cell carcinoma: prognosis and treatment of patients from a single institution. *Journal of*

*clinical oncology*: official journal of the American Society of Clinical Oncology, 2005. 23(10): p. 2300-9.

10. Amé JC, Spenlehauer C, and de Murcia G. (2004) The PARP superfamily. *Bioessays* 26: 882-893.
11. Amere Subbarao Sreedhara, va Kalmára EŁ, Peéter Csermelya, Yu-Fei Shenb, Hsp90 isoforms: functions, expression and clinical importance (PDF), in *FEBS Letters*, vol. 562, n° 1, 08 03 2004, p. 11.
12. An Ping, Sáenz Robles MT Pipas, JM. (13 October 2012). "Large T Antigens of Polyomaviruses: Amazing Molecular Machines". *Annual Review of Microbiology*. 66 (1): 213–236. doi:10.1146/annurev-micro-092611-150154. PMID 22994493.
13. Andersson L, and Porath J. (1986). Isolation of phosphoproteins by immobilized metal (Fe3+) affinity chromatography. *Anal Biochem* 154, 250-254.
14. Arockiaraj J, Gnanam AJ, Kumaresan V, Palanisamy R, Bhatt P, Thirumalai MK, Roy A, Pasupuleti M, Kasi M (November 2013). "An unconventional antimicrobial protein histone from freshwater prawn Macrobrachium rosenbergii: analysis of immune properties". *Fish & Shellfish Immunology*. 35 (5): 1511–22. doi:10.1016/j.fsi.2013.08.018. PMID 23994279.
15. Atkin SJ, Griffin BE, Dilworth SM. Polyoma virus and simian virus 40 as cancer models: history and perspectives. *Semin. Cancer Biol.* 2009 Aug; 19(4):211-7.
16. Atwood WJ and Norkin LC. Class I major histocompatibility proteins as cell surface receptors for simian virus 40. *J. Virol.* 63, 4474-4477 (1989).
17. Babakir-Mina M, Ciccozzi M, Lo Presti A, Greco F, Perno CF, Ciotti M. Identification of Merkel cell polyomavirus in the lower respiratory tract of Italian patients. *J. Med. Virol.* 2010 Mar; 82(3):505-9.
18. Baltimore D. RNA-dependent DNA polymerase in virions of RNA tumour viruses. *Nature*, 1970. 226(5252): p. 1209-11

19. Banerjee S1, Mazumdar S. Electrosprayionization mass spectrometry: a technique to access the information beyond the molecular weight of the analyte. *J. Anal. Chem.* 2012; 2012:282574. doi: 10.1155/2012/282574. Epub 2011 Dec 15.
20. Barbeau D, et al. Functional interactions within adenovirus E1A protein complexes. *Oncogene*, 1994. 9(2): p. 359-73.
21. Bargonetti J, Reynisdóttir I, Friedman PN, Prives C. Site-specific binding of wild-type p53 to cellular DNA is inhibited by SV40 T antigen and mutant p53. Genes & development. *Genes & Developm*. 1992. 6(10): p. 1886-98.
22. Basu A, Rose KL, Zhang J, Beavis RC, Ueberheide B, Garcia BA, Chait B, Zhao Y, Hunt DF, Segal E, Allis CD, Hake SB. Proteome-wide prediction of acetylation substrates. *Proc Natl Acad Sci U S A.* 2009 Aug 18;106(33):13785-90. doi: 10.1073/pnas.0906801106. Epub 2009 Aug 3. PMID: 19666589
23. Belmadani S, Poüs C, Fischmeister R, Méry PF. Post-translational modifications of tubulin and microtubule stability in adult rat ventricular myocytes and immortalized HL-1 cardiomyocytes. 2004 *Mol Cell Biochem* 258, 35–48.
24. Berger JR and Concha M. Progressive multifocal leukoencephalopathy: the evolution of a disease once considered rare. 1995 *J Neurovirol*. 1(1): p. 5-18.
25. Berger LC, Smith DB, Davidson I, Hwang JJ, Fanning E, Wildeman AG. Interaction between T antigen and TEA domain of the factor TEF-1 derepresses simian virus 40 late promoter in vitro: identification of T-antigen domains important for transcription control. *Journal of virology*, 1996. 70(2): p. 1203-12.
26. Bern M1, Kil YJ, Becker C. Byonic: advanced peptide and protein identification software. *Curr Protoc Bioinformatics.* 2012 Dec; Chapter 13:Unit13.20. doi: 10.1002/0471250953.bi1320s40.
27. Bialasiewicz S, Whiley DM, Lambert SB, Wang D, Nissen MD, Sloots TP. A newly reported human polyomavirus, KI virus, is present in the respiratory tract of

Australian children. *Journal of clinical virology*: the official publication of the Pan American Society for Clinical Virology, 2007. 40(1): p. 15-8.

28. Bialasiewicz S, Rockett R, Whiley DW, Abed Y, Allander T, Binks M, Boivin G, Cheng AC, Chung JY, Ferguson PE, Gilroy NM, Leach AJ, Lindau C, Rossen JW, Sorrell TC, Nissen MD, Sloots TP. Whole-genome characterization and genotyping of global WU polyomavirus strains. *Journal of virology*, 2010. 84(12): p. 6229-34.
29. Black MM and Keyser P. Acetylation of alpha- tubulin in cultured neurons and the induction of alpha- tubulin acetylation in PC12 cells by treatment with nerve growth factor. 1987 *J Neurosci* 7, 1833–1842.
30. Block SL1, Nolan T, Sattler C, Barr E, Giacoletti KE, Marchant CD, Castellsagué X, Rusche SA, Lukac S, Bryan JT, Cavanaugh PF Jr, Reisinger KS; Protocol 016 Study Group. Comparison of the immunogenicity and reactogenicity of a prophylactic quadrivalent human papillomavirus (types 6, 11, 16, and 18) L1 virus-like particle vaccine in male and female adolescents and young adult women. *Pediatrics*. 2006 Nov;118 (5):2135-45.
31. Boni S, Lavergne JP, Boulant S, Cahour A (2005) Hepatitis C virus core protein acts as a trans- modulating factor on internal translation initiation of the viral RNA. *J Biol Chem* 280, 17737–17748.
32. Bonvoisin C, Weekers L, Xhignesse P, Grosch S, Milicevic M, Krzesinski JM. Polyomavirus in renal transplantation: a hot problem. *Transplantation.* 2008 Apr 15; 85 (7 Suppl): S42-8.
33. Borger DR and DeCaprio JA. Targeting of p300/CREB binding protein coactivators by simian virus 40 is mediated through p53. *Journal of virology*, 2006. 80(9): p. 4292-303.

34. Bosch A and Suau P. "Changes in core histone variant composition in differentiating neurons: the roles of differential turnover and synthesis rates". 1995 *European Journal of Cell Biology*. 68 (3): 220–5.

35. Bosch FX, Manos MM, Muñoz N, Sherman M, Jansen AM, Peto J, Schiffman MH, Moreno V, Kurman R, Shah KV.Prevalence of human papillomavirus in cervical cancer: a worldwide perspective. International biological study on cervical cancer (IBSCC) Study Group. *J Natl Cancer Inst*, 1995. 87(11): p. 796-802.

36. Bothner B, Dong XF, Bibbs L, Johnson JE, Siuzdak G. Evidence of viral capsid dynamics using limited proteolysis and mass spectrometry. 1998 *J. Biol. Chem.* 273:673–676.

37. Bradley DW. Hepatitis viruses: their role in human cancer. *Proc Assoc Am Physicians*, 1999. 111(6): p. 588-93.

38. Brady JN and Consigli RA. Chromatographic separation of the polyoma virus proteins and renaturation of the isolated VP1 major capsid protein. *J Virol*, 1978. 27(2): p. 436-42.

39. Broos K, Wei J, Marshall D, Brown F, Smith TJ, Johnson JE, Schneemann A, Siuzdak G. Viral capsid mobility: a dynamic conduit for inactivation. 2001 *Proc. Natl. Acad. Sci. U.S.A.* 98:2274–2277.

40. Brosh R and Rotter V. When mutants gain new powers: news from the mutant p53 field. *Nature reviews. Cancer*, 2009. 9(10): p. 701-13.

41. Buck CB, Phan GQ, Raiji MT, Murphy PM, McDermott DH, McBride AA. Complete genome sequence of a tenth human polyomavirus. *J. Virol.* 2012 Oct; 86(19):10887.

42. Bukreyev A and Belyakov IM. Expression of immunomodulating molecules by recombinant viruses: can the immunogenicity of live virus vaccines be improved? *Expert Rev Vaccines*, 2002. 1(2): p. 233-45.

43. Burkhart DL and Sage J. Cellular mechanisms of tumour suppression by the retinoblastoma gene. *Nature reviews. Cancer*, 2008. 8(9): p. 671-82.

44. Butel JS and Lednicky JA. Cell and molecular biology of simian virus 40: implications for human infections and disease. *J Natl Cancer Inst*, 1999. 91(2): p. 119-34.

45. Bzhalava D, Bray F, Storm H, Dillner J. Risk of second cancers after the diagnosis of Merkel cell carcinoma in Scandinavia. *Br J. Cancer.* 2011 Jan 4; 104(1):178-80.

46. Caldarelli-Stefano R, Boldorini R, Monga G, Meraviglia E, Zorini EO, Ferrante P. JC virus in human glial-derived tumors. *Human pathology*, 2000. 31(3): p. 394- 5.

47. Cambray-Deakin MA and Burgoyne RD.Posttranslational modifications of alpha-tubulin: acetylated and detyrosinated forms in axons of rat cerebellum. 1987 *J Cell Biol* 104, 1569–1574.

48. Campbell KS, Mullane KP, Aksoy IA, Stubdal H, Zalvide J, Pipas JM, Silver PA, Roberts TM, Schaffhausen BS, DeCaprio JA. DnaJ/hsp40 chaperone domain of SV40 large T antigen promotes efficient viral DNA replication. *Genes & development*, 1997. 11(9): p. 1098-110.

49. Cann AJ. Principles of Molecular Virology. 3rd ed. 2001: *Academic press*.

50. Carbone M, Reale A, Di Sauro A, Sthandier O, Garcia MI, Maione R, Caiafa P, Amati P. PARP-1 interaction with VP1 capsid protein regulates polyomavirus early gene expression. *J Mol Biol*. 2006 Nov 3;363(4):773-85. Epub 2006 Jun 30.

51. Carbone M, Ascione G, Chichiarelli S, Garcia M I, Eufemi M, Amati P. Chromosome-protein interactions in polyomavirus virions. 2004 *J Virol*. 78, 513–519.

52. Carbone M, Rizzo P, Pass HI. Simian virus 40, poliovaccines and human tumors: a review of recent developments. *Oncogene*, 1997. 15(16): p. 1877-88.

53. Caruso M, Belloni L, Sthandier O, Amati P, Garcia MI. Alpha4beta1 integrin acts as a cell receptor for murine polyomavirus at the postattachment level. *J. Virol.* 77, 3913-3921 (2003).

54. Caruso M, Busanello A, Sthandier O, Cavaldesi M, Gentile M, Garcia MI, Amati P. Mutation in the VP1-LDV motif of the murine polyomavirus affects viral infectivity and conditions virus tissue tropism in vivo. *J. Mol. Biol.* 367, 54-64 (2007).

55. Chace DH. Mass spectrometry in the clinical laboratory. 2001 *Chem. Rev.* 101:445–477.

56. Chan HM, Narita M, Lowe SW, Livingston DM. The p400 E1A-associated protein is a novel component of the p53 --> p21 senescence pathway. *Genes & development*, 2005. 19(2): p. 196-201.

57. Chang Y, Cesarman E, Pessin MS, Lee F, Culpepper J, Knowles DM, Moore PS. "Identification of herpesvirus-like DNA sequences in AIDS-associated Kaposi's sarcoma". 1994 *Science*. 266 (5192): 1865–1869.

58. Chen T, Hedman L, Mattila PS, Jartti T, Ruuskanen O, Söderlund-Venermo M, Hedman K. Serological evidence of Merkel cell polyomavirus primary infections in childhood. *J. Clin. Virol.* 2011 Feb; 50(2):125-9.

59. Chen T, Mattila PS, Jartti T, Ruuskanen O, Söderlund-Venermo M, Hedman K. Seroepidemiology of the newly found trichodysplasia spinulosa-associated polyomavirus. *J. Infect Dis.* 2011 Nov 15; 204(10):1523-6.

60. Chen S, Paucha E. Identification of a region of simian virus 40 large T antigen required for cell transformation. *Journal of virology*, 1990. 64(7): p. 3350-7.

61. Cheng J, DeCaprio JA, Fluck MM, Schaffhausen BS. Cellular transformation by Simian Virus 40 and Murine Polyoma Virus T antigens. 2009 *Semin. Cancer Biol. 19*, 218–228.

62. Chertova E, Chertov O, Coren LV, et al. Proteomic and biochemical analysis of purified human immunodeficiency virus type 1 produced from infected monocyte-derived macrophages. *J. Virol* 2006;80(18):9039–9052.

63. Choudhary C, Kumar C, Gnad F, Nielsen ML, Rehman M, Walther TC, Olsen JV, Mann M. Lysine acetylation targets protein complexes and co-regulates major cellular functions. 2009 Science 325 834–840. 10.1126/science.1175371.

64. Chromy LR, Oltman A, Estes PA, Garcea RL. Chaperone-mediated in vitro disassembly of polyoma- and papillomaviruses. 2006 *J Virol*. 80, 5086–5091.

65. Chromy LR, Pipas JM, Garcea RL. Chaperone-mediated in vitro assembly of polyomavi-rus capsids. 2003 *Proc. Natl Acad. Sci. USA*, 100, 10477–10482.

66. Clayson ET, Compans RT, Characterization of simian virus 40 receptor moieties on the surfaces of Vero C1008 cells. *J Virol*, 1989. 63(3): p. 1095-100.

67. Cole CN, Conzen SD. Polyomaviridae: the viruses and their replication. *In: Knipe DM, Howley PM, editors. Fields virology. 4th edition. Philadelphia: Lippincott Williams & Wilkins.* pp. 2141–2174.

68. Comar M, Zanotta N, Croci E, Murru I, Marci R, Pancaldi C, Dolcet O, Luppi S, Martinelli M, Giolo E, Ricci G, Tognon M. Association between the JC Polyomavirus Infection and Male Infertility. *PLoS One.* 2012; 7(8):e42880.

69. Comings DE. A general theory of carcinogenesis. *Proceedings of the National Academy of Sciences of the United States of America*, 1973. 70(12): p. 3324-8.

70. Conzen SD, Cole CN. The three transforming regions of SV40 T antigen are required for immortalization of primary mouse embryo fibroblasts. *Oncogene*, 1995. 11(11): p. 2295-302.

71. Corallini A, Altavilla G, Carra L, Grossi MP, Federspil G, Caputo A, Negrini M, Barbanti-Brodano G. Oncogenity of BK virus for immunosuppressed hamsters. *Archives of virology*, 1982. 73(3-4): p. 243-53.

72. Costanzi C, Pehrson JR. "Histone macroH2A1 is concentrated in the inactive X chromosome of female mammals". 1998 *Nature*. 393 (6685): 599–601. Bibcode:1998Natur.393..599C. doi:10.1038/31275. PMID 9634239.

73. Cotsiki M, Lock RL, Cheng Y, Williams GL, Zhao J, Perera D, Freire R, Entwistle A, Golemis EA, Roberts TM, Jat PS, Gjoerup OV. Simian virus 40 large T antigen targets the spindle assembly checkpoint protein Bub1.*Proceedings of the National Academy of Sciences of the United States of America,* 2004. 101(4): p. 947-52.

74. Cottrell JS. Protein identification by peptide mass fingerprinting. *Pept. Res.* 1994 May-Jun; 7 (3):115-24.

75. Cox MM, Lehninger AL, Nelson DL. Lehninger principles of biochemistry (4th ed). 2005 New York: W.H. Freeman. ISBN 978-0-7167-4339-2.

76. Crawford LV, Crawford EM, Watsondh, The physical characteristics of polyoma virus. I. Two types of particle. *Virology*, 1962. 18: p. 170-6.

77. Cripe TP, Delos SE, Estes PA, Garcea RL. In vivo and in vitro association of hsc70 with polyomavirus capsid proteins. 1995 *J Virol* 69, 7807–7813.

78. Cueva JG, Hsin J, Huang KC, Goodman MB. Posttranslational acetylation of a-tubulin constrains protofilament number in native microtubules. 2012 *Curr Biol* 22, 1066–1074.

79. D'Amours D, Desnoyers S, D'Silva I, Poirier G. Poly(ADP-ribosyl)ation reactions in the regulation of nuclear functions. 1999 *Biochem. J*. 342: 249-268.

80. Da Costa SR, Wang Y, Vilalta PM, Schönthal AH, Hamm-Alvarez SF. Changes in cytoskeletal organization in polyoma middle T antigen-transformed fibroblasts: involvement of protein phosphatase 2A and src tyrosine kinases. 2000 *Cell Motil Cytoskeleton* 47, 253– 268.

81. Dang X, Bialasiewicz S, Nissen MD, Sloots TP, Koralnik IJ, Tan CS. Infrequent detection of KI, WU and MC polyomaviruses in immunosuppressed individuals

with or without progressive multifocal leukoencephalopathy. *PloS one*, 2011. 6(3): p. e16736.

82. Dasgupta D, Rajgopalan R, Gurnani S. Involvement of colchicine binding site of tubulin in the polymerisation process. 1983 *FEBS Lett* 152, 101–104.
83. De Hoffmann E, Stroobant V. Mass Spectrometry: Principles and Applications, 2007.
84. De la Lastra CA, Villegas I, Sanchez-Fidalgo S. Poly(ADP-ribose) polymerase inhibitors: new pharmacological functions and potential clinical implications. 2007 *Curr Pharm Des* 13: 933-962.
85. DeCaprio JA, Garcea RL. "A cornucopia of human polyomaviruses". 2013 *Nature* Reviews. Microbiology. 11(4): 264–76. doi:10.1038/nrmicro2992. PMC3928796.PMID 23474680.
86. DeCaprio JA, Ludlow JW, Figge J, Shew JY, Huang CM, Lee WH, Marsilio E, Paucha E, Livingston DM. SV40 large tumor antigen forms a specific complex with the product of the retinoblastoma susceptibility gene. *Cell*, 1988. 54(2): p. 275-83.
87. DeCaprio JA. How the Rb tumor suppressor structure and function was revealed by the study of Adenovirus and SV40. *Virology,* 2009. 384(2): p. 274-84.
88. Delchambre M, Gheysen D, Thines D, Thiriart C, Jacobs E, Verdin E, Horth M, Burny A, Bex F. The GAG precursor of simian immunodeficiency virus assembles into virus-like particles. *Embo J*, 1989. 8(9): p. 2653-60.
89. Deppert W, Steinmayer T, Richter W. Cooperation of SV40 large T antigen and the cellular protein p53 in maintenance of cell transformation. *Oncogene,* 1989. 4(9): p. 1103-10.
90. Deribe YL, Pawson T, Dikic I. Post-translational modifications in signal integration. 2010 *Nat. Struct. Mol. Biol.* 17 666–672. 10.1038/nsmb.1842.
91. Dessel BH. Cultivation of papova-like virus from human brain with progressive multifocal leucoencephalopathy. *Lancet* 1, 1257-1260 (1971).

92. Dickmanns A, Zeitvogel A, Simmersbach F, Weber R, Arthur AK, Dehde S, Wildeman AG, Fanning E. The kinetics of simian virus 40-induced progression of quiescent cells into S phase depend on four independent functions of large T antigen. *Journal of virology*, 1994. 68(9): p. 5496-508.

93. Dilworth SM. Polyoma virus middle T antigen and its role in identifying cancer-related molecules. *Nat Rev Cancer*, 2002. 2(12): p. 951-6.

94. Dittmer D, Pati S, Zambetti G, Chu S, Teresky AK, Moore M, Finlay C, Levine AJ. Gain of function mutations in p53. *Nature genetics*, 1993. 4(1): p. 42-6.

95. Donnelly JJ, Wahren B, Liu MA. DNA vaccines: progress and challenges. *J Immunol*, 2005. 175(2): p. 633-9.

96. Drews K, Bashir T, Dorries K. Quantification of human polyomavirus JC in brain tissue and cerebrospinal fluid of patients with progressive multifocal leukoencephalopathy by competitive PCR. *J. Virol. Methods.* 2000 Jan; 84(1):23-36.

97. Droit A, Hunter JM, Rouleau M, Ethier C, Picard-Cloutier A, Bourgais D, Poirier, GG. PARPs Database: A LIMS systems for protein-protein interaction data mining or Laboratory Information management system. 2002 *BMC Bioinformatics* 8: 483.

98. Dyson N, Buchkovich K, Whyte P, Harlow E. The cellular 107K protein that binds to adenovirus E1A also associates with the large T antigens of SV40 and JC virus. *Cell,* 1989. 58(2): p. 249-55.

99. Dyson N, Howley PM, Münger K, Harlow E. The human papilloma virus-16 E7 oncoprotein is able to bind to the retinoblastoma gene product. *Science*, 1989. 243(4893): p. 934-7.

100. Eash S, Manley K, Gasparovic M, Querbes W, Atwood WJ. The human polyomaviruses. *Cell Mol. Life Sci.* 2006 Apr; 63(7-8):865-76.

101. Eash S, Querbes W, Atwood WJ. Infection of vero cells by BK virus is dependent on caveolae. 2004 *J Virol* 78: 11583–11590.

102. Echeverria PC, Picard D. Molecular chaperones, essential partners of steroid hormone receptors for activity and mobility. 2010 *Biochim Biophys Acta* 1803, 641–649.

103. Eckhart W. Polyomavirinae and their replication. In *Virology* 2004 (Fields, B. N., Knipe, D. M. & Howley, P. M., eds), pp. 1593–1607, Raven, New York.

104. Eckner R, Ludlow JW, Lill NL, Oldread E, Arany Z, Modjtahedi N, DeCaprio JA, Livingston DM, Morgan JA. Association of p300 and CBP with simian virus 40 large T antigen. Molecular and cellular biology, 1996. 16(7): p. 3454-64.

105. Eddy BE, Stewart SE, Berkeley W. Cytopathogenicity in tissue culture by a tumor virus from mice. *Proc Soc Exp Biol Med*, 1958. 98(4): p. 848-51.

106. Edlich RF, Hill LG, Williams FM. Global epidemic of human T-cell lymphotrophic virus type-I (HTLV-I): an update. 2003 *J Long Term Eff Med Implants* 13: 127–140.

107. Edman P. A metod for the determination of the amino acid sequence of peptides. 1949 *Arch. Biochem. Biophys*, 22:475-483.

108. Edwards RA, Jickling G, Turner RJ. Development of indole chemistry to label tryptophan residues in protein for determination of tryptophan surface accessibility *Photochem. Photobiol*. 2002, 75, 362-368.

109. Egli A, Infanti L, Dumoulin A, Buser A, Samaridis J, Stebler C, Gosert R, Hirsch HH. Prevalence of polyomavirus BK and JC infection and replication in 400 healthy blood donors. *The Journal of infectious diseases*, 2009. 199(6): p. 837-46.

110. Elliott G, O'Hare P. Herpes simplex virus type 1 tegument protein VP22 induces the stabilization and hyperacetylation of microtubules. 1998 *J Virol* 72, 6448–6455.

111. Elphick GF, Querbes W, Jordan JA, Gee GV, Eash S, Manley K, Dugan A, Stanifer M, Bhatnagar A, Kroeze WK, Roth BL, Atwood WJ. The human polyomavirus, JCV, uses serotonin receptors to infect cells. *Science*, 2004. 306(5700): p. 1380-3.

112. Erickson KD, Garcea RL, Tsai B. Ganglioside GT1b is a putative host cell receptor for the Merkel cell polyomavirus. *J Virol.* 2009 Oct;83(19):10275-9.

113. Epstein MA, Achong BG, Barr YM. Virus Particles in cultured Lymphoblasts from Burkitt's Lymphoma. *Lancet* 1964 Mar 28; 1(7335):702-3.

114. Erickson KD, Garcea RL, Tsai B. Ganglioside GT1b is a putative host cell receptor for the Merkel cell polyomavirus. *Journal of virology*, 2009. 83(19): p. 10275-9.

115. Erstad DJ, and Jr, JCC. (2014). Mutational analysis of merkel cell carcinoma. *Cancers* (Basel). *6*, 2116–2136.

116. Ewen ME, Ludlow JW, Marsilio E, DeCaprio JA, Millikan RC, Cheng SH, Paucha E, Livingston DM.An N-terminal transformation-governing sequence of SV40 large T antigen contributes to the binding of both p110Rb and a second cellular protein, p120. *Cell*, 1989. 58(2): p. 257-67.

117. Fanning E, Zhao K. SV40 DNA replication: from the A gene to a nanomachine. *Virology*, 2009. 384(2): p. 352-9.

118. Faust H, Pastrana DV, Buck CB, Dillner J, Ekstrom J. Antibodies to merkel cell polyomavirus correlate to presence of viral DNA in the skin. *J. Infect Dis.* 2011 Apr; 203(8):1096-100.

119. Fei ZL, D'Ambrosio C, Li S, Surmacz E, Baserga R. Association of insulin receptor substrate 1 with simian virus 40 large T antigen. *Molecular and cellular biology*, 1995. 15(8): p. 4232-39.

120. Feng H, Taylor JL, Benos PV, Newton R, Waddell K, Lucas SB, Chang Y, Moore PS. Human transcriptome subtraction by using short sequence tags to search for tumor viruses in conjunctival carcinoma. *J Virol.* 2007 Oct; 81(20):11332-40.

121. Feng H, Kwun HJ, Liu X, Gjoerup O, Stolz DB, Chang Y, Moore PS. (2011). Cellular and viral factors regulating Merkel cell polyomavirus replication. *PLoS One 6*, e22468.

122. Feng H, Taylor JL, Benos PV, Newton R, Waddell K, Lucas SB, Chang Y, Moore PS. Human transcriptome subtraction by using short sequence tags to search for tumor viruses in conjunctival carcinoma. *J Virol*, 2007. 81(20): p. 11332-40.

123. Feng H, Shuda M, Chang Y, Moore PS. Clonal integration of a polyomavirus in human Merkel cell carcinoma. 2008 *Science 319*, 1096–1100.

124. Fischer H, Sauer G. Identification of virus-induced proteins in cells productively infected with simian virus 40. *Journal of virology,* 1972. 9(1): p. 1-9.

125. Fletcher MA, Saliou P, Ethevenaux C, Plotkin SA. The efficacy of whole cell pertussis immunisation: collected data on a vaccine produced in France. *Public Health,* 2001. 115(2): p. 119-29.

126. Flint SJ, Enquist LW, Racaniello VR, Skalka AM. in *Principle of virology* , (2009).

127. Fonteneau JF, Kavanagh DG, Lirvall M, Sanders C, Cover TL, Bhardwaj N, Larsson M. Characterization of the MHC class I cross-presentation pathway for cell-associated antigens by human dendritic cells. *Blood*, 2003. 102(13): p. 4448-55.

128. Foster RH, Noble S. Bivalent cholera and typhoid vaccine. *Drugs*, 1999. 58(1): p. 91-6; discussion 97-8.

129. Fostinis Y, Theodoropoulos PA, Gravanis A,Stournaras C. Heat shock protein HSP90 and its association with the cytoskeleton: a morphological study. 1992 *Biochem Cell Biol* 70, 779–786.

130. Foulongne V, Courgnaud V, Champeau W, Segondy M. Detection of Merkel cell polyomavirus on environmental surfaces. *J. Med. Virol.* 2011 Aug; 83(8):1435-9.

131. Foulongne V, Dereure O, Kluger N, Moles JP, Guillot B, Segondy M. Merkel cell polyomavirus DNA detection in lesional and nonlesional skin from patients with Merkel cell carcinoma or other skin diseases. *Br J. Dermatol.* 2010 Jan; 162(1):59-63.

132. Fountoulakis M, Langen H. Identification of proteins by matrix-assisted laser desorption ionization-mass spectrometry following in-gel digestion in low-salt, nonvolatile buffer and simplified peptide recovery. *Anal. Biochem.* 1997 Aug 1; 250(2):153-6.

133. French TJ, Marshall JJ, Roy P. Assembly of double-shelled, viruslike particles of bluetongue virus by the simultaneous expression of four structural proteins. *J Virol*, 1990. 64(12): p. 5695-700.

134. Fried H, Cahan LD, Paulson JC, Polyoma virus recognizes specific sialyligosaccharide receptors on host cells. *Virology*, 1981. 109(1): p. 188-92.

135. Fuchs M, Gerber J, Drapkin R, Sif S, Ikura T, Ogryzko V, Lane WS, Nakatani Y, Livingston DM. The p400 complex is an essential E1A transformation target. *Cell*, 2001. 106(3): p. 297- 307.

136. Furuse Y, Suzuki A, Kishi M, Galang HO, Lupisan SP, Olveda RM, Oshitani H. Detection of novel respiratory viruses from influenza-like illness in the Philippines. *Journal of medical virology*, 2010. 82(6): p. 1071-4.

137. Crevel G, Bates H, Huikeshoven H, Cotterill S. The Drosophila Dpit47 protein is a nuclear Hsp90 co-chaperone that interacts with DNA polymerase alpha, in *J Cell. Sci.*, vol. 114, n° 11, giugno 2001, pp. 2015–25.

138. Gardner SD, Field AM, Coleman DV, Hulme B. New human papovavirus (B.K.) isolated from urine after renal transplantation. *Lancet.* 1971 Jun 19;1(7712):1253-7.

139. Gaynor AM, Nissen MD, Whiley DM, Mackay IM, Lambert SB, Wu G, Brennan DC, Storch GA, Sloots TP, Wang D. Identification of a novel polyomavirus from patients with acute respiratory tract infections. *PLoS pathogens*, 2007. 3(5): p. e64.

140. Geller R, Taguwa S, Frydman J (2012) Broad action of Hsp90 as a host chaperone required for viral replication. *Biochim Biophys Acta* 1823, 698–706.

141. Gheysen D, Jacobs E, de Foresta F, Thiriart C, Francotte M, Thines D, De Wilde M. Assembly and release of HIV-1 precursor Pr55gag virus-like particles from recombinant baculovirus-infected insect cells. *Cell*, 1989. 59(1): p. 103-12.

142. Gilbert J, Benjamin T. Uptake pathway of polyomavirus via ganglioside GD1a. *J Virol*, 2004. 78(22): p. 12259-67.

143. Gingras AC, Gstaiger M, Raught B, Aebersold R. Analysis of protein complexes using mass spectrometry. *Nat. Rev. Mol. Cell. Biol.* 2007 Aug; 8(8):645-54. Review. PMID:17593931.

144. Giustiniani J, Daire V, Cantaloube I, Durand G, Pous C, Perdiz D, Baillet A. Tubulin acetylation favors Hsp90 recruitment to microtubules and stimulates the signaling function of the Hsp90 clients Akt/PKB and p53. 2009 *Cell Signal* 21, 529–539.

145. Gjoerup O, Chang Y. Update on human polyomaviruses and cancer. *Adv. Cancer Res.* 2010; 106:1-51.

146. Godbout R, Dryja TP, Squire J, Gallie BL, Phillips RA. Somatic inactivation of genes on chromosome 13 is a common event in retinoblastoma. *Nature*, 1983. 304(5925): p. 451-3.

147. Goldie SJ, Kohli M, Grima D, Weinstein MC, Wright TC, Bosch FX, Franco E. Projected clinical benefits and cost-effectiveness of a human papillomavirus 16/18 vaccine. *Journal of the National Cancer Institute,* 2004. 96(8): p. 604-15.

148. Gowans JL. The lymphocyte--a disgraceful gap in medical knowledge. *Immunol Today*, 1996. 17(6): p. 288-91

149. Graves PR, Haystead TA Molecular Biologist's Guide to Proteomics *Microbiol Mol. Biol.* Rev. 2002 Mar;66(1):39-63; table of contents. Review. PMID: 11875127.

150. Griffin BE. Epstein-Barr virus (EBV) and human disease: facts, opinions and problems. *Mutation research*, 2000. 462(2-3): p. 395-405.

151. Gross L. "Spontaneous" leukemia developing in C3 H mice following inoculation in infancy, with AK-leukemic extracts, or AK-embrvos. *Proc Soc Exp Biol Med*. 1951, 76: 27-32.

152. Gross L. A filterable agent, recovered from Ak leukemic extracts, causing salivary gland carcinomas in C3H mice. *Proc Soc Exp Biol Med*, 1953. 83(2): p. 414-21.

153. Grossi MP, Caputo A, Meneguzzi G, Corallini A, Carra L, Portolani M, Borgatti M, Milanesi G, Barbanti-Brodano G. Transformation of human embryonic fibroblasts by BK virus, BK virus DNA and a subgenomic BK virus DNA fragment. *The Journal of general virology*, 1982. 63(2): p. 393-403.

154. Guo YH, Li YN, Zhao JR, Zhang J, Yan Z. HBc binds to the CpG islands of HBV cccDNA and promotes an epigenetic permissive state. 2011 *Epigenetics* 6, 720–726.

155. Haeberle H, Fujiwara M, Chuang J, Medina MM, Panditrao MV, Bechstedt S, Howard J, Lumpkin EA. Molecular profiling reveals synaptic release machinery in Merkel cells. *Proceedings of the National Academy of Sciences of the United States of America,* 2004. 101(40): p. 14503-8.

156. Halata Z, Grim M, Bauman KI. Friedrich Sigmund Merkel and his "Merkel cell", morphology, development, and physiology: review and new results. The anatomical record. Part A, *Discoveries in molecular, cellular, and evolutionary biology*, 2003. 271(1): p. 225-39.

157. Hanahan D, Weinberg RA. Hallmarks of cancer: the next generation. *Cell*, 2011. 144(5): p. 646-74.

158. Hannon GJ, Demetrick D, Beach D. Isolation of the Rb-related p130 through its interaction with CDK2 and cyclins. *Genes & development*, 1993. 7(12A): p. 2378-91.

159. Haun G, Keppler OT, Bock CT, Herrmann M, Zentgraf H, Pawlita M. The cell surface receptor is a major determinant restricting the host range of the B-lymphotropic papovavirus. *J Virol*, 1993. 67(12): p. 7482- 92.

160. Heath M, Jaimes N, Lemos B, Mostaghimi A, Wang LC, Peñas PF, Nghiem P. Clinical characteristics of Merkel cell carcinoma at diagnosis in 195 patients: the AEIOU features. *J Am Acad Dermatol*, 2008. 58(3): p. 375-81.

161. Hermannstadter A, Ziegler C, Kühl M, Deppert W, Tolstonog GV. Wild-type p53 enhances efficiency of simian virus 40 large-T-antigen-induced cellular transformation. *Journal of virology*, 2009. 83(19): p. 10106-18.

162. Hershey AD, Chase M. Independent functions of viral protein and nucleic acid in growth of bacteriophage. *J Gen Physiol*, 1952. 36(1): p. 39-56.

163. Herzig M, Novatchkova M, Christofori G. An unexpected role for p53 in augmenting SV40 large T antigen-mediated tumorigenesis. *Biological chemistry,* 1999. 380(2): p. 203-11.

164. Hillenkamp F, Karas M, Beavis RC, Chait BT (1991) Matrix-assisted laser desorption ionization mass spectrometry of biopolymers. *Anal. Chem.* 63:A1193-A1202.

165. Hodgson NC. Merkel cell carcinoma: changing incidence trends. J Surg Oncol, 2005. 89(1): p. 1-4.

166. Hollstein M. Database of p53 gene somatic mutations in human tumors and cell lines. Nucleic acids research, 1994. 22(17): p. 3551-5.

167. Horie Y, Motoi M, Ogawa K. Early stages of development of rat brain tumors induced by JC virus: a sequential histological and immunohistochemical study. *Acta medica Okayama*, 1989. 43(5): p. 271-9.

168. Horníková L, Fraiberk M, Man P, Janovec V, Forstová J. VP1, the major capsid protein of the mouse polyomavirus, binds microtubules, promotes their

acetylation and blocks the host cell cycle. *FEBS J*. 2017 Jan;284(2):301-323. doi: 10.1111/febs.13977. Epub 2017 Jan 9.

169. Houff SA. Neuroradiological studies of JCV-induced astrocytomas in nonhuman primates. *Progress in clinical and biological research*, 1983. 105: p. 253-9.

170. Howard J, Basic Concepts in Immunology, in Immunobiology, C.A. Janeway, Editor. 2005, Garland Science Publishing: New York. p. 1-35. human tumour virology. *Nat Rev Cancer* 2010;10(12): 878-89.

171. Howe JA. Retinoblastoma growth suppressor and a 300-kDa protein appear to regulate cellular DNA synthesis. Proceedings of the National Academy of Sciences of the United States of America, 1990. 87(15): p. 5883-7.

172. Huber F, Boire A, Lòpez MP, Koenderink GH. (2015) Cytoskeletal crosstalk: when three different personalities team up. *Curr Opin Cell Biol* 32, 39–47.

173. Husain M, Cheung CY. (2014) Histone deacetylase 6 inhibits influenza A virus release by downregulating the trafficking of viral components to the plasma membrane via its substrate, acetylated microtubules. *JVirol.* 2014 Oct;88(19):11229-39. doi: 10.1128/JVI.00727-14. Epub 2014 Jul 16.

174. Husain M, Harrod KS. (2011) Enhanced acetylation of alpha-tubulin in influenza A virus infected epithelial cells. *FEBS Lett* 585, 128–132.

175. Imperiale MJ. The human polyomaviruses, BKV and JCV: molecular pathogenesis of acute disease and potential role in cancer. *Virology,* 2000. 267(1): p. 1-7.

176. Iyer NG, Ozdag H, Caldas C. p300/CBP and cancer. *Oncogene*, 2004. 23(24): p. 4225-31.

177. Jakobovits EB, Bratosin S, Aloni Y. (1980). A nucleosome-free region in SV40 minichromosomes. Nature, 285, 263–265.

178. Jartti T, Jartti L, Ruuskanen O, Söderlund-Venermo M. New respiratory viral infections. *Curr Opin Pulm Med*. 2012 May;18(3):271-8.doi: 10.1097/MCP.0b013e328351f8d4.

179. Jiang M, Abend JR, Johnson SF, Imperiale MJ. The role of polyomaviruses in human disease. *Virology*. 2009 Feb 20; 384(2):266-73.

180. Jay G. Identification of the SV40 agnogene product: a DNA binding protein. *Nature*, 1981. 291(5813): p. 346-9.

181. Jiang M.The role of polyomaviruses in human disease. *Virology*, 2009. 384(2): p. 266-73.

182. Johne R, Müller H. Polyomaviruses of birds: etiologic agents of inflammatory diseases in a tumor virus family. *J. Virol.* 2007; 81: 11554–11559.

183. Johne R. Rolling-circle amplification of viral DNA genomes using phi29 polymerase. *Trends in microbiology*, 2009. 17(5): p. 205-11.

184. Johne R. Taxonomical developments in the family Polyomaviridae. Archives of virology, 2011. 156(9): p. 1627-34.

185. Jung WT. JC virus T-antigen expression in sporadic adenomatous polyps of the colon. *Cancer*, 2008. 112(5): p. 1028-36.

186. Kaae J, Hansen AV, Biggar RJ, Boyd HA, Moore PS, Wohlfahrt J. Merkel cell carcinoma: incidence, mortality, and risk of other cancers. *J. Natl. Cancer Inst.* 2010 Jun 2; 102(11):793-801.

187. Kanda T, Takemoto KK. Analysis of T antigen and viral DNA in mouse cells transformed by K virus, a nononcogenic murine papovavirus. *J Virol,* 1984. 50(3): p. 954-6.

188. Kang D, Gho YS, Suh M, Kang C. Highly Sensitive and Fast Protein Detection with Coomassie Brilliant Blue in Sodium Dodecyl Sulfate-Polyacrylamide Gel Electrophoresis Bull. *Korean Chem. Soc*. 2002, vol. 23, No. 11 1511-1512.

189. Kantola K, Sadeghi M, Lahtinen A, Koskenvuo M, Aaltonen LM, Mottonen M. Merkel cell polyomavirus DNA in tumor-free tonsillar tissues and upper respiratory tract samples: implications for respiratory transmission and latency. *J. Clin. Virol.* 2009 Aug; 45(4):292-5.

190. Kasper JS. Simian virus 40 large T antigen's association with the CUL7 SCF complex contributes to cellular transformation. Journal of virology, 2005. 79(18): p. 11685-92.

191. Kassem A, Schöpflin A, Diaz C, Weyers W, Stickeler E, Werner M, Zur HA. (2008). Frequent detection of Merkel cell polyomavirus in human Merkel cell carcinomas and identification of a unique deletion in the VP1 gene. *Cancer Res. 68*, 5009–5013.

192. Kast J, Parker CE, van der Drift K, Dial JM, Milgram SL, Wilm M, Howell M, Borchers CH. Matrix-assisted laser desorption/ionization directed nano-electrospray ionization tandem mass spectrometric analysis for protein identification. *Rapid Commun Mass Spectrom.* 2003; 17(16):1825-34.

193. Kazem S, van der Meijden E, Kooijman S, Rosenberg AS, Hughey LC, Browning JC. Trichodysplasia spinulosa is characterized by active polyomavirus infection. *J. Clin. Virol.* 2012 Mar; 53(3):225-30.

194. Kazem S, van der Meijden E, Wang RC, Rosenberg AS, Pope E, Benoit T, Fleckman P, Feltkamp MCW. Polyomavirus-associated trichodysplasia spinulosa involves hyperproliferation, pRB phosphorylation and upregulation of p16 and p21. *PLOS One*, 2014, Oct 7; 9(10):e108947. doi: 10.1371/journal.pone.0108947. eCollection 2014. PubMed PMID: 25291363.

195. Kazmin D, Edwards RA, Turner RJ, Larson E, Starkey J. Visualization of Proteins in Acrylamide Gels Using Ultraviolet Illumination. Anal Biochem. 2002 Feb; 301(1):91–6.

196. Kean JM, Rao S, Wang M, Garcea RL. Seroepidemiology of human polyomaviruses. *PLoS Pathog.* 2009 Mar; 5(3):e1000363.

197. Kelly GL, Rickinson AB. Burkitt lymphoma: revisiting the pathogenesis of a virus-associated malignancy. Hematology / the Education Program of the American

Society of Hematology. American Society of Hematology. *Education Program*, 2007: p. 277-84.

198. Keppler OT. Biosynthetic modulation of sialic acid-dependent virus- receptor interactions of two primate polyoma viruses. J Biol Chem, 1995. 270(3): p. 1308-14.

199. Khalili K, Sariyer IK, Safak M. (2008). Small tumor antigen of polyomaviruses: role in viral life cycle and cell transformation. *J. Cell. Physiol. 215*, 309–319.

200. Kierstead TD, Tevethia MJ. Association of p53 binding and immortalization of primary C57BL/6 mouse embryo fibroblasts by using simian virus 40 T-antigen mutants bearing internal overlapping deletion mutations. Journal of virology, 1993. 67(4): p. 1817-29.

201. Kilham L, Murphy HW. A pneumotropic virus isolated from C3H mice carrying the Bittner Milk Agent. Proc Soc Exp Biol Med, 1953. 82(1): p. 133-7.

202. Kim HY, Ahn BY, Cho Y. Structural basis for the inactivation of retinoblastoma tumor suppressor by SV40 large T antigen. EMBO J, 2001. 20(1-2): p. 295-304.

203. Klose J. (1975). Protein mapping by combined isoelectric focusing and electrophoresis of mouse tissues. A novel approach to testing for induced point mutations in mammals. Humangenetik 26, 231-243.

204. Klug A. Structure of Viruses of the Papilloma-Polyoma Type.Ii. Comments on Other Work. *J. Mol.Biol.* 11,424-431 (1965).

205. Knight LM, Stakaityte G, Wood JJ, Abdul-Sada H, Griffiths DA, Howell GJ, Wheat R, Blair GE, Steven NM, Macdonald A. Merkel cell polyomavirus small T antigen mediates microtubule destabilization to promote cell motility and migration. 2015 *J Virol* 89, 35–47.

206. Knowles WA. Discovery and epidemiology of the human polyomaviruses BK virus (BKV) and JC virus (JCV). *Adv. Exp. Med. Biol.* 2006; 577:19-45.

207. Knowles WA. Population-based study of antibody to the human polyomaviruses BKV and JCV and the simian polyomavirus SV40. *Journal of medical virology*, 2003. 71(1): p. 115-23.

208. Knudson AG, Jr. Mutation and cancer: statistical study of retinoblastoma. *Proceedings of the National Academy of Sciences of the United States of America*, 1971. 68(4): p. 820-3.

209. Kotsakis A, Pomeranz LE, Blouin, Blaho JA. Microtubule reorganization during herpes simplex virus type 1 infection facilitates the nuclear localization of VP22, a major virion tegument protein. 2001 *J Virol* 75, 8697–8711.

210. Krishna RG, Wold F. Post-translational modification of proteins. 1993 *Adv Enzymol Relat Areas Mol Biol* 67, 265-298.

211. Kuwamoto S. Recent advances in the biology of Merkel cell carcinoma. *Hum. Pathol.* 2011 Aug; 42(8):1063-77.

212. Ladner CL, Edwards RA, Schriemer DC, Turner RJ. Identification of trichloroethanol visualized proteins from two-dimensional polyacrylamide gels by mass spectrometry. *Anal Chem*. 2006 Apr 1;78(7):2388-96.

213. Ladner CL, Raymond JT, Robert A. Edwards RA. Development of indole chemistry to label tryptophan residues in protein for determination of tryptophan surface accessibility *Protein Sci*. 2007 Jun; 16(6): 1204–1213. doi: 10.1110/ps.062728407

214. Ladner CL, Tran K, Le M, Turner RJ, Edwards RA. Excited State Photoreaction between the Indole Side Chain of Tryptophan and Halocompounds Generates New Fluorophores and Unique Modifications. *Photochem Photobiol*. 2014 Apr;n/a-n/a.

215. Ladner CL, Yang J, Turner RJ, Edwards RA. Visible fluorescent detection of proteins in polyacrylamide gels without staining. *Anal Biochem*. 2004 Mar;326(1):13–20.

216. Lagatie O, Tritsmans L, Stuyver LJ. The miRNA world of polyomaviruses. *Virol J*. 2013 Aug 28;10:268. doi: 10.1186/1743-422X-10-268.

217. Laghi L. JC virus DNA is present in the mucosa of the human colon and in colorectal cancers. Proceedings of the National Academy of Sciences of the United States of America, 1999. 96(13): p. 7484-9.

218. Lambert PH, Liu M, Siegrist CA. Can successful vaccines teach us how to induce efficient protective immune responses? *Nat Med*, 2005. 11(4 Suppl): p. S54-62.

219. Lane DP, Crawford LV. T antigen is bound to a host protein in SV40-transformed cells. *Nature*, 1979. 278(5701): p. 261-3.

220. Lane DP. Cancer. p53, guardian of the genome. *Nature*, 1992. 358(6381): p. 15-6.

221. Lavanchy D. Hepatitis B virus epidemiology, disease burden, treatment, and current and emerging prevention and control measures. *Journal of viral hepatitis*, 2004. 11(2): p. 97-107.

222. Lee WH. Human retinoblastoma susceptibility gene: cloning, identification, and sequence. *Science*, 1987. 235(4794): p. 1394-9.

223. Lewis JK, Bendahmane M, Smith TJ, Beachy RN, Siuzdak G (1998) Identification of viral mutants by mass spectrometry. *Proc. Natl. Acad. Sci.*, USA 95:8596–8601.

224. Lewis JK, Chiang J, Siuzdak, G (1999) Monitoring protein-drug interactions with mass spectrometry. *J. Assoc. Lab Automat.* 4:46–48.

225. Li PP, Itoh N, Watanabe M, Shi Y, Liu P, Yang HJ, Kasamatsu H (2009) Association of Simian virus 40 VP1 with 70-kilodalton heat shock proteins and viral tumor antigens. J Virol 83, 37–46.

226. Li PP, Nakanishi A, Shum D, Sun PC, Salazar AM, Fernandez CF. Simian virus 40 Vp1 DNA-binding domain is functionally separable from the overlapping nuclear localization signal and is required for effective virion formation and full viability. 2001 *J. Virol.* 75, 7321–7329.

227. Lill NL. p300 family members associate with the carboxyl terminus of simian virus 40 large tumor antigen. *Journal of virology,* 1997. 71(1): p. 129-37.

228. Lilyestrom W. Crystal structure of SV40 large T-antigen bound to p53: interplay between a viral oncoprotein and a cellular tumor suppressor. *Genes & development*, 2006. 20(17): p. 2373-82.

229. Linzer DI, Levine AJ. Characterization of a 54K dalton cellular SV40 tumor antigen present in SV40- transformed cells and uninfected embryonal carcinoma cells. *Cell*, 1979. 17(1): p. 43-52.

230. Litovchick L. Evolutionarily conserved multisubunit RBL2/p130 and E2F4 protein complex represses human cell cycle-dependent genes in quiescence. *Molecular cell*, 2007. 26(4): p. 539-51.

231. Liu CK, Wei G, Atwood WJ. Infection of glial cells by the human polyomavirus JC is mediated by an N-linked glycoprotein containing terminal alpha(2-6)-linked sialic acids. *J Virol*, 1998. 72(6): p. 4643-9.

232. London WT. Brain tumors in owl monkeys inoculated with a human polyomavirus (JC virus). *Science*, 1978. 201(4362): p. 1246-9.

233. Low JA, Magnuson B, Tsai B, Imperiale MJ. Identification of gangliosides GD1b and GT1b as receptors for BK virus. *J. Virol.* 2006 Feb;80(3):1361-6.

234. Lucarz A, Brand G. Current considerations about Merkel cells. *European journal of cell biology*, 2007. 86(5): p. 243-51.

235. Maginnis MS, Atwood WJ. JC virus: an oncogenic virus in animals and humans? Seminars in cancer biology, 2009. 19(4): p. 261-9.

236. Magnuson B, Rainey EK, Benjamin T, Baryshev M, Mkrtchian S, Tsai B. (2005). ERp29 triggers a conformational change in polyomavirus to stimulate membrane binding. Mol. Cell. 20, 289–300.

237. Mann M, Jensen ON. (2003). Proteomic analysis of post-translational modifications. Nat Biotechnol 21, 255-261.

238. Mannova P, Forstova J. Mouse polyomavirus utilizes recycling endosomes for a traffic pathway independent of COPI vesicle transport. *J Virol,* 2003. 77(3): p. 1672-81.

239. Marcoval J, Ferreres JR, Penín RM, Pérez D, Viñals JM. (2014). Merkel Cell Carcinoma: Differences between Sun-Exposed and Non-Sun-Exposed Variants - A Clinical Analysis of 36 Cases. *Dermatology 229*, 205–209.

240. Margaret E, McLaughlin-Drubin, Karl Munger Viruses Associated with Human *Cancer Biochim Biophys Acta*. 2008 Mar; 1782(3): 127–150. PMCID: PMC2267909 NIHMSID: NIHMS41780 PMID: 18201576.

241. Maricich SM. Merkel cells are essential for light-touch responses. *Science*, 2009. 324(5934): p. 1580-2.

242. Martel-Jantin C. Genetic variability and integration of Merkel cell polyomavirus in Merkel cell carcinoma. Virology, 2012. 426(2): p. 134-42.

243. Marx JL. Cancer gene research wins medicine Nobel. *Science*, 1989. 246(4928): p. 326-7.

244. Masumi A. The histone acetylase PCAF is a phorbol-ester-inducible coactivator of the IRF family that confers enhanced interferon responsiveness. *Mol Cell Biol*, 1999. 19(3): p. 1810-20.

245. Mayol X. Cloning of a new member of the retinoblastoma gene family (pRb2) which binds to the E1A transforming domain. *Oncogene*, 1993. 8(9): p. 2561-6.

246. Meraldi P, Sorger PK. A dual role for Bub1 in the spindle checkpoint and chromosome congression. *The EMBO journal*, 2005. 24(8): p. 1621-33.

247. Mertz KD, Junt T, Schmid M, Pfaltz M, Kempf W. Inflammatory monocytes are a reservoir for Merkel cell polyomavirus. *J. Invest Dermatol.* 2010 Apr; 130(4):1146-51. doi: 10.1038/jid.2009.392.

248. Mezes B, Amati, P. (1994). Mutations of poly-omavirus VP1 allow in vitro growth in undifferen-tiated cells and modify in vivo tissue replication specificity. J. Virol. 68, 1196–1199.

249. Michel MR, Hirt B, Weil R. Mouse cellular DNA enclosed in polyoma viral capsids (pseudovirions). *Proc Natl Acad Sci USA*, 1967. 58(4): p. 1381-8.

250. Miller RW, Rabkin CS. Merkel cell carcinoma and melanoma: etiological similarities and differences. Cancer epidemiology, biomarkers & prevention : a publication of the American Association for Cancer Research, cosponsored by the American Society of Preventive Oncology, 1999. 8(2): p. 153-8.

251. Miyanohara A. Expression of hepatitis B virus core antigen gene in Saccharomyces cerevisiae: synthesis of two polypeptides translated from different initiation codons. *J Virol*, 1986. 59(1): p. 176-80.

252. Montross L. Nuclear assembly of polyomavirus capsids in insect cells expressing the major capsid protein VP1. *J Virol*, 1991. 65(9): p. 4991-8.

253. Morris EJ, Dyson NJ. Retinoblastoma protein partners. Advances in cancer research, 2001. 82: p. 1- 54.

254. Muller U, Zentgraf H, Eicken I, Keller W. Higher order structure of simian virus 40 chromatin. *Science* 201, 406-415 (1978).

255. Munger K. Complex formation of human papillomavirus E7 proteins with the retinoblastoma tumor suppressor gene product. *The EMBO journal*, 1989. 8(13): p. 4099-105.

256. Murai Y. High JC virus load in gastric cancer and adjacent non-cancerous mucosa. *Cancer science*, 2007. 98(1): p. 25-31.

257. Murata K. Immunization with hepatitis C virus-like particles protects mice from recombinant hepatitis C virus-vaccinia infection. *Proc Natl Acad Sci U S A*, 2003. 100(11): p. 6753-8.

258. Murphy RM, Lamb GD. Important considerations for protein analyses using antibody based techniques: down-sizing Western blotting up-sizes outcomes: Quantitative Western blotting. *J Physiol*. 2013 Dec 1;591(23):5823–31.

259. Neske F, Prifert C, Scheiner B, Ewald M, Schubert J, Opitz A. High prevalence of antibodies against polyomavirus WU, polyomavirus KI, and human bocavirus in German blood donors. *BMC Infect Dis.* 2010;10: 215.

260. Nesvizhskii AI. Computational and informatics strategies for identification of specific protein interaction partners in affinity purification mass spectrometry experiments. *Proteomics* 12(10), 1639–1655 (2012).

261. Neu U, Stehle T, Atwood WJ. The Polyomaviridae: Contributions of virus structure to our understanding of virus receptors and infectious entry. *Virology* 384, 389-399 (2009).

262. Norja P, Ubillos I, Templeton K, Simmonds P. No evidence for an association between infections with WU and KI polyomaviruses and respiratory disease. *J. Clin. Virol.* 2007 Dec; 40(4):307-11.

263. Norkin LC, Anderson HA, Wolfrom SA, Oppenheim A. (2002). Caveolar endocytosis of simian virus 40 is followed by brefeldin A-sensitive transport to the endoplasmic reticulum, where the virus dis-assembles. *J Virol*. 76, 5156–5166.

264. O'Farrel PH. (1975). High resolution two dimensional electrophoresis of proteins. *J. Biol. Chem*. 250: 4007- 4021.

265. O'Donnell PH, Swanson K, Josephson MA, Artz AS, Parsad SD, Ramaprasad C. BK virus infection is associated with hematuria and renal impairment in recipients of allogeneic hematopoetic stem cell transplants. *Biol. Blood Marrow Transplant.* 2009 Sep; 15(9):1038-48 e1. Oct; 18(10):1737-43.

266. Ohsumi S. Induction of undifferentiated brain tumors in rats by a human polyomavirus (JC virus). Japanese journal of cancer research : Gann, 1985. 76(6): p. 429-31.

267. Ohsumi S, Motoi M, Ogawa K. Induction of undifferentiated tumors by JC virus in the cerebrum of rats. Acta pathologica japonica, 1986. 36(6): p. 815-25.

268. Csermely P, Schnaider T, Soti C, Prohászka Z, Nardai G. The 90-kDa molecular chaperone family: structure, function, and clinical applications. A comprehensive review, in Pharmacol. Ther. vol. 79, n°2, agosto 1998, pp. 129–68, DOI:10.1016/S0163-7258(98)00013-8, PMID 9749880.

269. Padgett BL, Walker DL, ZuRhein GM, Eckroade RJ, Parton RG, Simons K. The multiple faces of caveolae. *Nat. Rev. Mol. Cell Biol*. 8, 185-194 (2007).

270. Padgett BL, Walker DL, ZuRhein GM, Eckroade RJ, Dessel BH. Cultivation of papova-like virus from human brain with progressive multifocal leucoencephalopathy. *Lancet.* 1971 Jun 19; 1(7712):1257-60.

271. Padgett BL, Walker DL, ZuRhein, GM, Eckroade, R J, Pantulu ND, Pallasch CP, Kurz AK, Kassem A, Frenzel L, Sodenkamp S. Detection of a novel truncating Merkel cell polyomavirus large T antigen deletion in chronic lymphocytic leukemia cells. *Blood.* 2010 Dec 9; 116(24):5280-4.

272. Paliard X. Priming of strong, broad, and long-lived HIV type 1 p55gag- specific CD8+ cytotoxic T cells after administration of a virus-like particle vaccine in rhesus macaques. AIDS Res Hum Retroviruses, 2000. 16(3): p. 273- 82.

273. Pandey A, Mann M. (2000). Proteomics to study genes and genomes. *Nature* 405, 837-846.

274. Parkin DM. Global cancer statistics in the year 2000. *Lancet Oncol*, 2001. 2(9): p. 533-43.

275. Parkin DM. The global health burden of infection-associated cancers in the year 2002. *Int J Cancer,* 2006. 118(12): p. 3030-44.

276. Parton RG, Simons K. The multiple faces of caveolae. *Nat. Rev. Mol. Cell Biol.* 8, 185-194 (2007).

277. Pashine A, Valiante NM, Ulmer JB. Targeting the innate immune response with improved vaccine adjuvants. *Nat Med*, 2005. 11(4 Suppl): p. S63- 8.

278. Pastrana DV. Quantitation of human seroresponsiveness to Merkel cell polyomavirus. PLoS Pathog, 2009. 5(9): p. e1000578.

279. Pastrana DV, Pumphrey KA, Çuburu N, Schowalter RM, Buck CB. Characterization of monoclonal antibodies specific for the Merkel cell polyomavirus capsid. *Virology*, 2010. 405(1): p. 20-5.

280. Patterson SD, Aebersold RH. (2003). Proteomics: the first decade and beyond. *Nat Genet* 33 Suppl, 311-323.

281. Patton WF. A thousand points of light: The application of fluorescence detection technologies to two-dimensional gel electrophoresis and proteomics. *Electrophoresis*. 2000;21(6):1123–1144.

282. Pearse AG. The neuroendocrine (APUD) cells of the skin. *The American Journal of dermatopathology*, 1980. 2(2): p. 121-3.

283. Petry H. The use of virus-like particles for gene transfer. *Curr Opin Mol Ther*, 2003. 5(5): p. 524-8. PMID:12563305.

284. Pipas JM. Common and unique features of T antigens encoded by the polyomavirus group. *J Virol,* 1992. 66(7): p. 3979-85.

285. Pipas JM. SV40: Cell transformation and tumorigenesis. *Virology*, 2009. 384(2): p. 294-303.

286. Poiesz BJ, Ruscetti FW, Gazdar AF, Bunn PA, Minna JD, Gallo RC. Detection and isolation of type C retrovirus particles from fresh and cultured lymphocytes of a patient with cutaneous T-cell lymphoma. *Proc Natl Acad Sci USA* 1980; 77: 7415–9

287. Portolani M, Borgatti M. Stable transformation of mouse, rabbit and monkey cells and abortive transformation of human cells by BK virus, a human papovavirus. *The Journal of general virology*, 1978. 38(2): p. 369-74.

288. Posch A, Kohn J, Oh K, Hammond M, Liu N. V3 Stain-free Workflow for a Practical, Convenient, and Reliable Total Protein Loading Control in Western Blotting. J Vis Exp [Internet]. 2013 Dec 30;(82). Available from: http://www.jove.com/video/50948/v3-stain-free-workflow-for-practical-convenient-reliable-total.

289. Poulin DL, Kung AL, DeCaprio JA. p53 targets simian virus 40 large T antigen for acetylation by CBP. *Journal of virology*, 2004. 78(15): p. 8245-53.

290. Poulin DL, DeCaprio JA. (2006). Is there a role for SV40 in human cancer? *J. Clin. Oncol. 24*, 4356–4365.

291. Schowalter RM, Buck CB. The Merkel Cell Polyomavirus Minor Capsid Protein PLoS Pathog. 2013 Aug; 9(8): e1003558. Published online 2013 Aug 22. doi: 10.1371/journal.ppat.1003558 PMCID: PMC3749969.

292. Rappsilber J, Mann M, Ishihama Y. Protocol for micro-purification, enrichment, pre-fractionation and storage of peptides for proteomics using StageTips. Nat Protoc. 2007;2(8):1896-906.

293. Raptis L, Vultur A. Neoplastic transformation assays. Methods Mol Biol, 2001. 165: p. 151-64.

294. Rathi AV. Simian virus 40 T-antigen-mediated gene regulation in enterocytes is controlled primarily by the Rb-E2F pathway. Journal of virology, 2009. 83(18): p. 9521-31.

295. Rathje LS, Nordgren N, Pettersson T, Rönnlund D, Widengren J, Aspenström P, Gad AK. (2014) Oncogenes induce a vimentin filament collapse mediated by HDAC6 that is linked to cell stiffness. *Proc Natl Acad Sci USA* 111, 1515–1520.

296. Arora R, Chang Y, Moore PS. MCV and Merkel Cell Carcinoma: A Molecular Success Story *Curr Opin Virol*. 2012 Aug; 2(4): 489–498. Published online 2012 Jun 17. doi: 10.1016/j.coviro.2012.05.007.

297. Ren L. WU and KI polyomavirus present in the respiratory tract of children, but not in immunocompetent adults. Journal of clinical virology: the official publication of the Pan American Society for Clinical Virology, 2008. 43(3): p. 330-3.

298. Rencic A. Detection of JC virus DNA sequence and expression of the viral oncoprotein, tumor antigen, in brain of immunocompetent patient with oligoastrocytoma. Proceedings of the National Academy of Sciences of the United States of America, 1996. 93(14): p. 7352-7.

299. Ricci L, Maione R, Passananti C, Felsani A, Amati P. (1992). Mutations in the VP1 coding region of polyomavirus determine differentiating stage spe-cificity. *J Virol.* 66, 7153–7158.

300. Ricciardiello L. JC virus DNA sequences are frequently present in the human upper and lower gastrointestinal tract. *Gastroenterology,* 2000. 119(5): p. 1228-35.

301. Ricciardiello L. Mad-1 is the exclusive JC virus strain present in the human colon, and its transcriptional control region has a deleted 98-base-pair sequence in colon cancer tissues. *Journal of virology*, 2001. 75(4): p. 1996-2001.

302. Robey RC, Mletzko S, Gotch FM. The T-Cell Immune Response against Kaposi's Sarcoma-Associated Herpesvirus Adv Virol. 2010; 2010: 340356. Published online 2011 Jan 16. doi: 10.1155/2010/340356.

303. Ronald T. Javier and Janet S. Butel The History of Tumor Virology Cancer Res. 2008 Oct 1; 68(19): 7693–7706. doi: 10.1158/0008-5472.CAN-08-3301

304. Rose RC. Expression of human papillomavirus type 11 L1 protein in insect cells: in vivo and in vitro assembly of viruslike particles. J Virol, 1993. 67(4): p. 1936-44.

305. Rouleau M, Aubin AR, Poirier GG. (2004). Poly(ADP-ribosyl)ated chromatin domains: access granted. *J Cell Sci.* 117, 815–825.

306. Rous P. A transmissible avian neoplasm. (Sarcoma of the common fowl) by Peyton Rous, M.D., *Experimental Medicine* for Sept. 1, 1910, vol. 12, pp.696-705.

307. Rous P. Landmark article (JAMA 1911;56:198). Transmission of a malignant new growth by means of a cell-free filtrate. By Peyton Rous. JAMA : the *journal of the American Medical Association,* 1983. 250(11): p. 1445-9.

308. Rubin H. (2011). The early history of tumor virology: Rous, RIF, and RAV. *Proc. Natl. Acad. Sci. USA 108*, 14389–14396.

309. Sablina AA, Hahn WC. SV40 small T antigen and PP2A phosphatase in cell transformation. Cancer metastasis reviews, 2008. 27(2): p. 137-46.

310. Sadeghi M, Riipinen A, Vaisanen E, Chen T, Kantola K, Surcel HM. Newly discovered KI, WU, and Merkel cell polyomaviruses: no evidence of mother-to-fetus transmission. *Virol. J.* 2010; 7:251.

311. Sakaguchi S. Immunologic self-tolerance maintained by activated T cells expressing IL-2 receptor alpha-chains (CD25). Breakdown of a single mechanism of self-tolerance causes various autoimmune diseases. J Immunol, 1995. 155(3): p. 1151-64.

312. Salunke DM, Caspar DL, Garcea RL. "Self-assembly of purified polyomavirus capsid protein VP1". 1986 *Cell*. 46 (6): 895–904. doi:10.1016/0092-8674(86)90071-1. PMID 3019556.

313. Samuelson AV. p400 is required for E1A to promote apoptosis. The Journal of biological chemistry, 2005. 280(23): p. 21915-23.

314. Sapp M, Day PM. Structure, attachment and entry of polyoma- and papillomaviruses. *Virology* 384, 400-409 (2009).

315. Sariyer IK. Infection by agnoprotein-negative mutants of polyomavirus JC and SV40 results in the release of virions that are mostly deficient in DNA content. Virology journal, 2011. 8: p. 255.

316. Sarnaik AA, Lien MH, Nghiem P, Bichakjian CK. Clinical recognition, diagnosis, and staging of merkel cell carcinoma, and the role of the multidisciplinary management team. *Curr. Probl. Cancer.* 2010 Jan-Feb; 34(1):38-46.

317. Scheele GA. Two-dimensional gel analysis of soluble proteins. Charaterization of guinea pig exocrine pancreatic proteins. 1975 *J Biol Chem* 250, 5375-5385.

318. Scheffner M. The E6 oncoprotein encoded by human papillomavirus types 16 and 18 promotes the degradation of p53. *Cell*, 1990. 63(6): p. 1129-36.

319. Schowalter RM, Buck CB. (2013). The Merkel cell polyomavirus minor capsid protein. *PLoS Pathog. 9*, e1003558.

320. Schowalter RM, Pastrana DV, Pumphrey KA, Moyer AL, Buck CB. Merkel cell polyomavirus and two previously unknown polyomaviruses are chronically shed from human skin. *Cell Host Microbe.* 2010 Jun 25; 7(6):509-15.

321. Schrama D. No evidence for association of HPyV6 or HPyV7 with different skin cancers. The Journal of investigative dermatology, 2012. 132(1): p. 239-41.

322. Schwartz RH. T cell anergy. Annu Rev Immunol, 2003. 21: p. 305-34.

323. Scuda N, Hofmann J, Calvignac-Spencer S, Ruprecht K, Liman P, Kuhn J. A novel human polyomavirus closely related to the african green monkey-derived lymphotropic polyomavirus. *J. Virol.* 2011 May; 85(9):4586-90.

324. Seidler J, Zinn N, Boehm ME, Lehmann WD. De novo sequencing of peptides by MS/MS. Proteomics 2010;10(4): 634–49.

325. Seo GJ, Chen CJ, Sullivan CS. Merkel cell polyomavirus encodes a microRNA with the ability to autoregulate viral gene expression. Virology, 2009. 383(2): p. 183-7.

326. Shah KV. Simian virus 40 and human disease. J Infect Dis, 2004. 190(12): p. 2061-4.

327. Shimizu J, Yamazaki S, Sakaguchi S. Induction of tumor immunity by removing CD25+CD4+ T cells: a common basis between tumor immunity and autoimmunity. *J Immunol*, 1999. 163(10): p. 5211-8.

328. Shin SK. Oncogenic T-antigen of JC virus is present frequently in human gastric cancers. *Cancer*, 2006. 107(3): p. 481-8.

329. Shishido-Hara Y, Ichinose S, Higuchi K, Hara Y, Yasuj K (2004) Major and minor capsid proteins of human polyomavirus JC cooperatively accumulate to nuclear domain 10 for assembly into virions. *J Virol* 78, 9890-9903.

330. Shuda M. T antigen mutations are a human tumor-specific signature for Merkel cell polyomavirus. Proceedings of the National Academy of Sciences of the United States of America, 2008. 105(42): p. 16272-7.

331. Sibley RK, Dehner LP, Rosai J. Primary neuroendocrine (Merkel cell?) carcinoma of the skin. I. A clinicopathologic and ultrastructural study of 43 cases. *The American journal of surgical pathology*, 1985. 9(2): p. 95-108.

332. Sickmann A, Mreyen M, Meyer HE. Identification of modified proteins by mass spectrometry. *IUBMB Life.* 2002 Aug; 54(2):51-7.

333. Siebrasse EA, Reyes A, Lim ES, Zhao G, Mkakosya RS, Manary MJ. Identification of MW Polyomavirus, a Novel Polyomavirus in Human Stool. *J. Virol.* 2012 Oct; 86(19):10321-6.

334. Simmons DT. SV40 large T antigen functions in DNA replication and transformation. *Advances in virus research*, 2000. 55: p. 75-134.

335. Sinibaldi L. Involvement of gangliosides in the interaction between BK virus and Vero cells. *Arch Virol*, 1990. 113(3-4): p. 291-6.

336. Siuzdak G. Probing viruses with mass spectrometry. 1998 *J. Mass Spectrom.* 33:203–211.

337. Smith AE, Helenius A. How viruses enter animal cells. *Science*, 2004. 304(5668): p. 237-42.

338. Sontag E. Protein phosphatase 2A: the Trojan Horse of cellular signaling. Cellular signalling, 2001. 13(1): p. 7-16.

339. Spink KM, Fluck MM. Polyomavirus hr-t mutant-specific induction of a G2/M cell-cycle arrest that is not overcome by the expression of middle T and/or small T. 2003 *Virology* 307, 191–203.

340. Srinivasan A. The amino-terminal transforming region of simian virus 40 large T and small t antigens functions as a J domain. *Molecular and cellular biology*, 1997. 17(8): p. 4761-73.

341. Stakaityt G, Wood JJ, Knight LM, Abdul-Sada H, Adzahar NS, Nwogu N, Macdonald A, Whitehouse A. (2014). Merkel cell polyomavirus: molecular insights into the most recently discovered human tumour virus. *Cancers* (Basel). *6*, 1267–1297.

342. Steen H, Mann M. The ABC's (and XYZ's) df peptide sequencing. *Nat. Rev. Mol. Cell Biol.* 2004 Sep; 5(9):699-711. Review. PMID: 15340378.

343. Stensballe A, Andersen S, Jensen ON. (2001). Characterization of phosphoproteins from electrophoretic gels by nanoscale Fe(III) affinity chromatography with off-line mass spectrometry analysis. Proteomics 1, 207-222.

344. Stewart SE, Eddy BE, Borgese N. Neoplasms in mice inoculated with a tumor agent carried in tissue culture. *J Natl Cancer Inst*, 1958. 20(6): p. 1223- 43.

345. Stewart SE. Leukemia in mice produced by a filterable agent present in AKR leukemic tissues with notes on a sarcoma produced by the same agent. *Anat. Record.*, 1953. 117: p. 532.

346. Stolt A, Sasnauskas K, Koskela P, Lehtinen M, Dillner J. Seroepidemiology of the human transmission. *Int. J. Cancer* 126, 2991-2996 (2010).

347. Stubdal H. Inactivation of pRB-related proteins p130 and p107 mediated by the J domain of simian virus 40 large T antigen. *Molecular and cellular biology*, 1997. 17(9): p. 4979-90.

348. Stubdal H, Zalvide J, DeCaprio JA. Simian virus 40 large T antigen alters the phosphorylation state of the RB-related proteins p130 and p107. *J Virol*, 1996. 70(5): p. 2781-8.

349. Sullivan CS, Pipas JM. T antigens of simian virus 40: molecular chaperones for viral replication and tumorigenesis. *Microbiology and molecular biology reviews*: MMBR, 2002. 66(2): p. 17

350. Sullivan CS. SV40-encoded microRNAs regulate viral gene expression and reduce susceptibility to cytotoxic T cells. *Nature*, 2005. 435(7042): p. 682-6.

351. Sullivan CS, Cantalupo P, Pipas JM. The molecular chaperone activity of simian virus 40 large T antigen is required to disrupt Rb-E2F family complexes by an ATP-dependent mechanism. *Molecular and cellular biology*, 2000. 20(17): p. 6233-43.

352. Sweet BH, Hilleman MR. The vacuolating virus, SV 40, in *Proc. Soc. Exp. Biol Med.*, Vol 105, November 1960, pp. 420-427, PMID 13774265

353. Talalay P, Ashman GW, Bryan WR. 1966 nobel laureates in medicine or physiology. *Science*, 1966. 154(3747): p. 362-5.

354. Talbert PB, Henikoff S. (April 2010). "Histone variants--ancient wrap artists of the epigenome". *Nature Reviews*. Molecular Cell Biology. 11 (4): 264–75. doi:10.1038/nrm2861. PMID 20197778.

355. Tan BH, Busam KJ. Virus-associated Trichodysplasia spinulosa. *Advances in anatomic pathology*, 2011. 18(6): p. 450-3.

356. Tegerstedt K. Murine pneumotropic virus VP1 virus-like particles (VLPs) bind to several cell types independent of sialic acid residues and do not serologically cross react with murine polyomavirus VP1 VLPs. *J Gen Virol*, 2003. 84(Pt 12): p. 3443-52.

357. Temin, H.M. and S. Mizutani, RNA-dependent DNA polymerase in virions of Rous sarcoma virus. Nature, 1970. 226(5252): p. 1211-3.

358. Tiemann F, Deppert W Stabilization of the tumor suppressor p53 during cellular transformation by simian virus 40: influence of viral and cellular factors and biological consequences. *Journal of virology*, 1994. 68(5): p. 2869-78.

359. Tognon M. Oncogenic transformation by BK virus and association with human tumors. *Oncogene*, 2003. 22(33): p. 5192-200.

360. Toker C. Trabecular carcinoma of the skin. *Archives of dermatology*, 1972. 105(1): p. 107-10.

361. Tolstov YL, Pastrana DV, Feng H, Becker JC, Jenkins FJ, Moschos S. Human Merkel cell polyomavirus infection II. MCV is a common human infection that can be detected by conformational capsid epitope immunoassays. *Int. J. Cancer.* 2009 Sep 15;125(6):1250-6.

362. Topalis D, Andrei, G, Snoeck R. "The large tumor antigen: A "Swiss Army knife" protein possessing the functions required for the polyomavirus life cycle". 2013 *Antiviral Research*. 97 (2): 122–136. doi:10.1016/j.antiviral.2012.11.007. PMID 23201316.

363. Toracchio S, Foyle A, Sroller V, Reed JA, Wu J, Kozinetz CA. Lymphotropism of Merkel cell polyomavirus infection, Nova Scotia, Canada. *Emerg. Infect. Dis.* 2010 Nov;16(11):1702-9.

364. Trusch F, Klein M, Finsterbusch T, Kuhn J, Hofmann J, Ehlers B. Seroprevalence of human polyomavirus 9 and cross-reactivity to African green monkey-derived lymphotropic polyomavirus. *J. Gen. Virol.* 2012 Apr; 93(Pt 4):698-705.

365. Tsai B. Gangliosides are receptors for murine polyoma virus and SV40.Embo J, 2003. 22(17): p. 4346-55.

366. Tsang SH, Wang R; Nakamaru-Ogiso E, Knight SAB, Buck CB, Jianxin Y, Banks L. "The Oncogenic Small Tumor Antigen of Merkel Cell Polyomavirus Is an Iron-Sulfur Cluster Protein That Enhances Viral DNA Replication".2016 *Journal of Virology*. 90 (3): 1544–1556. doi:10.1128/JVI.02121-15

367. Turk B. Simian virus 40 small-t antigen binds two zinc ions. *Journal of virology*, 1993. 67(6): p. 3671-3.

368. Valenzuela-Fern´andez A, Alvarez S, Gordon-Alonso M, Barrero M, Ursa A, Cabrero JR, Fern´andez G, Naranjo-Su´arez S, Y´an~ez-Mo M, Serrador JM. (2005) Histone deacetylase 6 regulates human immunodeficiency virus type 1 infection. *Mol Biol Cell* 16, 5445–5454.

369. Van der Meijden E, Janssens RW, Lauber C, Bouwes Bavinck JN, Gorbalenya AE, Feltkamp MC. Discovery of a new human polyomavirus associated with trichodysplasia spinulosa in an immunocompromized patient. *PLoS Pathog*. 2010; 6(7):e1001024.

370. Van der Meijden E, Kazem S, Burgers MM, Janssens R, Bouwes Bavinck JN, de Melker H. Seroprevalence of trichodysplasia spinulosa-associated polyomavirus. *Emerg. Infect. Dis.* 2011 Aug; 17(8):1355-63.

371. Van Ghelue M, Khan MT, Ehlers B, Moens U. Genome analysis of the new human polyomaviruses. *Rev. Med. Virol.* 2012 Mar 28.

372. Van Keymeulen, A. Epidermal progenitors give rise to Merkel cells during embryonic development and adult homeostasis. *The Journal of cell biology*, 2009. 187(1): p. 91-100.

373. Venter M, Visser A, Lassauniere R. Human polyomaviruses, WU and KI in HIV exposed children with acute lower respiratory tract infections in hospitals in South Africa. *Journal of clinical virology*: the official publication of the Pan American Society for Clinical Virology, 2009. 44(3): p. 230-4.

374. Viscidi RP, Rollison DE, Sondak VK, Silver B, Messina JL, Giuliano AR. Agespecific seroprevalence of Merkel cell polyomavirus, BK virus, and JC virus. *Clin. Vaccine Immunol.* 2011.

375. Viscidi RP, Clayman B. Serological cross reactivity between polyomavirus capsids. *Advances in experimental medicine and biology*, 2006. 577: p. 73-84.

376. Vogel C, Marcotte EM. Insights into the regulation of protein abundance from proteomic and transcriptomic analyses. *Nat Rev Genet*. 2012 Mar 13;13(4):227-32. doi: 10.1038/nrg3185.

377. Walker DL. Human papovavirus (JC): induction of brain tumors in hamsters. *Science,* 1973. 181(4100): p. 674-6.

378. Wang T, Yu B, Lin L, Zhai X, Han Y, Qin Y, Guo Z, Wu S, Zhong X, Wang Y. (2012) A functional nuclear localization sequence in the VP1 capsid protein of coxsackievirus B3. *Virology* 433, 513–521.

379. Wang HG. Identification of specific adenovirus E1A N-terminal residues critical to the binding of cellular proteins and to the control of cell growth. *Journal of virology*, 1993. 67(1): p. 476-88.

380. Wattier RL. Role of human polyomaviruses in respiratory tract disease in young children. *Emerging infectious diseases*, 2008. 14(11): p. 1766-8.

381. Weinberg RA. the biology of cancer2007: *Garland Science*.

382. White MK, Gordon J, Reiss K. "Human polyomaviruses and brain tumors". 2005 *Brain Research Reviews* 50 (1): 69–85. doi:10.1016/j.brainresrev.2005.04.007. PMID15982744.

383. Whyte P. Association between an oncogene and an anti-oncogene: the adenovirus E1A proteins bind to the retinoblastoma gene product. *Nature*, 1988. 334(6178): p. 124-9.

384. Wilkins MR1, Hochstrasser DF, Sanchez JC, Bairoch A, Appel RD. Integrating two-dimensional gel databases using the Melanie II software. *Trends Biochem Sci*. 1996 Dec;21(12):496-7.

385. Winocour E. Further studies on the incorporation of cell DNA into polyoma-related particles. *Virology*, 1968. 34(4): p. 571-82.

386. Winocour E. Purification of polyoma virus. *Virology*, 1963. 19: p. 158-68.

387. Wu J, Shuichi T, Wong C-H, Siuzdak G. (1997) Quantitative electrospray mass spectrometry for the rapid assay of enzyme inhibitors. *Chem. Biol.* 4:653–657.

388. Wyatt AJ.Virus-associated trichodysplasia spinulosa. *The American journal of surgical pathology*, 2005. 29(2): p. 241-6.

389. Yaciuk P. Simian virus 40 large-T antigen expresses a biological activity complementary to the p300-associated transforming function of the adenovirus E1A gene products. *Mol Cell Biol*, 1991. 11(4): p. 2116-24.

390. Yates JR 3rd, McCormack AL, Link AJ, Schieltz D, Eng J, Hays L. Future prospects for the analysis of complex biological systems using micro-column liquid chromatography-electrospray tandem mass spectrometry. *Analyst.* 1996 Jul;121(7):65R-76R.

391. Yew PR, Berk AJ. Inhibition of p53 transactivation required for transformation by adenovirus early 1B protein. *Nature*, 1992. 357(6373): p. 82-5.

392. Yuen LK, Consigli RA. (1985). Identification and protein analysis of polyomavirus assembly intermedi-ates from infected primary mouse embryo cells. Virology, 144, 127–138.

393. Zalvide J, Stubdal H, DeCaprio JA. The J domain of simian virus 40 large T antigen is required to functionally inactivate RB family proteins. *Mol Cell Biol*, 1998. 18(3): p. 1408-15.

394. Zerrahn J, Knippschild U, Winkler T, Deppert W. Independent expression of the transforming amino-terminal domain of SV40 large I antigen from an alternatively spliced third SV40 early mRNA *EMBO J.,* 12 (1993), pp. 4739-4746.

395. Zhao L. Identification of WU polyomavirus from pediatric patients with acute respiratory infections in Beijing, China. *Archives of virology*, 2010. 155(2): p. 181-6.

396. Zhao R. The transcriptional program following p53 activation. *Cold Spring Harbor symposia on quantitative biology*, 2000. 65: p. 475-82.

397. Zhong M, Zheng K, Chen M, Xiang Y, Jin F, Ma K, Qiu X, Wang Q, Peng T, Kitazato K, Wang Y. Heat-shock protein 90 promotes nuclear transport of herpes simplex virus 1 capsid protein by interacting with acetylated tubulin. *PLoS One.* 2014 Jun 5;9(6):e99425. doi: 10.1371/journal.pone.0099425. eCollection 2014.

398. Zhuang WL. [Detection and clinical characterization of WU polyomavirus in acute respiratory tract infection in children]. Zhonghua er ke za zhi. *Chinese journal of pediatrics*, 2010. 48(2): p. 90-4.

399. Zuehlke AD, Beebe K, Neckers L, Prince T. (2015) Regulation and function of the human HSP90AA1 gene. *Gene* 570, 8–16.

400. Zur Hausen H. Viruses in human cancers. *Eur J Cancer*, 1999. 35(14): p. 1878- 85.